1993

Analysis of Immediate-Early Gene Expression in the Songbird Brain Following Song Presentation

Claudio Vianna de Mello

ANALYSIS OF IMMEDIATE-EARLY GENE EXPRESSION IN THE SONGBIRD BRAIN FOLLOWING SONG PRESENTATION

Claudio Vianna de Mello
New York, NY, 1993

A thesis submitted to the faculty of
The Rockefeller University
in partial fulfillment
of the requirements for the degree of
Doctor of Philisophy

Acknowledgments

The work presented in this thesis would not have been possible if I could not count on the precious help of several people who I wish to acknowledge here. I thank Maria Huecas, who guided me through the initial steps in the lab, and played a fundamental role in ZENK isolation and sequencing; the birdkeepers in the Field Research Center in Millbrook, Dawn and Sharon, who did the really hard-work; my friends and colleagues in the Clayton, Nottebohm and Alvarez-Buylla labs, who provide such an enjoyable working atmosphere. My particular thanks to Kaleb Yohay, for his help during the preparation of this manuscript, Soshi Okuhata, who made some of the most difficut tracer injections possible, Hubert Schwabl, who collaborated in the field study of song sparrows and David Vicario for the very stimulating discussion sessions and for his insights into some very fundamental issues. I want to thank Fernando Nottebohm for the enthusiasm and appreciation he has shown for this work, for his crucial help in building a coherent and convincing story out of fairly complicated anatomical data and for his agreeing on being co-advisor of my thesis work, together with David Clayton. Fernando's essential contributions to the biology of songbirds have provided the basic framework for the studies described here. Finally, I'd like to thank my advisor David Clayton for his support and for always being available; he gave me a lot of freedom to develop my projects in his lab, but his constant feedback was essential in defining the main directions and goals of this research, especially in such a vast and unexplored territory.

I thank Lucia for her love, care and support throughout the most difficult moments and for helping me grow as a more complete human being.

ABSTRACT

The song system of oscine songbirds consists of the auditory and motor pathways used in the acquisition and production of learned song and provides powerful material for the study of neuronal and behavioral plasticity, both developmentally and during adult life. The purpose of this thesis is to begin to study molecular mechanisms underlying plasticity in the songbird brain. To test whether genomic mechanisms are involved, the expression of an immediate-early gene (IEG) was studied. The isolation of the canary ZENK homologue is described, an IEG that encodes a zinc-finger protein and which is highly sensitive to growth factors and depolarizing stimulation, including stimuli leading to LTP induction in the mammalian hippocampus. Two methods were used to study gene regulation: administration of metrazole, a strong depolarizing agent, and playbacks of birdsong, a natural stimulus of well-defined behavioral relevance. Both stimuli result in significant increases in ZENK mRNA levels in the brain. Metrazole experiments demonstrate that ZENK is differentially regulated and may be selectively repressed in some neuronal populations, including cells of the song control pathway. Mapping of depolarized areas after song playbacks with ZENK probes defines a series of brain areas activated by song; some of these had not been described as being related to song production or perception and neuroanatomical tract-tracing techniques were used to define their connections. Some of these areas are intimately associated with auditory structures; a subset of these is closely apposed to nuclei of the motor pathway for song control and could represent sites for

sensory motor integration, an essential aspect of song learning. ZENK induction in the caudo-medial neostriatum (NCM, the area with the most marked response) shows a preference for conspecific song and can be habituated by repetitive presentations of the same song, but does not enter an absolute refractory period after habituation, since another song will elicit a full genomic response; these results suggest that cells showing ZENK response are related to auditory processing and song discrimination.

CONTENTS

CHAPTER 1: GENERAL INTRODUCTION

Immediate-early genes and the brain

The adult vertebrate brain can be viewed as the result of a complex interaction between genes expressed in neuronal cells and the environmental stimuli the animal encounters throughout its life history. This process is usually thought to occur predominantly at an early age, when neuronal morphology, connectivity and function can be most easily shaped according to patterns of external stimulation (as shown in detail, for instance, in the mammalian visual system; see Wiesel, 1982; Shatz, 1990). Such periods of intense remodelling and organization, usually temporally restricted to defined times after birth, have been termed sensitive periods (reviewed in Bornstein, 1989).

Evidence has rapidly accumulated, though, demonstrating that various brain processes related to morphological and functional change and usually grouped under the denomination of neuronal plasticity, are not restricted to developmental periods but are also expressed during adult life or in mature brain tissue. Some examples are modulations in gene expression, synaptic plasticity and regulation of neuronal and synaptic morphology and function in various paradigms (a few samples from this literature are: Bliss and Lomo, 1973; Berry et al., 1980; Lee et al. 1980; Cotman et al., 1981; Nottebohm, 1981; Chang and Greenough, 1984; Cotman and Nieto-Sampedro, 1984; Purves et al., 1986 and 1987; Greenough and Bailey, 1988). In some more extreme cases, modifications in the neuronal

population during adult life through cell death, neurogenesis and neuronal replacement have also been described (Goldman and Nottebohm, 1983; Alvarez-Buylla et al., 1990). This continued ability to change, in many cases in direct response to external stimulation, may indeed be a most essential aspect of brain function and could be the underlying basis of learning and memory processes.

The ability to change patterns of gene expression in response to various extracellular stimuli is a remarkable example of plasticity in neuronal cells. Even though their functional significance is not yet clear, many genes respond rapidly and transiently to membrane depolarizing signals and to signals related to growth and differentiation such as growth factors and serum (Bartel et al., 1989; Ginty et al, 1992; Morgan and Curran, 1989; Sheng and Greenberg, 1990); they have thus been named immediate-early genes (IEGs). Many IEGs analysed so far encode DNA-binding proteins of various classes, several of which have been shown to possess transcriptional regulatory activity (reviewed in McMahon and Monroe, 1992). They can, thus, coordinately influence the expression of other genes and could potentially be the early steps in a cellular program leading from depolarization to changes in cell shape, size and function (Goelet et al., 1986; Sheng and Greenberg, 1990). For example, addition of Nerve Growth Factor (NGF) to PC-12 cells, an undifferentiated cell line derived from a rat pheochromocytoma, results in neuronal-like differentiation of these cells, including extension of neurites and expression of so-called "late" or "effector" genes encoding neuronal-specific proteins such as peripherin (an intermediate filament protein), transin (a metalloprotease), subunits of neurofilaments,

neural cell adhesion molecule (N-CAM), S-100-like proteins and GAP-43, a phosphoprotein related to neurite outgrowth and synaptic potentiation (Milbrandt, 1987; Changelian et al., 1989). These changes affecting cell differentiation are preceded by rapid and transient induction of various IEGs including transcription factors which could coordinate the whole process by regulating, directly or indirectly, the expression of late genes (Goelet et al., 1986; Milbrandt, 1987 and 1988). In summary, IEGs would function as the mediators of long-term cellular changes in response to external stimulation (Goelet et al., 1986).

The initial studies on IEG regulation were performed in established cell lines and proved instrumental in the investigation of molecular events following administration of growth factors or membrane depolarizing stimuli such as KCl and neurotransmitter agonists, and in the actual isolation of IEGs. IEGs encoding DNA-binding proteins can be further subdivided according to the class of DNA-binding motifs they express. Some examples are: genes of the leucine-zipper family (c-fos, c-jun and respective families; as reviewed in McMahon and Monroe, 1992), genes related to the steroid hormone receptor superfamily (NGFI-B, Milbrandt, 1988) and genes encoding other classes of zinc-finger proteins (Milbrandt, 1987; and see chapter 2). C-fos, c-jun and related genes are the most extensively studied IEGs. They seem to be fairly ubiquitous and are sensitive to a wide variety of extracellular stimuli tested in cell cultures from various sources (Sheng and Greenberg, 1990). In neuronal cells, c-fos responds well to strong depolarizing stimuli and

has been used as a mapping tool for activated cells in various in vivo paradigms (see below).

Studies with cell lines have also revealed that various steps such as activation of specific classes of neurotransmitter receptors, calcium entry, activation of specific kinases and eventual phosphorylation and activation of pre-existing DNA-binding proteins such as CREB (cAMP response element binding protein) are essential components of the signal transduction pathway leading from cellular activation to IEG induction (Sheng et al., 1990; Sheng and Greenberg, 1990). Cell cultures have also been the choice system for determining the molecular consequences of IEG induction such as transcriptional regulation of downstream genes. Experiments involving promoter deletion, in vitro binding assays and intracellular injection of antisense mRNA and co-transfection of cultured cells with a plasmid containing an IEG and a plasmid containing a specific promoter anchored to a reporter gene have been used to demonstrate the effect of IEGs on promoter function. Using this methodology, Fos and Jun proteins have been shown to form homo- and heterodimers that are believed to influence transcription of genes like proenkephalin, tyrosine hydroxilase, nerve growth factor, transin and some IEGs, all of which contain AP-1 (binding activity defined by Fos/Jun complexes) binding sites in their promoters (Sonnenberg et al., 1989b; reviewed in Ginty et al., 1992 and McMahon and Monroe, 1992).

In order, though, to investigate whether IEG activation has any relevance to the study of mechanisms of behavioral modification, some basic questions need to be addressed: 1) Is the activation of

IEGs regulated by behaviorally meaningful stimuli? This is a critical issue that can only be addressed in in vivo situations involving the whole animal under physiological (non-pathological) conditions and the presentation of non-invasive stimuli. Of particular relevance is the use of natural stimuli that can elicit the full expression of naturally occurring behaviors; further steps would be to perform experiments in nature (such as field studies) or under conditions that most closely mimic that situation. 2) What are the functional consequences of IEG activation? Is IEG induction in neuronal cells linked to behavioral modifications? A direct way to causally relate gene induction to behavioral changes is to somehow try to block the induction and assess the consequences on behavior. A more complete knowledge of which genes are activated by the stimulus presentation and as a direct result of IEG activation is needed before educated guesses can be made about the most interesting or relevant genes to be blocked. 3) A central question that would still remain after the demonstration of gene induction in the context of behavior, is exactly how changes in gene expression can translate into behavioral changes. The general hypothesis derived from cell culture studies is that IEGs may mediate physiological and/or morphological changes (i.e. modulations of cell shape, size, neurotransmitter profile, classes of ionic channels expressed, etc.) that could eventually underlie behavioral modifications.

The first demonstrations of IEG activation in vivo involved artificial conditions such as direct neuronal activation by electrode stimulation of various brain structures, kindling stimulation and seizure activity after administration of convulsant drugs (Dragunow

and Robertson, 1987; Morgan et. al, 1987; Saffen et al. 1988; Sagar et al. 1988; Watson and Milbrandt, 1989). Even though a significant induction of various genes was seen in depolarized areas in those experiments, the question still remained whether more physiological stimuli would be equally effective in inducing gene expression. Several attempts were made in this direction; these include water deprivation in the study of the activation of regulatory centers for water intake in the hypothalamus (Sagar et al., 1988), analysis of activated pathways in the spinal cord after stimulation of the paw with nociceptive stimuli (Hunt et al., 1987; Wisden et al., 1992) and studies of visual pathways using light stimuli (Sagar and Sharp, 1990; Worley et al., 1991).

One of the most interesting examples of IEG induction in the context of a behavioral modification is the study of the regulation of circadian rhythms in rodents by light stimuli (Kornhauser et al., 1990; Rusak et al., 1990). In these experiments, animals kept in 12h/12h (light/dark) photoperiod cycles are exposed to flashes of light at various times during their subjective day or night and are then examined for IEG induction in the suprachiasmatic nucleus (SCN), a hypothalamic area thought to function as a biological clock in mammals. The correlation found in these studies is that IEG induction in the SCN only occurs after light stimuli given during the subjective night, i.e., a time during which a light stimulus most probably results in a shift of the biological clock, but not during the subjective day.

Some earlier studies have suggested that induction of genes such as IEGs could be related to processes of learning and memory. These include, first, experiments involving the use of inhibitors of protein

synthesis in various learning paradigms in vertebrates (reviewed in Davis and Squire, 1984). Although intrinsically not conclusive, these experiments suggested that new protein synthesis in a narrow time window during the training period was essential for the long-term retention of memories related to the task being learnt. Secondly, Kandel's experiments on the sea snail *Aplysia californica* have led to the definition of distinct biochemical events underlying the formation of short- and long-term memories during behavioral training (Goelet et al., 1986; Montarolo et al., 1986). Whereas short-term memories seem to be independent of new protein synthesis and to rely on modifications of pre-existing proteins, long-term memories are critically dependent on proteins being synthesized during the training period (Montarolo et al., 1986) and are associated with morphological changes (Bailey and Chen, 1983). Indeed, a whole series of proteins with different induction kinetics (some are immediately activated, whereas others have variously delayed induction times) has been detected as a consequence of behavioral training in these animals (Castellucci et al., 1988). The early steps might be represented by transcription factor-like activities that could then coordinate the whole cascade.

Recent evidence suggesting a relation between IEG induction and associative learning in vertebrates comes from work done in chicks (Anohkin and Rose, 1991; Anohkin et al., 1991; Rose, 1991). These studies represent the first direct demonstration of IEG induction in a telencephalic area after non-invasive stimulation; the changes in gene expression occur in areas that had been previously detected by increases in metabolic activity during the learning period. Some

criticism on these studies, however, includes the lack of more precise knowledge about circuits regulating the behavior, the complication of separating effects specifically related to learning from developmental processes (this is inherent to any study made during developmental phases or sensitive periods), especially because uninduced levels are usually higher in younger animals than in adults, and the little understanding of the effects of sensory stimulation alone (this is an important control, especially because some forms of learning - such as habituation - may be intrinsically associated with any stimulus presentation). Some more recent attempts to correlate IEG induction and learning in rodents include sexual learning (Bialy et al., 1992) and the learning of a two-way active avoidance reaction (Nikolaev et al., 1992a and b) in rats and the formation of olfactory memories in mice (Brennan et al., 1992).

Songbirds

The song system of oscine songbirds has emerged, in the last three decades, as a powerful model for the study of neuronal and behavioral plasticity, both developmentally and during adult life (Nottebohm, 1981 and 1989; Konishi, 1989). Study of brain areas related to song production, a learned motor behavior, has revealed a specialized circuit that includes a well-defined series of discrete and interconnected nuclei essential for normal singing behavior (Nottebohm et al., 1976; Nottebohm et al., 1982; Konishi, 1989). This circuit ultimately controls the output of motoneurons of the XIIth cranial nerve, which then project to muscle fibers of the syrinx, the

vocal organ of songbirds. Some other nuclei have been identified which are intimately connected with this descending motor pathway and seem to be essential during the song learning period (Bottjer et al., 1984; Sohrabji et al., 1990; Scharff and Nottebohm, 1991).

One can usually divide songbirds into two general categories, according to the patterns of song learning. Sensitive period birds learn their song only once in their lives (during the sensitive period), and are exemplified by the zebra finch, Taeniopygia guttata (Immelman, 1969; Arnold, 1975). Seasonal or open-ended learners like canaries, on the other hand, retain the ability to change their vocal output during adult life (Nottebohm et al, 1986; Nottebohm and Nottebohm, 1988). The nuclei that constitute the song control circuit show extensive rearrangements of cell number, shape and connectivity during the song learning period in zebra finches (Konishi and Akutagawa, 1985; Nordeen and Nordeen, 1988). In seasonal learners, these morphological changes occur during adult life in cyclic patterns that are tightly correlated with fluctuations in singing behavior and hormonal levels (Nottebohm, 1981 and 1989; Nottebohm et al., 1986; Alvarez-Buylla et al., 1990). Such birds seem to be able, to some extent, to recapitulate developmental processes during adult life. Comparisons of species belonging to these different categories can be very useful in testing various general hypothesis related to development and plasticity and are used in the present work whenever relevant.

The song control nuclei are also characterized by marked sexual dimorphism, the result of either direct or indirect hormonal action (Nottebohm and Arnold, 1976; Herrmann and Arnold, 1991). Sex

steroids such as testosterone, estradiol and their metabolites, in particular, are important for the anatomical integrity of the song circuit and for the development and maintenance of normal singing behavior (DeVoogd and Nottebohm, 1981; Gurney, 1981). Treatment of females with the adequate hormonal regime results in masculinization of both the song circuit and singing behavior and castration, in turn, depresses the incidence of stable adult song (Arnold, 1975; DeVoogd and Nottebohm, 1981). Annual fluctuations in hormonal levels have also been postulated as a main modulator of morphological and functional changes in the song system (Nottebohm, 1981 and 1989). The tight control exerted by steroids on the biology of birdsong suggests that transcriptional regulation of target genes related to cell growth and differentiation may play a key regulatory role in this system.

Song learning involves a combination of genetic, sensory and social factors. Inherited components are represented by a preference for learning elements from the song of the same species (conspecific song) as opposed to other species song (heterospecific) in juveniles previously unexposed to song (Marler and Peters, 1977 and 1987), as well as the preservation of some temporal features of the species song in birds raised in isolation from song models (Thorpe, 1958; Marler, 1970). The social component is represented by stimuli coming from the father or tutor, the most important of which being presentation of the learned trait itself, song (Thorpe, 1958; Kroodsma, 1982). Complete isolation of juveniles from a model results in the development of aberrant song patterns, called isolate song, that fail to match the characteristic patterns of normal song and

are not recognized by females during courtship (Searcy and Marler, 1987). In certain species song learning can be obtained just from playbacks of tape-recorded song, whereas other species, including zebra finches, seem to rely more heavily on a combination of auditory stimuli and social interactions, possibly including visual cues and more direct tactile stimuli (Immelman, 1969; Morrison, 1992).

A considerable amount of effort has been devoted to developing techniques for recording and analysing song through sonograms, a two-dimensional display of changes in the distribution of frequencies from an auditory stimulus over time. Analysis of sonograms permits a definition of the structure of song according to syllable types and the way in which these are syntactically combined; it also allows the evaluation of the learning process by comparing patterns of motor output between juveniles and tutors (for example, see Price, 1979). Song learning has thus been subdivided into various phases, according to the degree of stereotipy of the vocal output; early phases are characterized by large variability in vocal output patterns, that gradually decrease as song becomes more stereotyped or crystallized, as typical of adult males.

The formation of memories related to the songs the bird encounters throughout its life is essential for both song learning and for the development and expression of reproductive behaviors (as further discussed in chapter 4). It is still unclear, however, how an auditory stimulus like song can affect neuronal physiology and/or morphology and eventually lead to changes related to learning and memory. It is hypothesized here that, in order to understand the

mechanisms underlying the formation of long lasting memories related to song, one must study whether and how song can affect cellular and molecular processes in brain structures that normally respond to song.

The specific purpose of the present work is to study regulation of IEG expression in the song system of oscine songbirds. The species initially chosen was the canary and the first step consisted in the isolation of the canary homologue of a representative IEG, since some previous work done in the lab showed that cross-hybridizations using mammalian or even chicken probes were not adequate for this purpose (David Clayton, unpublished observations). In chapter 2, the isolation of the canary homologue of an IEG (ZENK) is presented, which encodes a zinc-finger protein and which is highly sensitive to growth factors and depolarization. Two methods were then used to study gene regulation: 1) administration of metrazole, a strong depolarizing agent, that constitutes a simple and sensitive test for IEG inducibility by depolarizing stimuli and allows the study of general patterns of induction in the brain (chapter 3); and 2) playbacks of birdsong, a natural stimulus of well-defined behavioral relevance (chapter 4). A series of brain areas is defined, which are activated by song. Some of the areas mapped had not been previously described as being related to song production or perception. Genomic response in at least one area, the caudo-medial neostriatum (NCM), seems to reflect some aspects of auditory processing: it shows a preference for conspecific stimuli, habituation to repeated presentation of the same stimulus and a preference for novelty (new stimuli). Neuroanatomical tract-tracing techniques

were then used to define the connections of some of the areas found to be activated by song (chapters 5 and 6). These are found to be intimately associated with auditory brain pathways; a subset of them are closely apposed to nuclei of the motor pathway for song control (chapter 6) and could represent sites for sensory-motor integration.

A possible criticism of using songbirds for studying cellular and molecular mechanisms underlying neuronal plasticity in vertebrates is that the results may not be extended to mammals. However, at least two lines of evidence indicate the opposite: 1) contrary to earlier interpretations, recent comparative neuroanatomical studies have suggested that much of the basic brain circuitry has been evolutionarily preserved between birds and mammals, in spite of marked differences in their overall forebrain organization (nuclear vs. cortical); this applies especially to thalamo-telencephalic and intra-telencephalic circuits (see discussion in chapters 4 and 5); 2) recent cloning efforts in the songbird brain has revealed that genes related to various functions such as signal transduction, transcriptional regulation or neurite extension and growth have been evolutionarily preserved, sometimes to an extraordinary degree of conservation (Clayton, unpublished observations; George and Clayton, 1992); these results suggest that molecular brain mechanisms are also shared between these two vertebrate groups.

CHAPTER 2: ISOLATION OF CANARY ZENK

INTRODUCTION

In this chapter, the cloning of an avian version of ZENK, an IEG induced by growth factors and membrane depolarizing stimuli in cell cultures is described (ZENK is the acronym for zif-268, egr-1, NGFI-A and Krox-24, as the same gene is known in other systems; see Milbrandt, 1987; Christy et al., 1988; Lemaire et al., 1988; Sukhatme et al., 1988). ZENK encodes a "zinc-finger" motif DNA-binding protein with proven transcriptional regulatory activity that seems to closely correlate with neuronal growth and plasticity. For instance, ZENK is induced by Nerve Growth Factor in PC-12 cells, where it could be a regulator of a genetic program leading to neuronal differentiation (Milbrandt, 1987). ZENK also shows a high sensitivity to membrane depolarization, both in cell cultures and in vivo (Saffen et al., 1988; Sukhatme et al., 1988; Bartel et al., 1989; Cole et al., 1989). After metrazole treatment, ZENK expression seems to be enriched in brain areas thought to be particularly plastic during adult life (see chapter 3). Of particular relevance, ZENK is induced in an NMDA receptor-dependent manner by electrode stimulation that leads to long term potentiation (LTP), a widely studied form of synaptic plasticity in the mammalian hippocampus (Cole et al., 1989; Wisden et al., 1990). Interest in hippocampal LTP and the mechanisms of its induction and maintenance derives from the possibility that it may represent a physiological substrate for memory formation in vertebrates (reviewed in Bliss and Collingridge, 1993). In the experiments

mentioned above, ZENK induction correlated well with LTP induction, whereas induction of c-fos, a more widely studied IEG of almost ubiquitous distribution, failed to do so. ZENK expression, thus, could be a more powerful indicator of cell depolarization and of brain sites undergoing plastic changes.

c-DNA sequence analysis (Milbrandt, 1987; Sukhatme et al., 1988) shows that the mammalian ZENK encodes a protein of predicted 54 kilodaltons containing 3 tandemly repeated zinc-finger sequences which confer binding activity to specific DNA sequences, as well as a highly conserved unit of 8 amino acids (8aa) that occurs at least 11 times, both upstream and downstream of the zinc-fingers, which could represent a structural and modular domain of defined but unknown function. The gene structure has been determined in the rat (Changelian et al., 1989): the coding sequence is interrupted by a single intron at nucleotide (nt) 588 and the 3 zinc-fingers are not separated by an intron, in contrast to other genes containing zinc-finger motivs. Sequencing of the promoter region reveals the presence of a TATA box, various serum responsive elements, a cAMP responsive element and a Sp-1 binding site, all of which could potentially play a role in regulating ZENK transcription. By expressing ZENK in E. coli, a large amount of protein was produced to obtain crystals which were then used in the determination of the molecular structure of the DNA-protein complexes (Pavletich and Pabp, 1991).

ZENK synthesized in bacterial cells was also used to determine its binding site (Christy and Nathans, 1989). ZENK was initially shown to bind strongly to its own promoter, as well as to the promoters of some other IEGs. By comparing the sequences of these binding sites,

a consensus sequence was defined: GCG$^{G}/_{T}$GGGCG. This consensus was then found to be present in the promoters of other genes, including other IEGs activated by growth factors and extracellular stimuli, as well as other classes of genes, such as c-Ha-ras, int-2, c-abl, hsc73 and the genes encoding the histone H3.3, the A chain of PDGF and the mouse metallothionein and neurofilament proteins. In muscle, ZENK has been shown to be a transactivator of the muscle specific α-myosin heavy chain gene (Gupta et al., 1991). Although a clear picture of ZENK function cannot yet be formed based on this information, all these genes are potential ZENK targets. Binding to the promoters of IEGs may subserve negative regulatory roles that could explain the rapid decline in mRNA levels after the induction peak; for example, Fos has been shown to repress its own transcription, as well as transcription of ZENK (Sassone-Corsi et al., 1988; Gius et al., 1990). Binding to other promoters could be related to either gene activation or inactivation. Further search may reveal that ZENK binds to a multiplicity of genes; it will then be particularly important to determine whether ZENK has any regulatory role on transcription of late genes activated within any given paradigm where ZENK is rapidly induced.

METHODS

Cloning

Rat and mouse probes used in the screening were provided by Milbrandt and Sukhatme (see results for details).

Sequencing

The nucleotide sequence of isolated clones was performed by the chain termination method (Sanger et al., 1977).

Preparation of riboprobes for Northern hybridization

Plasmids obtained from mini-preps were further purified by running through NACS columns. Plasmids were then digested with the appropriate restriction enzyme to prevent transcription of vector DNA, extracted with phenol, precipitated with ethanol and ressuspended in TE at the concentration of 1µg/µl, under ribonuclease(RNase)-free conditions. The riboprobe synthesis reaction contained (added in this order, at room temperature): 5µl of ^{32}P-UTP (50µC), 2µl of 5X ribo-12 buffer (2.5mM ATP, CTP and GTP each, 50mM DTT, 0.2M Tris, pH 7.5, 30 mM $MgCl_2$, 10mM spermidine, 50mM NaCl and 60µM UTP), 0.5µl of RNase inhibitor (40µg/µl, Promega), 0.1 to 1.0µl of plasmid DNA (0.1 to 1.0µg) and distilled water up to 9µl. To this solution was added 1.0 µl (5 to 20U, usually split in two halves, the second half added 30 minutes later) of the appropriate RNA polymerase and the reaction was then incubated for 1 to 1.5 hour at 42°C. The reaction was then run through a G-50 column after addition of 40µl of equilibration buffer (TE containing 50mM Na) and 20µg of tRNA; 1µl samples were taken for scintilation counting.

Northern blot

Canary and zebra finch brain RNA, total (30 µg/lane) or polyA$^+$ (1µg/lane), were run on a 1.5% agarose/8% formaldehyde gel and transferred to nytron filters in 10XSSPE overnight; filters were then rinsed in 2XSSPE, air-dried and baked for 2 hours.

Filters were pre-hybridized in 10ml of a solution containing 2.5mM $NaHPO_4$, 0.5ml of 5M NaCl, 0.7g of SDS, 2.0ml of 2M PEG8000, 20µl of 0.5M EDTA, 5 ml of formamide and 10µl of 20mg/ml polyA; ^{32}P-labeled riboprobes were added to this solution at a final concentration of 10^5cpm/ml and filters were hybridized overnight at 65^{o}C. Filters were then washed with several changes of 0.1X SSPE/0.1% SDS at 65^{o}C; the high stringency wash consisted of two final washes in 0.1% SDS/1mM sodium pyrophosphate/1mM $NaHPO_4$/1mM EDTA at 65^{o}C.

RESULTS

Cloning

Preliminary studies using Southern hybridizations (carried out by Maria Huecas and David Clayton), had established the probable existence of a single canary homologue of the rodent ZENK gene. Several candidate cDNA clones were then isolated by reduced-stringency hybridization of a cDNA library (made from the dorsal posterior hyperstriatum and neostriatum of adult male canaries, George and Clayton, 1992) with probes derived from the mouse egr-1 and rat NGFI-A genes. Inserts from six of these clones were subcloned into pBluescript for further analysis.

Sequence analysis and species comparisons

To determine whether any of the candidate clones in fact encoded the canary ZENK gene, their complete nucleotide sequences were determined and one clone identified (e-12) which predicted a protein closely related to the mouse and rat sequences. Analysis of e-12 sequence (figure 2.1) shows the presence of 3 zinc-finger domains and a short degenerate sequence repeated 10 times upstream and downstream of the zinc-fingers; these features are also characteristic of the mammalian gene (Milbrandt, 1987; Sukhatme et al., 1988). A comparison with the rat NGFI-A (figure 2.2) reveals an overall identity of 70% at the amino acid level, which rises to 100% throughout the zinc-finger domain. Most of the substitutions are conservative and many of them fall within the short repeats, which exhibit considerable divergence both within and between species

Figure 2.1 - Nucleotide sequence and translated peptide sequence of the e-12 cDNA clone. The short degenerate amino acid repeats are underlined, and the zinc fingers are boxed.

```
GGCAGCAATCCCCTATGGCCAGAGCCCCTCTTCAGCCTCGTCAGTGGGCTTGTGGGCATGGCTAATGCACCTCCCACATCTACGCCTACT      90
G  S  N  P  L  W  P  E  P  L  F  S  L  V  S  G  L  V  G  M  A  N  A  P  P  T  S  T  P  T

TCATCATCACCATCCTCCTCCTCGCAGAGCTCCCCACTGAGCTGTTCTGTCCAAGCCAGCGACAACAATCCAATTTATTCAGCTGCACCA     180
S  S  S  P  S  S  S  S  Q  S  S  P  L  S  C  S  V  Q  A  S  D  N  N  P  I  Y  S  A  A  P

ACATTTCCCAATTCCAGCTCTGACATTTTTCCTGAATCCCAGACCCAGTCTTTCCCCAACCCCTCTGGAGCCCCTATCCAGTATCCACCT     270
T  F  P  N  S  S  S  D  I  F  P  E  S  Q  T  Q  S  F  P  N  P  S  G  A  P  I  Q  Y  P  P

CCAGCTTATCCGACTGCTAAAACCAACTTTCAGGTGCCGATGATCCCGGATTACTTGTTCCCTCAGCAACAGGGTGAGCTCAGTCTTGTT     360
P  A  Y  P  T  A  K  T  N  F  Q  V  P  M  I  P  D  Y  L  F  P  Q  Q  Q  G  E  L  S  L  V

CCAGCTGATCAGAAGCCCTTCCCAGCTCTTGAGACCAGAGCACAGCAGCCTTCCCTCACACCACTGTCCACCATCAAGGCATTTGCTACT     450
P  A  D  Q  K  P  F  P  A  L  E  T  R  A  Q  Q  P  S  L  T  P  L  S  T  I  K  A  F  A  T

CAGACTGGCTCCCAAGAGCTGAAGACCCTCAATGCTAATTATCAGTCCCAGCTGATCAAGCCCAGCAGGATGAGGAAATACCCCAACCGT     540
Q  T  G  S  Q  E  L  K  T  L  N  A  N  Y  Q  S  Q  L  I  K  P  S  R  M  R  K  Y  P  N  R

CCCAGCAAGACGCCTCCTCATGAGCGTCCCTATGCCTGCCCAGTGGAGTCCTGTGACCGGAGGTTTTCACGATCCGATGAGCTAACGCGG     630
P  S  K  T  P  P  H  E  R  P  Y  A  C  P  V  E  S  C  D  R  R  F  S  R  S  D  E  L  T  R

CACATACGCATCCACACGGGACAGAAACCTTTCCAGTGCCGCATTTGCATGCGGAACTTCAGCAGGAGTGACCATTTGACTACGCACATC     720
H  I  R  I  H  T  G  Q  K  P  F  Q  C  R  I  C  M  R  N  F  S  R  S  D  H  L  T  T  H  I

CGCACGGCACACAGGAGAGAAGCCGTTTGCTTGTGACATTTGTGGCAGAAAGTTTGCCAGAAGTGATGAGAGGAAGAGGCACACTAAAATC     810
R  T  H  T  G  E  K  P  F  A  C  D  I  C  G  R  K  F  A  R  S  D  E  R  K  R  H  T  K  I

CATCTTAGGCAGAAGGACAAGAAAGTGGAAAAGGCAGCACCAGCCTCAACTGCTTCCCCAATTCCTGCGTATTCATCCTCTGTGACTACG     900
H  L  R  Q  K  D  K  K  V  E  K  A  A  P  A  S  T  A  S  P  I  P  A  Y  S  S  S  V  T  T

TCCTACCCTTCCTCTATTGCCACCACTTATCCCTCCCCAGTGCGCACAGCGTATTCTTCTCCTGCTCCCTCTTCCTATCCCTCCCCTGCA     990
S  Y  P  S  S  I  A  T  T  Y  P  S  P  V  R  T  A  Y  S  S  P  A  P  S  S  Y  P  S  P  A

CACACCACATTCCCATCCCCTTCTATAGCAACCACTTACCCCTCTGGCACTGCCACTTTTCAGACCCAAGTGGCCACTTCCTTCTCATCT    1080
H  T  T  F  P  S  P  S  I  A  T  T  Y  P  S  G  T  A  T  F  Q  T  Q  V  A  T  S  F  S  S

CCAGGAGTCACCAACAATTTCAGCTCACAGGTAACCTCATCACTTTCAGACATGAACTCAGCCTTTTCTCCAAGGACAATTGAGATCTGC    1170
P  G  V  T  N  N  F  S  S  Q  V  T  S  S  L  S  D  M  N  S  A  F  S  P  R  T  I  E  I  C

TGAGACTACCTTCTGGAACAGGATAATTCACCTTTTCCATTGGTATTATCAGACACGGAGTCTCCAATTACTCCCACAACACCATACGTT    1260
GCAAGGCTATTTAGTTGAAACTTCAGCTGCCTGAATCGACTGCTGCTTAAGTTTTCCACCTCTGTTGAATGACTTAATTTCGATGGACTG    1350
TGGATATAAGTTCAATATAACTTTCCCTGTAAACAATAATCTTTTATTAGGAAGAAAGACTTTTGATTAAGTATCTAGCTAATGTAAATT    1440
GTACATGTGCCATGGTTTTGCTTTCCTTTAGGTACTATTGATGTGGAAAAAATCTTTGCATATTCATATTGTATAATTTGGAGTTTGCAG    1530
GGCCATATTTNGTAAATGTTAATTCTATTTCAGTGATAATGCTATAATGCGNTTCAAACTTCTTTGGGAACAGCACTTACTGTATTTGAG    1620
CATGTTGGAGTGATGCTATGTAATTATCATCTGATGAGACACTCACATGTGGCAGAAGTTTTGTTTTAAAAGTTACAAGTCTTGGTGCCT    1710
TTTTGTGAAGCCTTGCTGACGTCATGCGTTTGTGTGAGTGGATGCTTTGCATCTTGCCTTAAAGTGGAAGGGATGTTACTCAAAGAATGT    1800
AAGGAAGAGCAGGGAATGGGTGGGGAGAGGAGCAAGAGAAAGGGCCAGGGGATGGAATATAAGCAAAAAAAAAAAACCAAACCAAAGG      1887
```

Figure 2.2 - Alignment of the rat NGFI-A peptide sequence (RATNGFIA) with the predicted canary ZENK peptide (CANZENK) derived from the e-12 cDNA clone and the pge12 genomic clone. Regions of identity are boxed, and dashes indicate gaps in the alignment. The large vertical arrows indicate the position of the single intron in the respective genomic coding sequences, as determined by genomic clone analysis (note conserved placement). The horizontal arrow indicates the 5' end of the sequence contained in the e-12 cDNA clone (figure 1).

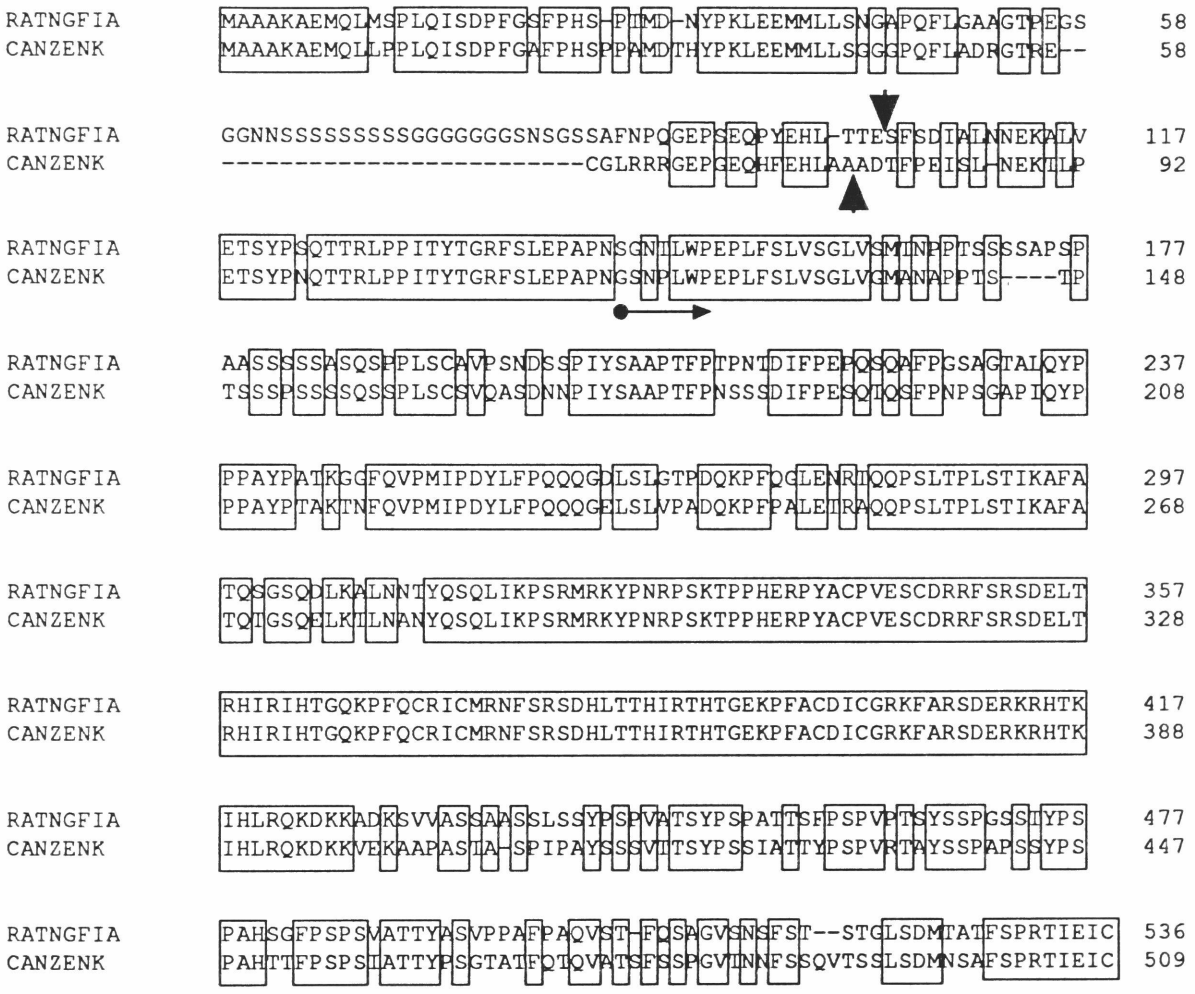
RATNGFIA MAAAKAEMQLMSPLQISDPFGSFPHS-PIMD-NYPKLEEMMLLSNGAPQFLGAAGTPEGS 58
CANZENK MAAAKAEMQLLPPLQISDPFGAFPHSPPAMDTHYPKLEEMMLLSGGGPQFLADRGTRE-- 58
RATNGFIA GGNNSSSSSSSSSGGGGGGGSNSGSSAFNPQGEPSEQPYEHL-TTESFSDIALNNEKALV 117
CANZENK ----------CGLRRRGEPGEQHFEHLAAADTFPEISL-NEKTLP 92
RATNGFIA ETSYPSQTTRLPPITYTGRFSLEPAPNSGNILWPEPLFSLVSGLVSMTNPPTSSSSAPSP 177
CANZENK ETSYPNQTTRLPPITYTGRFSLEPAPNGSNPLWPEPLFSLVSGLVGMANAPPTS----TP 148
RATNGFIA AASSSSSASQSPPLSCAVPSNDSSPIYSAAPTFPTPNTDIFPEPQSQAFPGSAGTALQYP 237
CANZENK TSSSPSSSSQSSPLSCSVQASDNNPIYSAAPTFPNSSSDIFPESQIQSFPNPSGAPIQYP 208
RATNGFIA PPAYPATKGGFQVPMIPDYLFPQQQGDLSLGTPDQKPFQGLENRIQQPSLTPLSTIKAFA 297
CANZENK PPAYPTAKTNFQVPMIPDYLFPQQQGELSLVPADQKPFPALETRAQQPSLTPLSTIKAFA 268
RATNGFIA TQSGSQDLKALNNTYQSQLIKPSRMRKYPNRPSKTPPHERPYACPVESCDRRFSRSDELT 357
CANZENK TQTGSQELKTLNANYQSQLIKPSRMRKYPNRPSKTPPHERPYACPVESCDRRFSRSDELT 328
RATNGFIA RHIRIHTGQKPFQCRICMRNFSRSDHLTTHIRTHTGEKPFACDICGRKFARSDERKRHTK 417
CANZENK RHIRIHTGQKPFQCRICMRNFSRSDHLTTHIRTHTGEKPFACDICGRKFARSDERKRHTK 388
RATNGFIA IHLRQKDKKADKSVVASSAASSLSSYPSPVATSYPSPATTSFPSPVPTSYSSPGSSIYPS 477
CANZENK IHLRQKDKKVEKAAPASTA-SPIPAYSSSVTTSYPSSIATTYPSPVRTAYSSPAPSSYPS 447
RATNGFIA PAHSGFPSPSMATTYASVPPAFPAQVST-FQSAGVSNSFST--STGLSDMTATFSPRTIEIC 536
CANZENK PAHTTFPSPSIATTYPSGTATFQTQVATSFSSPGVTNNFSSQVTSSLSDMNSAFSPRTIEIC 509

(the function of this repeat is yet unknown); conservation falls drastically outside these regions. The e-12 clone is not a complete cDNA and begins at amino acid 145 of the rat sequence.

To determine the remainder of the coding sequence, Maria Huecas in the lab identified and sequenced a genomic clone (pge12) which overlaps the 5' end of e-12, but extends to include the first exon and intron (both of which have been significantly conserved), as well as portions of the 5' flanking sequence. The complete predicted canary protein is included in the alignment shown in figure 2.2. One notable difference in the rodent and canary sequences revealed by this alignment is the apparent absence of a site near the NH_2-terminal portion of the predicted peptide, which contains a stretch of nine serine residues followed by seven glycine repeats. The fact that, in rodents, all serines are encoded by the same codon (AGC), and the glycine by GGNs (N is any nucleotide) which may constitute a distinct functional domain when clustered, has led to the suggestion that this region may be functionally defined by the nucleotide sequence rather than the aminoacid sequence; a possible function could then be the binding of a specific protein to the gene or to the mRNA (Milbrandt, 1987). This possible deletion still needs to be confirmed, for example by sequencing other clones independently isolated or by using PCR amplification.

Northern analysis

Northern blot analysis was used to determine both the specificity of single-stranded RNA probes (riboprobes) synthesized from the e-12 cDNA clone and the stringency of conditions to be used for the in

Figure 2.3 - Northern blot containing 30μg of total RNA from canary forebrain (A) and 1μg of poly-A^+ from canary (B) or zebra finch (C) forebrain, hybridized to a ^{32}P-labeled single-stranded antisense RNA probe, and washed in 0.1XSSPE/0.1% SDS at 65°C. The position of 18S and 28S ribosomal RNAs are shown for reference.

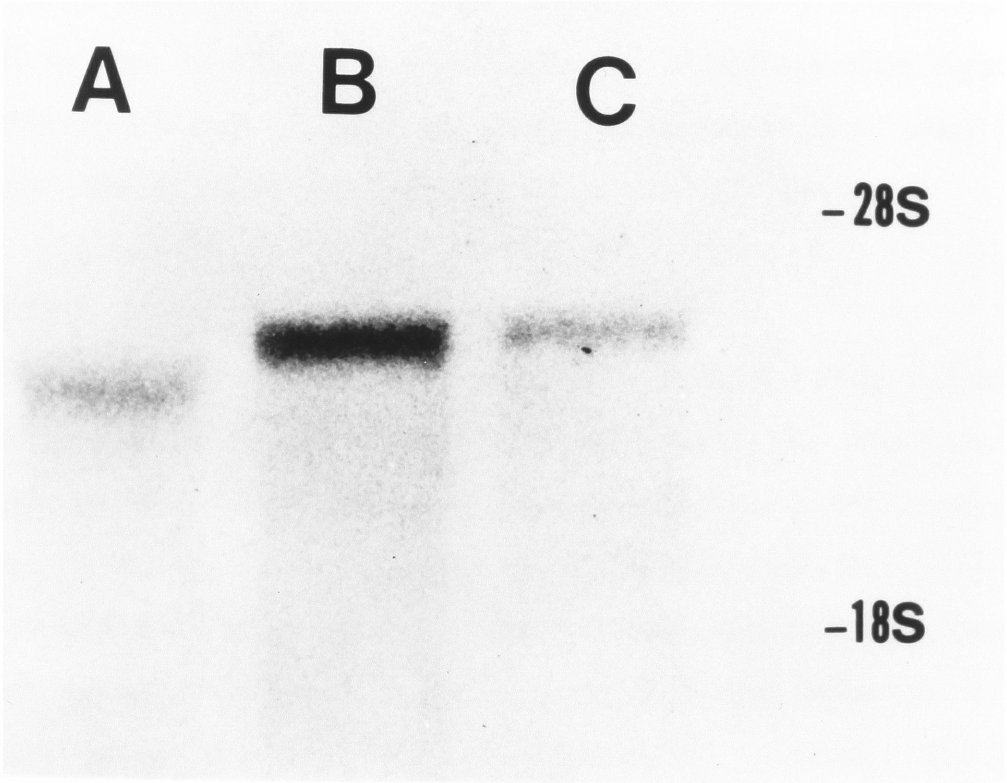
A
B
C
-28S
-18S

situ hybridizations. Under the conditions used for the blot in figure 2.3, (0.1X SSPE at 65°C during the final wash) a single band of approximately 3.5Kb is detected in lanes containing RNA from either canary (figure 2.3B) or zebra finch (figure 2.3C) brains, which shows that this probe can be successfully used in cross-hybridizations and is suitable for analysis of both canary and zebra finch brain material. Further increases in the stringency of the washes, such as elevating the temperature to 68°C or decreasing the salt concentration to 11mM sodium, resulted in a significant loss of hybridization signal in the zebra finch lane but did not affect the signal in the canary lane, whereas less stringent washes resulted in multiple bands.

Initial regulatory studies

ZENK mRNA levels were found to be very low, barely detectable, when in situ hybridization was used to measure its expression in sections of adult canary or zebra finch brains (see later chapters for details). However, since expression levels of this and other IEGs had been shown to depend on appropriate cellular stimulation in rodents, various stimuli were tested for a gene induction response in the songbird brain. The first class of experiments is briefly described here (for the other stimuli, metrazole and auditory stimulation, see chapters 3 and 4 respectively). Kent Nastiuk and David Clayton provided poly-A^+ mRNA from a fragment of dorso-caudal forebrain tissue that included HVC and the surrounding neo- and hyperstriatum from ovariectomized female canaries 1 hour, 6 hours or 7 days following systemic injection with testosterone or cholesterol (control). ^{32}P-labelled cDNA probes were made from

these RNAs and hybridized with dot blots containing cloned cDNAs representing various canary genes including ZENK. No difference was seen in the hybridization signal to ZENK plasmid DNA between testosterone and cholesterol treatments at any time investigated, suggesting that the ZENK gene may not be directly regulated by testosterone.

DISCUSSION

A cDNA clone (e-12) has been identified in the canary brain which is believed to represent the canary homologue of the ZENK gene. This conclusion is based on the following: 1- the sequence similarity with the mouse egr-1 and rat NGFI-A genes initially used in the screening, in particular the conservation of the zinc-fingers and the other repeats (figure 2); 2- the appropriate size of the mRNA identified on the Northern blot; and 3- its inducibility by depolarizing stimuli (see later chapters). Other studies in the lab have provided further support for this view, including the identification of additional upstream sequence (figure 2) and evidence for a single homologous gene as provided by Southern analysis (not shown).

The negative results on ZENK regulation by testosterone should be taken as preliminary. Some problems in the experiment include the following: 1- HVC in ovariectomized females is very small; the dissections included significant amounts of surrounding tissue and it is unclear how well the population of mRNAs expressed within HVC was represented; 2- although the effects of testosterone administration on singing behavior and neuronal morphology in the song control nuclei of ovariectomized females have been well documented and shown to take days to weeks to be expressed (for example, DeVoogd and Nottebohm, 1981), little is known about the time-course of testosterone action on gene expression and the best time to look for a genomic response; 3- systemic injections of testosterone yields only transient elevation of brain testosterone levels (Nastiuk, 1992). These preliminary negative results have been

somewhat extended in Kent Nastiuk's doctoral dissertation, however, where he reported small changes in androgen receptor and c-jun mRNAs but no change in ZENK mRNA following testosterone implants. As shown in subsequent chapters, other experiments have led to the suspicion that the ZENK gene may actually be repressed in brain areas known to bind testosterone.

CHAPTER 3: ZENK INDUCTION BY METRAZOLE

INTRODUCTION

Metrazole (pentylenetetrazole) is a potent GABAergic antagonist which exerts a strong depolarizing action on nervous tissue and has been widely used in studies of IEG regulation in neuronal cells in vivo (Morgan et al., 1987; Morgan and Curran, 1989). In mammals, metrazole administration is followed by generalized depolarization and eventually several recurring seizure episodes; this activity results in widespread IEG induction in the brain (Morgan et al., 1987). Various classes of IEGs have been shown to respond to metrazole with significant increases in mRNA and protein levels, including c-fos and related genes, c-jun and related genes and ZENK (Morgan et al., 1987; Saffen et al., 1988; Sukhatme et al., 1988; Watson and Milbrandt, 1989). Characteristically, the induction is not ubiquitous and is most pronounced in structures thought to represent sites of maintained plasticity during adult life, in particular the neocortex and hippocampus (Saffen et al., 1988).

The songbird constitutes a powerful model for the study of neuronal and behavioral plasticity (see chapter 1) and may be particularly useful for assessing the functional significance of specific molecular processes in the nervous system. In this chapter, the anatomical distribution of ZENK mRNA in the songbird brain after metrazole-induced depolarization is described. The specific aim was to address the following points: 1) Is ZENK subjected to the same regulatory control in the songbird brain as in mammals, i.e.,

induction by depolarizing stimulation? 2) In songbirds, do sites of ZENK induction correlate with sites where phenomena related to neural plasticity are known to occur? 3) Do ZENK induction patterns reveal any important aspects of the overall organization of the song control circuit and the songbird brain? 4) More generally, do the respective patterns of induction in songbirds and mammals reflect presumed evolutionary relationships in brain structure, and thus provide insight into the possible function of IEG induction?

METHODS

Animals

Male songbirds of two different species, zebra finches and canaries, were obtained from Canary Bird Farms (Englishtown, NJ) and from closed colonies maintained at the Rockefeller University Field Research Center (Millbrook, NY). A total of 40 birds, including adult and juvenile (32-day old) male zebra finches, adult female zebra finches, and adult male canaries in the Spring (May) or in the Fall (September/October/November) was examined.

Metrazole administration

Birds were injected intraperitonially or intramuscularly (pectoral muscle) with either metrazole or saline. The dose was adjusted to the minimum required to induce moderate seizure activity without death within the first hour. For canaries, this was in the 40-50mg/kg range; for zebra finches, the dose had to be increased to 60-70mg/kg for minimal seizure activity to be observed. Injections were made from a freshly prepared stock at the concentration of 20mg/ml. Uninjected controls were also compared to observe the effect of handling. Metrazole administration resulted in frequent repetitive seizures that usually began within 2 minutes after the injection and lasted for a few minutes, followed by prolonged quiet periods and occasional recurrent seizure episodes, either spontaneous or triggered by noise or stress; the behavioral response varied widely among birds, even using the same doses. In some cases, various anesthetic agents (chloropent, ketamine, xylazine, the last two variously combined)

were injected immediately before metrazole; in these birds, no convulsive activity was observed.

Preparation of slides for mounting sections

Pre-cleaned slides were washed in 1M HCl for 20 minutes, rinsed with distilled water, immersed in 100% ethanol for 20 minutes and air-dried. Slides were then coated with 3-aminopropyl triethoxysilane (TESPA) to enhance tissue adhesion, by following one of two protocols: 1) slides were heated overnight at 70°C in 1% (v/v) TESPA (pH 3.45 with HCl), washed for two hours in distilled water, baked overnight at 100°C, activated for 30 seconds with 10% glutaraldehyde in PBS (pH 7.0), rinsed with distilled water, dipped for 15 seconds in 0.1M sodium metaperiodate, rinsed with PBS (pH 7.0) and air-dried; or 2) slides were dipped for 10 seconds in 2% TESPA in dry acetone, followed by two brief rinses in acetone and one rinse in distilled water, and air-dried.

Protocol 2 was preferred for its simplicity and because slides can be stored for at least up to six months after coating. However, sections would occasionally fall off the slides during very stringent washes (11mM salt, 65°C); slides prepared according to protocol 1 can only be stored for shorter periods after the activation step with glutaraldehyde and periodate, but slides are more resistant to high stringency. Protocol 1 was used initially for all slides and later only for sections from canary brains; protocol 2 was used for most sections of zebra finch brains.

Tissue preparation

Animals were sacrificed at 30-45 minutes after the injection by decapitation. The brains were quickly dissected from the skulls,

frozen in Tissue-tek and stored at -70°C before sectioning. 10µm brain sections were cut in a cryostat after allowing the tissue block equilibrate to -18°C, thaw-mounted onto silanated slides, fixed in 4% paraformaldehyde in 0.1M phosphate buffer (pH 7.4) for 5 minutes, rinsed twice (a few dips) in 0.025M PBS (containing 0.14M NaCl and 5mM KCl, pH 7.2), dehydrated by dipping in 70%, 95% and 100% ethanol for 2 minutes each, air dried and stored dessicated at -70°C.

Preparation of riboprobes

Riboprobes for in situ hybridization were prepared and stored as described in chapter 2, with the following modifications: 1) ^{35}S-UTP was used, instead of ^{32}P-UTP; 2) riboprobes were stored at -20°C after addition of 1µl of 1M DTT. Probes were prepared from plasmids containing the canary homologues of ZENK, c-jun, n-myc, c-myc, GAP-43 and pCF-2.

In situ hybridization

Brain section were hybridized with ^{35}S-labeled riboprobes according to the protocol of Clayton et al., 1988, with some slight modifications. Slides were taken out of the freezer, dipped for 10 minutes in freshly prepared acetylation solution (containing 2.7ml of triethanolamine, 0.5ml of acetic anhydride and distilled water to 200ml), rinsed three times in 2XSSPE, dehydrated by dipping successively in 70%, 95% and 100% ethanol for 2 minutes each and air-dried. Riboprobes were diluted in hybridization solution containing 50% formamide, 2XSSPE, 2µg/µl tRNA, 2µg/µl BSA, 400 to 1000ng/µl polyA and 100mM DTT; 16 µl of this solution (0.25 to 0.5×10^{-6}dpm) was added to each section which was then covered with a 22x22mm coverslip. Slides were incubated under oil for 3

hours at 65°C, rinsed 3 times with chloroform and coverslips were removed in 2XSSPE containing 0.1% ß-mercaptoethanol (ß-ME). Sections were then washed for 1 hour at room temperature in fresh 2XSSPE/0.1% ß-ME, followed by a one-hour wash at 65°C in 50% formamide/2XSSPE/0.1% ß-ME and two 30-minute washes at 65°C in 0.1XSSPE (lower stringency, used for zebra finches and song sparrows) or in 2mM sodium pyrophosphate/1mM EDTA/1mM Na_2HPO_4 (higher stringency, used for canaries). Slides were again dehydrated by dipping successively in 70%, 95% and 100% ethanol for 2 minutes each, air-dried and exposed to X-ray films for 1-4 weeks, or dipped in NTB2 emulsion (KODAK) and exposed for 3-8 weeks. Emulsion-dipped slides were then developed, counterstained with cresyl-violet and coverslipped with Permount.

An alternative protocol which included RNase treatment was used in some cases to eliminate background problems. The procedure was essentially the same as above, except for the following modifications: 1) hybridization was performed at 50°C; 2) slides were equilibrated with 2XSSC (several washes) after the first wash at 65°C in 50% formamide/2XSSPE/0.1% ß-ME, incubated for 30 minutes at room temperature or at 37°C in a solution containing ribonuclease(RNase)-A (10µg/ml) and RNase T_1 (50U/ml) in 2XSSC and rinsed several times with 2XSSC; slides were then dehydrated and air-dried as above.

RESULTS

Autoradiography

Basal ZENK mRNA levels are very low throughout the brain of control animals; the signal is hardly detectable in autoradiograms at the exposures used and no apparent differences are seen between animals injected with saline (figure 3.1A) and uninjected controls (not shown). A dramatic increase in ZENK expression levels occurs in the brains of birds treated with metrazole (figures 3.1 and 3.2). ZENK induction occurs in all subdivisions of the telencephalon and is generally uniform throughout each subdivision (the exceptions are noted below); the patterns obtained with canaries (not shown) and zebra finches are remarkably similar.

The anatomical distribution of ZENK mRNA after metrazole was defined in a series of parasagittal brain sections (figure 3.2). The highest signal after metrazole is seen within the paleostriatal complex, in particular the lobus paraolfactorius (LPO, figures 3.2A and B), area X (figures 3.2A and B and 3.4A), and the paleostriatum augmentatum (PA, figure 3.2C). Area X is encircled by a thin rim of low hybridization signal, as can be seen in the shorter film exposures (figure 3.4A) and the density within X tends to be slightly higher than the surrounding paleostriatal tissue, possibly the result of a higher cellular density (figure 3.2B). High levels of induction are also seen in all subdivisions of the hyperstriatum (H, figure 3.2), including the hyperstriatum accessorium (HA), the hyperstriatum dorsale (HD) and the hyperstriatum ventrale (HV); ZENK levels within HV and HD are higher than within HA and comparable with paleostriatal levels

FIGURE 3.1 - *In situ* hybridization autoradiograms demonstrating ZENK induction after metrazole. Parasagittal sections of zebra finch brains at comparable levels (2.2mm lateral to midline) were hybridized with a riboprobe for ZENK: (A) control bird injected with saline; (B) bird treated with metrazole (arrow points to the High Vocal Center, HVC). (C) A section slightly more medial than (B) was hybridized with pCF-2. Orientation: dorsal is up and anterior is to the right. Bar size: 2mm.

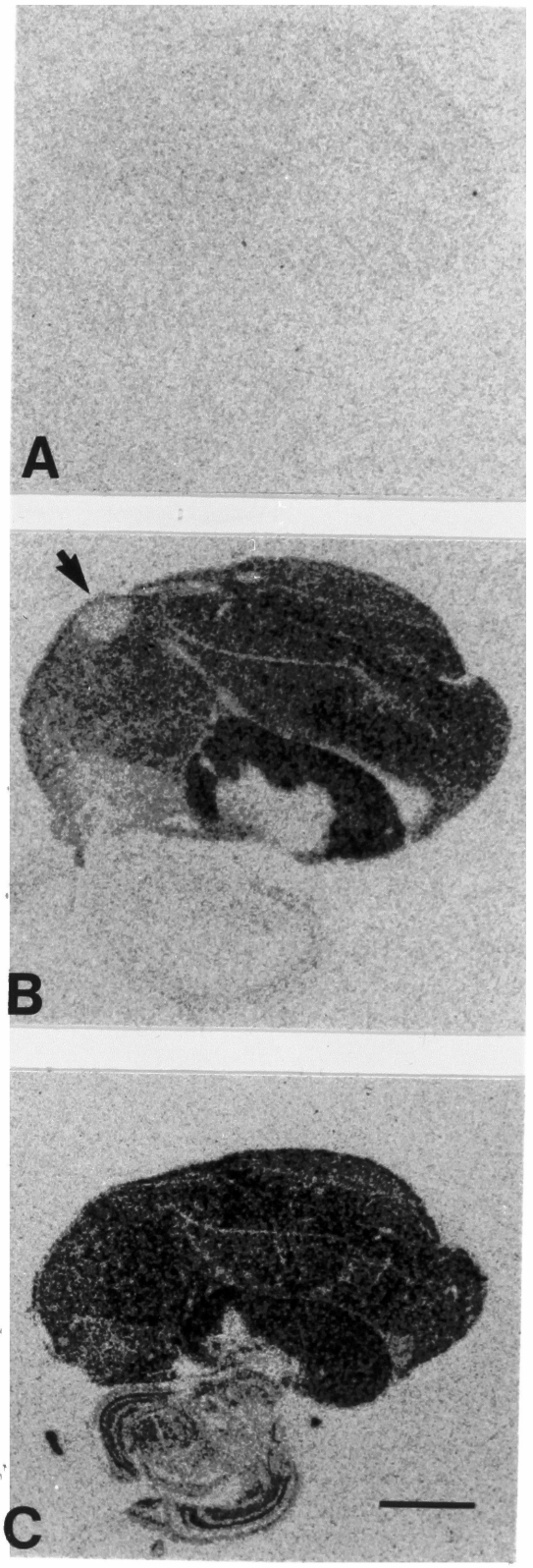
A
B
C

FIGURE 3.2 - Anatomical distribution of ZENK mRNA levels in the zebra finch brain after metrazole. Left column: in situ hybridization autoradiograms of sections hybridized with ZENK riboprobe: A to E represent a series of parasagittal sections, from 0.5mm (A) to 3.5mm (E) lateral to the midline, with intervals of approximately 0.75mm. Right column: diagrams represent camera lucida drawings of the sections whose autoradiograms are shown on the left column. The areas enclosed by the hatched rectangles in A, C and E are shown in detail in figure 3.3. Abbreviations: a, archistriatum; b, brain stem; cb, cerebellum; e, ectostriatum; h, hyperstriatum; ha, hyperstriatum accessorium; hd, hyperstriatum dorsale; hp, hippocampus and parahippocampal area; hv, hyperstriatum ventrale; hvc, high vocal center; L2a, subfield L2a of Field L; lpo, lobus paraolfactorius; m, nucleus magnocellularis lateralis of the anterior neostriatum; n, neostriatum; nb, nucleus basalis; nc, neostriatum caudale; om, tractus occipitomesencephalicus; p, paleostriatum; pa, paleostriatum augmentatum; pp, paleostriatum primitivum; ra, nucleus robustus archistriatalis; t, tectum; x, area X. Orientation: dorsal is up and anterior is to the left. Bar size: 2mm.

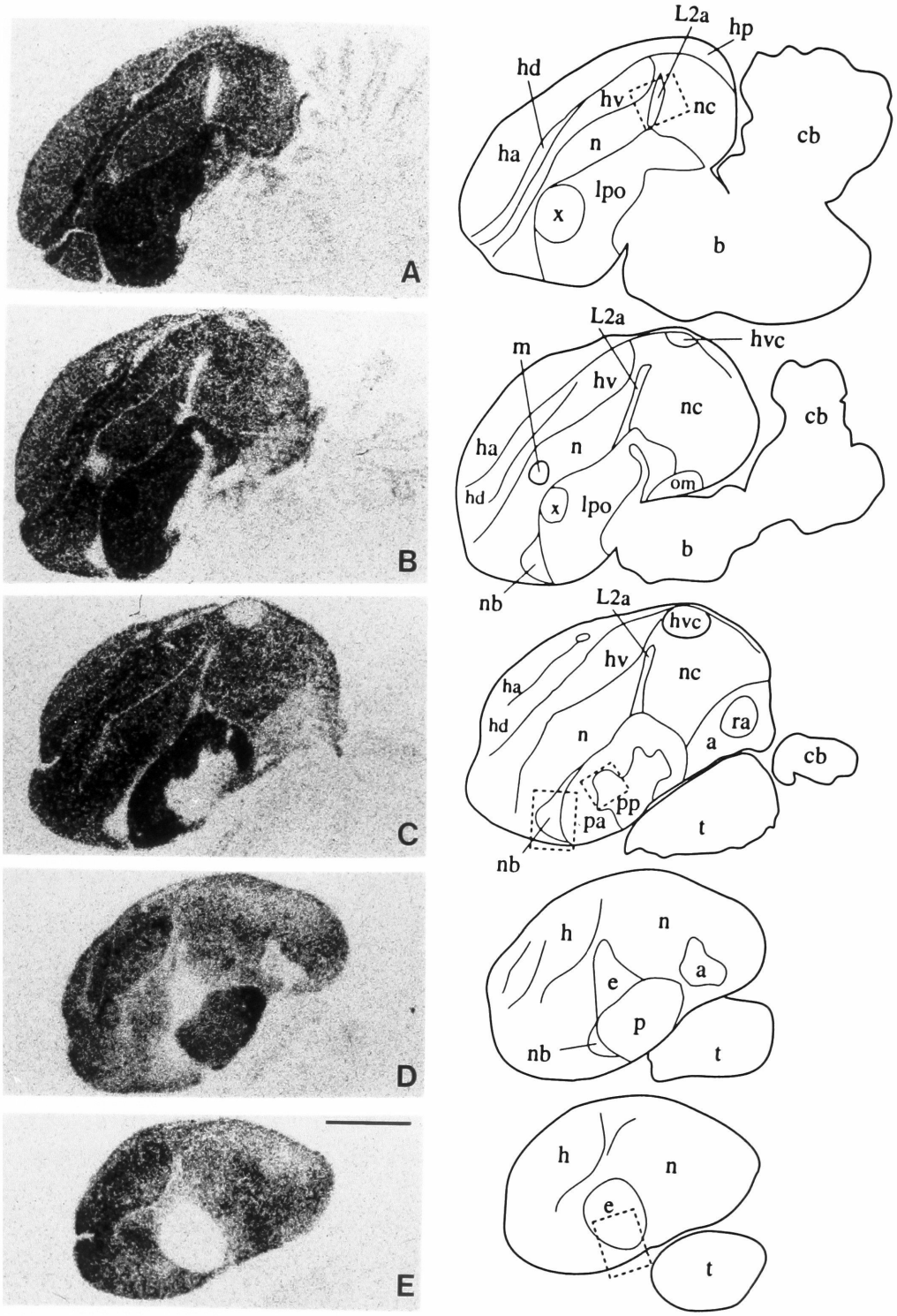
A
L2a
hp
hd
hv
nc
cb
ha
n
lpo
x
b
B
L2a
hvc
m
hv
nc
cb
ha
n
hd
om
x
lpo
b
nb
C
L2a
hvc
hv
nc
ha
hd
n
ra
a
cb
pp
pa
t
nb
D
h
n
a
e
p
nb
t
E
h
n
e
t

(figures 3.2A and 3.4A). ZENK levels comparable with those within HA are seen in the neostriatum (N), hippocampus (Hp) and parahippocampal area (transition zone between Hp and HA, figure 3.2); a much lower but still significant induction is seen in the archistriatum (A, figure 3.2C).

In contrast, ZENK mRNA induction is distinctly lower (by comparison with the immediately adjacent tissue) or absent in some discrete areas or nuclei of the forebrain. These include: 1- a subdivision of the paleostriatal complex, the paleostriatum primitivum (PP, figure 3.2C); 2- the ectostriatum (E, figure 3.2D and E); 3- nucleus basalis (B, figure 3.2B and C); 4- subfield "L2a", a subdivision of the auditory thalamo-recipient zone, Field L (figure 3.2A, B and C); 5- a small round area in the caudal hyperstriatum, at the tip of the lamina separating HA and HD (figure 3.2C), which has not been previously described as a distinct area or nucleus; 6- two nuclei within the neostriatum, the High Vocal Center (HVC, figures 3.1B, arrow, and 3.2C) and the lateral nucleus magnocellularis of the anterior neostriatum (lMAN, figures 3.2B and 3.4A, note the sharp contrast with area X); 7- the archistriatal nucleus robustus archistriatalis (RA, figure 3.2C). ZENK mRNA signal is also very low in the ventricular zone (for instance, in figure 3.5A, a thin layer of tissue separating HVC from overlying tissue) and in the laminae which separate the various telencephalic subdivisions and that are basically composed of neuronal fibers and glial elements (figure 3.2). Similarly, ZENK signal is remarkably low in the thalamus and brainstem (figure 3.2), although some signal is occasionally seen in the optic tectum and the cerebellar granular layer.

Microscopy

ZENK induction at the cellular level was investigated in emulsion-dipped slides. The exposure time was optimized to avoid saturation of brain sections from metrazole-treated animals with grains. With the exposures used (typically three times as long as for autoradiograms), the vast majority of cells in control brains are negative for ZENK mRNA; when longer exposure times are used, some cells can be seen within N and H that express ZENK at high levels (not shown, but see chapter 4). After metrazole, most or all cells in areas where ZENK is uniformily high in the film autoradiograms show high levels of ZENK expression by emulsion autoradiography, as represented by the white or positive areas in figures 3.3A, D, F and H, or the grain-labeled cells in figure 3.6C.

In contrast, most or all cells are negative in areas showing low or no ZENK induction in autoradiograms. The dashed rectangular areas enclosing L2a, NB, PP and E in the diagrams of figures 3.2A, C and E are represented in detail in figure 3.3. L2a (figure 3.3A), NB (figure 3.3D) and E (figure 3.3F) are all characterized by the absence of ZENK signal (with the exception of very few cells in NB, figure 3.3D, grain density in these areas is comparable to glass background). The respective bright-field images (figures 3.3B, E and G) show that these areas are characterized by numerous small and darkly staining cells that tend to be closely packed, with a resulting high cellular density. L2a is shown in further detail in figure 3.3C; the small and darkly staining cells, typically organized in short rows or columns aligned with the major axis of L2a (Fortune and Margoliash, 1992), which in this figure runs from the lower left to the upper right, are clearly

FIGURE 3.3 - Detailed view of areas showing low levels of ZENK expression after metrazole. Brain sections were hybridized with ZENK riboprobe, dipped in autoradiographic emulsion and stained with cresyl violet. (A), (D), (F) and (H) represent detailed dark-field views of Field L2a, Nucleus Basalis, Ectostriatum and PP respectively and correspond to the rectangles in figures 2A, C (larger rectangle), E and C (smaller rectangle); (B), (E), (G) and (I) represent their corresponding bright-field images. (C) is a high power view of the area enclosed by a rectangle in (B) and (J) a high power view of the area enclosed by a rectangle in (I). Orientation: dorsal is up and anterior is to the left. Bar sizes: (C) and (J), 30μm; (F) and all other panels, 100μm.

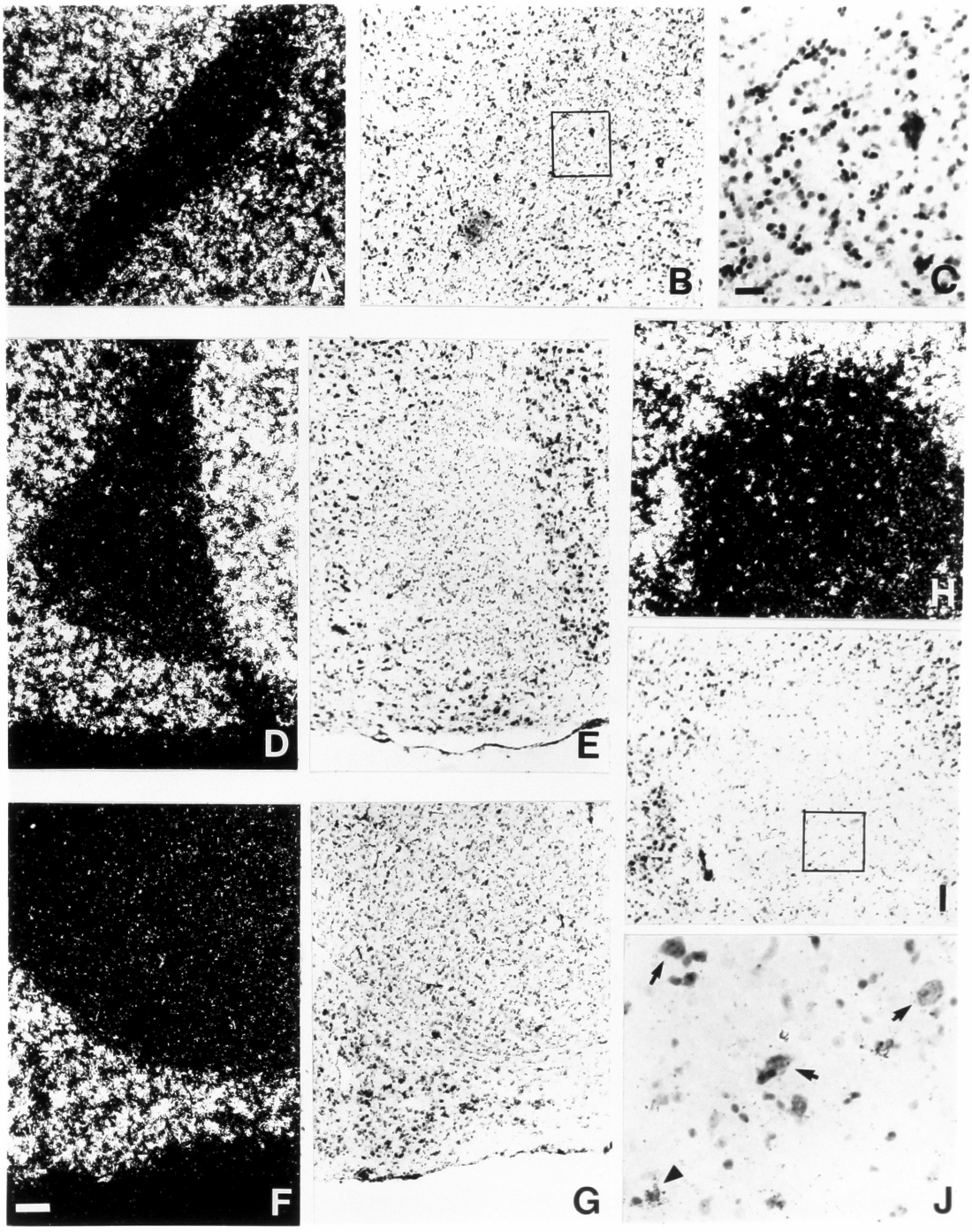
A
B
C
D
E
H
I
F
G
J

negative for ZENK. A number of ZENK positive cells are seen in PP (figure 3.3H), even though the cellular density is extremely low (figure 3.3I). A high power view (figure 3.3J) reveals that the typically large PP neurons are negative (arrows), whereas positive cells are represented by a population of small-sized cells (arrowhead).

Analysis of song control areas lMAN (figure 3.4), HVC (figure 3.5), and RA shows that these nuclei have a very low density of ZENK positive cells. ZENK induction within lMAN and RA occurs in a few small cells and spares the more numerous large cells (not shown). ZENK induction within HVC also occurs in a subpopulation (figure 3.5A) composed of small cells which are present either in isolation or in association with other cells (figure 3.6A and B). Large cells occurring either singly or in association with other cells are typically negative (figure 3.6B). In some cases, neuronal clusters are seen with a central larger cell surrounded by smaller cells; the central cells are negative and the small cells in the periphery of the clusters are positive (two examples are shown in figures 3.7A and B). The large negative cells have a clear neuronal morphology, including a pale-staining nucleus, clear nucleolus and abundant Nissl substance; smaller cells cannot be readily separated from glial cells with just cresyl-staining, but their presence in the cell clusters around the larger cells strongly suggests that they could represent a specific population of small neuronal cells (see discussion). The smaller and most darkly staining cells represent most probably glial elements and blood cells (animals were not perfused) and are usually negative. The cellular pattern within HVC contrasts sharply with the pattern

FIGURE 3.4 - Comparison between Area X (X) and the lateral nucleus Magnocellularis of the Anterior Neostriatum (MAN) in a zebra finch treated with metrazole. (A) In situ autoradiogram of a parasagittal brain section containing X and lateral MAN and hybridized with ZENK riboprobe. (B) Dark-field image of a cresyl violet-stained brain section at a level that includes lateral MAN and surrounding tissues. (C) bright field image of the same area as shown in (B), slightly enlarged. Orientation: dorsal is up and anterior is to the right.. Bar sizes: (B), 500μm; (C), 315μm.

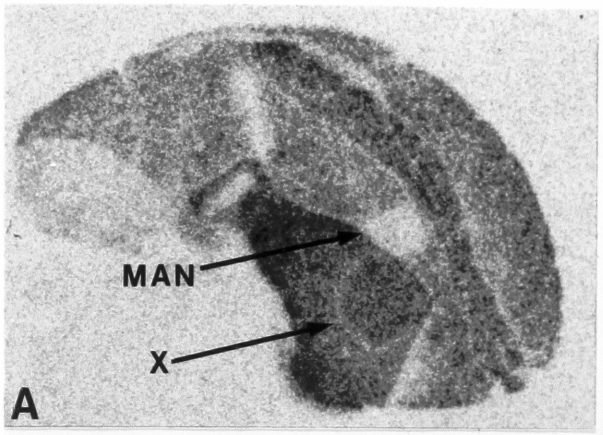
MAN
X
A

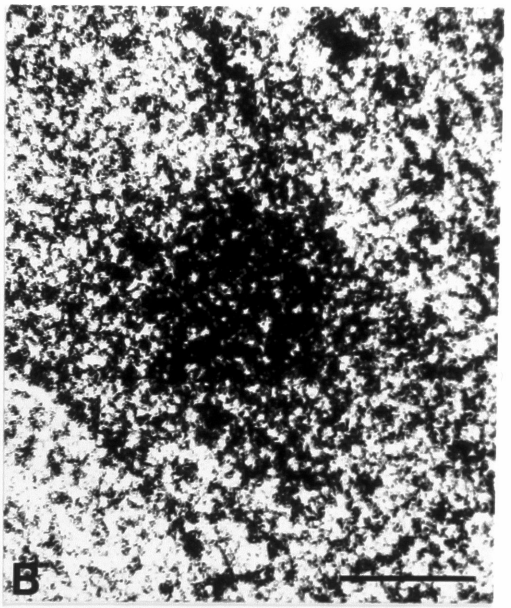
B

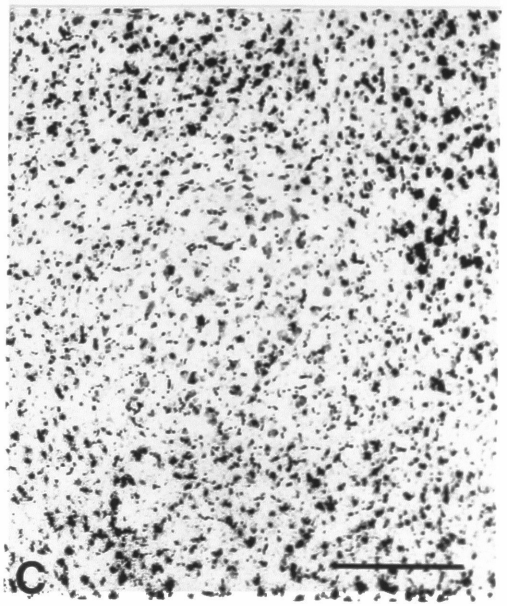
C

FIGURE 3.5 - Detailed view of the High Vocal Center (HVC) and surrounding tissues after metrazole in a zebra finch. Brain sections were treated as described in figure 3.3. (A) and (C) Dark-field images of adjacent brain sections hybridized with ZENK and pCF-2 riboprobes respectively. (B) Bright field image of the same section as shown in (A). Orientation: dorsal is up and anterior is to the left. Bar size: 500μm.

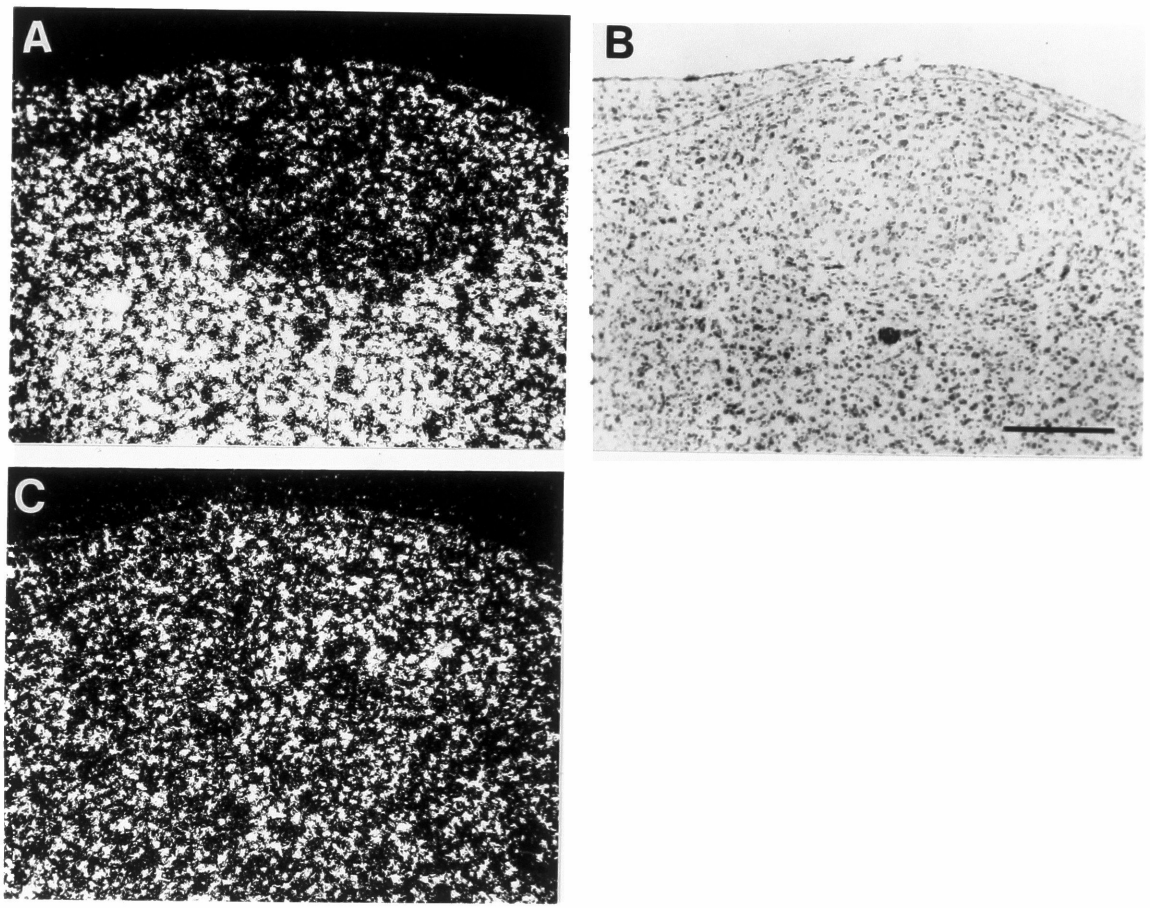
A
B
C

FIGURE 3.6 - High power view of cells within the High Vocal Center (HVC) and surrounding Neostriatum (N) after metrazole in a zebra finch. Brain sections were treated as described in figure 3.3. (A) Cells within HVC of a bird injected with saline; (B) cells within HVC of a bird injected with metrazole; (C) cells in N immediately surrounding HVC, from the same section as in (B). Bar size: 20μm.

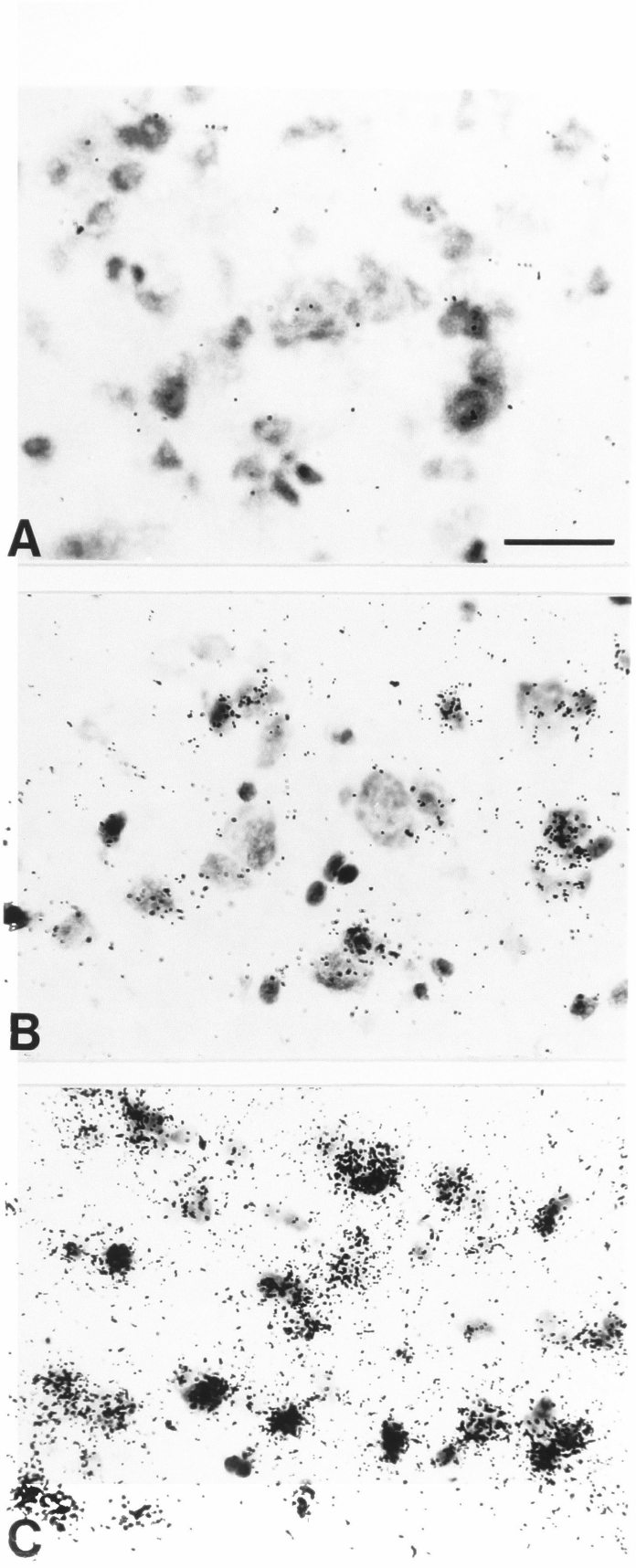
A
B
C

FIGURE 3.7 - High power view of neuronal clusters within the High Vocal Center (HVC) after metrazole in a zebra finch. Brain sections were treated as described in figure 3.3. (A) and (B) Clusters in sections hybridized with ZENK riboprobe, antisense strand; positive cells occur at the periphery of clusters; (C) section hybridized with ZENK riboprobe, sense strand. Bar size, 10μm.

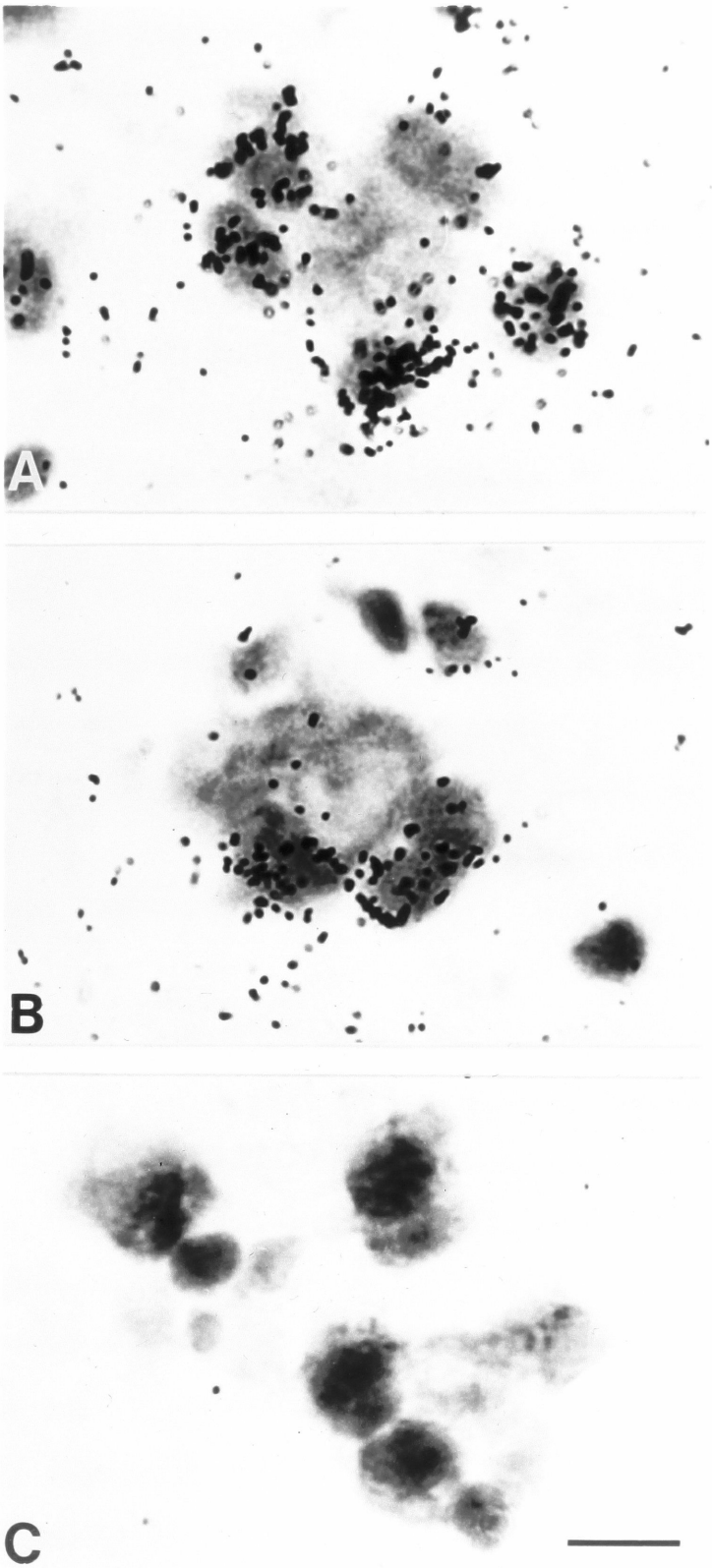
A
B
C

seen in the surrounding neostriatum, where all or the vast majority of cells express high levels of ZENK (figure 3.6C).

As an additional control for the possibility that regional differences in ZENK signal are the indirect result of variations in regional RNA content, the expression patterns of a gene not induced by metrazole, pCF-2 (Clayton et al., 1988), were analysed at both autoradiographic (figure 3.1C) and emulsion (figure 3.5C) levels. In the forebrain, pCF-2 expression is also highest in certain parts of the paleostriatum (LPO and PA) and lowest in PP. Otherwise, pCF-2 expression within the telencephalon is mostly uniform throughout the telencephalon and does not reveal local differences between HVC, RA and MAN and surrounding tissues (figures 3.1C and 3.5C for HVC; RA and MAN not shown). When sections are hybridized with riboprobes derived from the sense strand of ZENK, no signal above glass background is detected in autoradiograms (not shown) or in emulsion-coated sections (figure 3.7C).

Developmental, seasonal and sex comparisons

The effect of developmental age (in finches), season (in canaries) and sex on ZENK inducibility after metrazole was also investigated. No differences in ZENK induction patterns within the song control circuit were seen when adult finches were compared with 32-day old juveniles or when canaries in the Spring were compared with canaries in the Fall. The HVC of female finches is hardly detectable or unambiguously identified, which renders sex comparisons especially difficult, particularly in 10μm frozen sections, and results were not conclusive.

Other genes

Expression of other inducible genes such as c-jun, n-myc and c-myc and GAP-43, for which a canary probe is available, was analysed after metrazole administration. Of these, a significant increase was detected only in c-jun levels whereas the other genes did not seem to respond (data not shown). Basal expression of c-jun is higher than that of ZENK and c-jun induction by metrazole significantly lower than ZENK induction. The anatomical distribution of c-jun after metrazole is remarkably similar to ZENK, including a widespread increase throughout most of the forebrain and low levels within HVC, RA and MAN. However, one major difference was seen in another song control nucleus: c-jun levels in area X are much lower than ZENK and a sharp contrast is observed when adjacent sections are hybridized to either ZENK or c-jun. Even though the functional significance of this finding is not clear, it indicates that these two genes, representing different classes of transcriptional activators, can be differentially expressed in some parts of the song circuit.

DISCUSSION

Metrazole, a potent GABAergic antagonist, exerts a strong depolarizing action on nervous tissue and has been used to demonstrate IEG induction in neuronal cells in vivo (Morgan et al., 1987; Saffen et al., 1988; Sukhatme et al., 1988). The results presented here demonstrate that ZENK is also rapidly induced by metrazole in the songbird brain. ZENK induction occurs in vast areas of the telencephalon, including all of its main subdivisions, while lower brain structures are non-responsive. ZENK expression seems predominantly neuronal, although glial expression cannot be completely excluded.

Analysis of the anatomical distribution of ZENK mRNA after metrazole reveals that ZENK induction is not uniform throughout the telencephalon and that there are some dramatic regional differences. Some aspects of the general autoradiographic patterns on figures 3.1 and 3.2 can be explained by differences in cell density among various brain areas. For instance, the difference in autoradiographic densities between LPO/PA and PP are probably the result of a high cellular density in the former and an extremely low density in the latter (PP is probably the forebrain area with the lowest cellular density; figure 3.3I); the similar distribution of the control pCF-2 RNA (figure 3.1) is consistent with this interpretation. Cell density may also account for differences between LPO/PA and hyperstriatal and neostriatal fields, which together comprise the vast majority of the avian telencephalon, but does not explain the autoradiographic

patterns in other areas where ZENK expression is low or absent (see discussion below).

With a few exceptions (see below) this general induction pattern bears a striking resemblance to the distribution of cells born during adult life in the songbird brain (Alvarez-Buylla and Nottebohm, 1988). Both ZENK induction and the distribution of thymidine-labeled cells are sharply restricted to the telencephalon, and are highest in portions of the paleostriatum and hyperstriatum and lowest in PP and archistriatum. It is not clear what, if any, could be the logical connection between these two phenomena. ZENK is not expressed in proliferating or newly-divided and immature cells, since the ventricular zone and immediately surrounding tissue are negative (not shown). ZENK expression may include but is not restricted to migrating neuronal cells, since these comprise only a very small percentage of cells in the adult brain, whereas ZENK is expressed by the vast majority of cells in most brain areas. It is suggested, instead, that areas of high ZENK expression may represent areas of preferential migration or survival of newly-born cells. Recent reports have demonstrated that the mRNAs for growth-signaling factors like NGF and BDNF (brain-derived neurotrophic factor) are upregulated by seizure in hippocampus and neocortex (Gall and Isakson, 1989; Isakson et al., 1991), areas showing extensive IEG induction in the seizure paradigms (Morgan et al., 1987; Saffen et al., 1988). It is possible that, in birds, such regions could provide an adequate environment for the survival of migrating neurons and their incorporation into functional circuits.

In sharp contrast to this general pattern, very little or no ZENK mRNA induction is seen in some specific brain areas or nuclei. These can be divided into two groups: 1- primary forebrain areas for various sensory modalities: Field "L2a" (auditory), E (visual) and B (somatosensory of portions of the head); 2- forebrain testosterone-concentrating nuclei HVC, RA and lMAN. This aspect of the autoradiographic and dark-field patterns is not easily explained by a cell density or cell size effect. In fact, cellular analysis shows that B, E and Field L2a are characterized by a population of small and closely packed cells, with a high cellular density; ZENK is, nevertheless, absent in most or all cells within these nuclei. The fact that no significant difference is seen in the expression of another marker, pCF-2, when areas with low ZENK signal are compared with surrounding tissue (figures 3.1C and 3.5C), suggests that this effect may be specific to certain genes like ZENK and reflects specific mRNA regulation in different cellular populations.

Cellular analysis also reveals that certain subpopulations within the song control nuclei are specifically negative for ZENK. Within HVC, in particular, ZENK is absent in the larger cells and is present in some of the smaller cells, especially cells in the periphery of neuronal clusters characteristic of HVC. Neuronal tracing studies have demonstrated that Area X-projecting cells are large and tend to occur either in isolation or at the center of HVC clusters; in contrast, RA-projecting cells are smaller and occur at the periphery of these clusters (Kirn and Nottebohm, 1990). We therefore conclude that ZENK induction is absent in X-projecting cells but can occur in RA-

projecting cells. A similar pattern is seen in nuclei lMAN and RA: grains are absent in large cells and present in smaller cells.

Thus the various nuclei and cell types that comprise the song control circuit can differ in their molecular response to depolarization; unravelling the mechanisms of this differential gene regulation could be essential for understanding the physiological organization of the circuit. For example, since ZENK induction is high in Area X but low in HVC, RA and lMAN, it is suggested that testosterone action may result in ZENK repression in its brain targets (Arnold et al., 1976; DeVoogd and Nottebohm, 1981). This could be a direct effect (repression at the ZENK gene promoter) or an indirect one, for instance through repression of a component of the signal transduction machinery that leads to ZENK induction (it is interesting to note that NMDA receptors are also very low in the HVC, RA and lMAN of adults; see Ball and Casto, 1991).

A possible alternative explanation for the induction patterns described is that metrazole administration does not result in significant depolarization in certain brain areas, perhaps due to absence of appropriate receptors. However, no differential distribution of GABA or GABA receptors has yet been demonstrated which could explain the selective protection of discrete brain areas from metrazole action; if that were the case, such areas could still get activated indirectly, from their projection areas. Indeed, the few reports describing distribution of GABAergic immunoreactivity in the avian brain demonstrate that GABAergic nerve terminals and somata are present in all layers of the Field L complex (Müller, 1988) and in various song control nuclei, including HVC, RA and MAN (Zuschratter

et al., 1987; Grisham and Arnold, 1992); in addition, in vitro studies have described a release of GABA from brain slices containing RA after electrical stimulation of the pathway (Sakaguchi et al., 1987). This strongly suggests that GABA receptors are also expressed in these nuclei and that GABAergic transmission may play a role in these areas. The fact that ZENK is induced in Area X and in specific cell subpopulations within HVC, RA and lMAN (possibly cells related to GABAergic transmission?) precludes a general protection of the song control circuit from metrazole-induced depolarization (X is intimately connected with these other nuclei, receiving a direct projection from HVC and indirectly projecting to RA). Furthermore, ZENK inducibility in the songbird brain by presentation of conspecific song has been recently demonstrated (Mello et al., 1992, see chapter 4); in that paradigm, ZENK is markedly induced in discrete areas of the forebrain presumably involved in various aspects of auditory processing and is notably absent in nuclei of the song control circuit and in L2a, although increases in electrophysiological and metabolic activities are known to occur in these areas. Together with results from metrazole administration, this indicates that ZENK induction is not ubiquitous in depolarized areas of the brain, reinforcing the idea that ZENK induction has been uncoupled from depolarization in some specific brain nuclei and cell types.

The fact that ZENK is down-regulated or repressed in certain populations within nuclei of the song control circuit suggested that factors known to affect morphology and function of these nuclei might also influence ZENK inducibility by metrazole. However, no differences were seen in the expression patterns at different ages in

zebra finches or in seasonal comparisons in canaries. This indicates that ZENK repression in these areas may be independent of age or season, but the permanent result of early developmental processes.

The regional differences detected in ZENK mRNA levels may reflect important features of the vertebrate brain organization. As in songbirds, ZENK induction in mammals is most pronounced in the telencephalon, especially in the neocortex and hippocampus, structures thought to represent sites of continued plasticity during adult life. As a consequence of its nuclear rather than laminar organization, the avian telencephalon was long considered the homologue of mammalian basal ganglia and cortical-like structures were thought to be absent (reviewed in Karten and Shimizu, 1989). Recent neuroanatomical evidence, however, has suggested that much of the basic mammalian brain circuitry has been evolutionarily preserved in non-mammals and that structures corresponding to cortical elements may have been physically separated and distributed among the various subdivisions of the avian telencephalon during the course of evolution (Northcutt, 1981; Reiner et al., 1983 and 1984; Karten and Shimizu, 1989). For example, avian thalamo-recipient zones are distinctly separated from the archistriatum, where most sensory and motor descending systems originate; these sensory-recipient zones are still connected, though, through complex pathways involving other telencephalic subdivisions such as H and N, to specific archistriatal zones. This has been clearly demonstrated for the avian ectostriatal visual system and more recently for the auditory system as well (Karten and Shimizu, 1989; further discussed in chapter 6). One possible

consequence of these evolutionary rearrengements is a lesser heterogeneity in the neuronal population composing each avian telencephalic subdivision when compared with portions of the mammalian cortex; this would make the detection of molecular differences between different brain regions or cell types easier. Indeed, three avian telencephalic areas lacking a ZENK induction response to metrazole are primary sensory-recipient areas and are composed of cells with very similar morphology. The other important conclusion is that vast regions of the avian telencephalon where ZENK is induced such as H and N, may correspond, at least in part, to the complex mammalian cortical microcircuitry that connects granular or thalamo-recipient layers to infra-granular layers.

In summary, ZENK is also highly responsive to a strong depolarizing stimulus in songbirds. Brain induction patterns after metrazole may reflect aspects of neural plasticity such as distribution of specific classes of neurotransmitter receptors, synaptic plasticity and distribution of migrating neurons and occurs in structures that may represent an avian homologue of mammalian neocortex. In the next chapter, experiments testing ZENK induction by a more physiological stimulus, birdsong, are described.

CHAPTER 4: ZENK INDUCTION BY SONG

INTRODUCTION

Songbirds hear the song of other individuals of their species and respond by modifying their own vocal and social behavior (Kroodsma, 1976 and 1982; Marler and Peters, 1977; Falls, 1982; Welty, 1988; Godard, 1991). Auditory experience is, for example, an essential component of song learning: young birds learn their songs by imitating the models that they hear. In some seasonal learners, the ability to modify the vocal output according to the auditory experience is also preserved throughout adult life (Nottebohm et al., 1986; Nottebohm and Nottebohm, 1988). In adults, vocal communication through song plays a central role in reproduction and territoriality and presumably requires the formation and storage of auditory associations that involve other sensory modalities as well, such as visual representations of other birds and of the environment.

Birdsong constitutes, thus, a natural and noninvasive stimulus of high behavioral and ecological relevance. The cellular and molecular consequences of exposure to song, though, are still largely unknown, as well as how these responses may ultimately translate into physiological and behavioral changes. In this chapter, a series of experiments is presented that tests whether a genomic regulatory event is involved in the brain's response to a stimulus of this nature. The specific question asked is whether the expression of an IEG like ZENK can be regulated in the brain by birdsong playbacks. Studying induction of IEGs in this paradigm also allows addressing a key

question related to IEG regulation, namely, to what extent is IEG induction part of the physiological brain response to natural stimuli?

It was also reasoned that if a genomic event such as IEG induction can be detected in response to song presentation, it might be possible to use the phenomenon as a mapping tool in the investigation of brain areas activated by song. Mapping brain pathways with IEGs has the advantage of allowing a relatively easy survey of very extensive brain areas in a single experiment (potentially the whole brain of a single animal), which is virtually impossible with electrophysiological techniques. It also offers a higher resolution than markers of metabolic activity such as 2-DG or cytochrome oxidase, since with in situ hybridization one can determine individual cells which are activated by looking at the accumulation of mRNA in the cell body and proximal processes around the nuclei (Nissl substance), as opposed to the intense staining in the neuropil characteristic of metabolic methods.

Compared to areas involved in the motor control of song, brain areas related to perceptual tasks such as analysis and storage of complex auditory patterns are still poorly defined. A primary auditory area of the avian forebrain, Field L, has been described based on the projection from the thalamic auditory relay, nucleus ovoidalis (Karten, 1968; Kelley and Nottebohm, 1979). In songbirds, conspecific song is known to be an effective stimulus for neurons in Field L, and is the preferred stimulus in parts of the song control circuit (Margoliash, 1983 and 1986; Müller and Leppelsack, 1985; Müller and Scheich, 1985; Williams and Nottebohm, 1985). However, the detailed connectivity of auditory areas and the pathways that

convey information from these to song-selective brain areas, such as parts of the song control circuit (Margoliash, 1983 and 1986; Williams and Nottebohm, 1985), remain to be determined (the structure and connections of these areas are further discussed in chapters 5 and 6). Mapping with ZENK could thus provide a direct way to investigate which structures are activated by song and might be related to processing of complex auditory stimuli; it might as well reveal areas which have not yet been detected or studied in detail by electrophysiological or anatomical techniques.

A note of caution should be added, since in some situations no IEG induction is seen in cells known to be activated. The clearest example is the absence of IEG induction in cells of the dorsal root ganglion of the spinal cord or in the nuclei of the posterior column in the medulla after stimulation of the animal's paws (Hunt et al., 1987); this suggests that some classes of cells may not express IEGs, or at least the genes which have so far been isolated and for which probes are currently available. Other experiments suggests that certain brain structures only show IEG induction under certain functional states, as seems to occur in the suprachiasmatic nucleus (see chapter 2). Possible functional implications of this phenomenon will be discussed later, but it is important now to observe that whereas the detection of induction is a good indication of depolarization and, thus, cellular activation, a negative finding (no induction) does not necessarily indicate absence of depolarization, but could mean that depolarization and gene induction have been uncoupled in that particular cell type.

METHODS

Animals

155 songbirds of three different species, zebra finches (Taeniopygia guttata), canaries (Serinus canaria) and song sparrows (Melospiza melodia) were used: 110 adult male and 8 adult female finches, 8 juvenile male zebra finches, 25 adult male canaries and 4 adult male song sparrows. Adult male birds used for the various comparisons (specificity, time-course and habituation experiments) were in similar hormonal conditions, as judged by the amount of singing activity, by beak color (zebra finches) and testis size. For seasonal studies, 6 canaries in the Spring (May) and 6 in the Fall (October) were used; blood T levels and testis size were assessed to evaluate hormonal status. 3 breeding pairs of zebra finches were kept in isolation inside acoustic isolation chambers according to the following protocol: 1) breeding pairs were placed in the isolation chambers and checked frequently for eggs in the nesting sites (these pairs had been previously acclimatized to the chambers); 2) upon hatching, the male was withdrawn and individual hatchlings marked; 3) juveniles were separated from female and siblings on day 28 and placed in isolation in separate chambers until playbacks were performed. Adult male song sparrows were captured in the field, in collaboration with Dr. Hubert Schwabl, at the Field Research Center (see section 4.8 for details).

Song exposure

Each bird was typically placed in an acoustically and visually neutral environment (either plexiglass boxes or sound isolation

chambers) and kept isolated from other birds for at least 24 hours; it was then exposed to one of various tapes containing a recorded sound stimulus: either conspecific birdsong, heterospecific song, a non-song auditory stimulus or no auditory stimulus. The song stimuli lasted between 15 and 30 seconds (see below) and were presented every minute during the stimulation period (the specific content of the song tapes is presented in detail in the results section). The non-song auditory stimulus consisted of a tape containing either white noise (generated from SoundEdit software) or tone bursts at frequencies from 1-5.5kHz, similar to the frequency range of natural birdsong. Tone duration varied from 50-400msec and tones were presented in a random sequence either singly or in groups of 4 ascending or descending frequencies, separated by intervals of 5 seconds. In all cases the speakers were placed at 35cm from the center of a 47cm x 26cm x 23cm cage and the average sound intensity adjusted to 70dB at the center of the cage. A microphone was placed near the cage and the stimulus presentation together with the bird's vocal response were recorded. The stimulus presentation was always performed between noon and 3:00pm, unless otherwise indicated.

Tissue preparation and *in situ* hybridization.

After the stimulus presentation, the birds were sacrificed by decapitation. Processing of brain tissues and *in situ* hybridization were performed as described in chapter 3 (stringency conditions for song sparrow brain sections were the same as for zebra finches). Riboprobes were prepared from plasmids containing cDNA inserts of the canary homologues of ZENK, c-jun, n-myc, c-myc, GAP-43 and

pCF-2. Probes were routinely prepared in both orientations and control sections were hybridized to riboprobes derived from the sense strand of the cDNAs to allow for determination of hybridization background. Hybridized brain sections were exposed to X-ray films for 2-4 weeks, or dipped in NTB2 emulsion (KODAK) and exposed for 6-8 weeks. To minimize variability, all sections in each experiment that was quantified were hybridized and exposed simultaneously.

Image analysis and densitometry

Autoradiograms of canary and zebra finch brain sections hybridized to ZENK RNA probes were analysed using either an Eyecom II image processing system or a MacIntosh based system and Image software (NIH). Before measurements, a calibration curve was obtained using optical density standards and measurements were done within the linear range. For all birds in the experiments described in sections 4.2 to 4.5 and 4.7, the average optical density over the medial caudal neostriatum (NCM) was determined in two adjacent sections taken in a parasagittal plane 200-300μm from the midline (for example, the dark areas in figure 4.16), excluding the central area of low hybridization signal that corresponds to a portion of Field L (figure 4), whenever it was present in the section analysed. To control for variations in background, hybridization efficiency or section thickness, the initial density values obtained with ZENK for each bird (experimentals and controls) were divided by the values obtained from the next two adjacent sections hybridized with pCF-2 (a forebrain enriched gene of moderate abundance - see Clayton et al., 1988 - which was found not to change significantly in response to stimulation either with song or metrazole) or by the values obtained

from measurements over the hippocampal and parahippocampal areas in the same sections (ZENK levels were found not to differ among the various groups in these areas). All resulting NCM densities were then divided by the mean NCM signal obtained in unstimulated control birds to create a normalized scale (as a result of this normalization, mean unstimulated=1 on this scale).

RESULTS AND DISCUSSION

4.1 - ANATOMICAL ANALYSIS

A - General pattern

Substantial increases in ZENK mRNA levels occurred in the brain of all birds that were exposed to song compared to various control groups. The general anatomical distribution of ZENK mRNA signal was studied in series of parasagittal (figure 4.2) and coronal brain sections (figure 4.3), at the levels indicated in the upper and lower diagrams of figure 4.1 respectively. As can be seen in figures 4.2 and 4.3, song presentation results in marked ZENK induction in localized areas of the forebrain.

The parasagittal series (figure 4.2) demonstrates that the most marked induction occurs in the caudal forebrain. This effect is most pronounced in the more medial sections (figure 4.2A), where a homogeneously high signal covers a relatively large area of the caudal telencephalon. This particular area is formed by the caudo-medial neostriatum and hyperstriatum ventrale (see details below) and has an ovoid or drop-like shape, resembling the cut surface of a lobular structure. At more lateral levels, ZENK signal becomes less dense and appears more patchy. Notice that a conspicuous aspect of parasagittal sections is the presence of a central or core region which shows very low ZENK levels and is surrounded by areas of high ZENK induction, as can be seen in most panels of figure 4.2. In the more medial sections, this negative region is stripe-shaped and begins rostro-ventrally at the caudo-dorsal tip of the paleostriatal complex

FIGURE 4.1 - Diagramatic schemes of the songbird brain. Upper panel, dorsal view of the brain; lines represent levels of parasagittal sections (A to G) shown in figure 4.2. Lower panel, diagram of a parasagittal section at the level indicated by line A in the upper panel; lines represent levels of coronal sections (A to H) shown in figure 4.3. Drawings are not to scale.

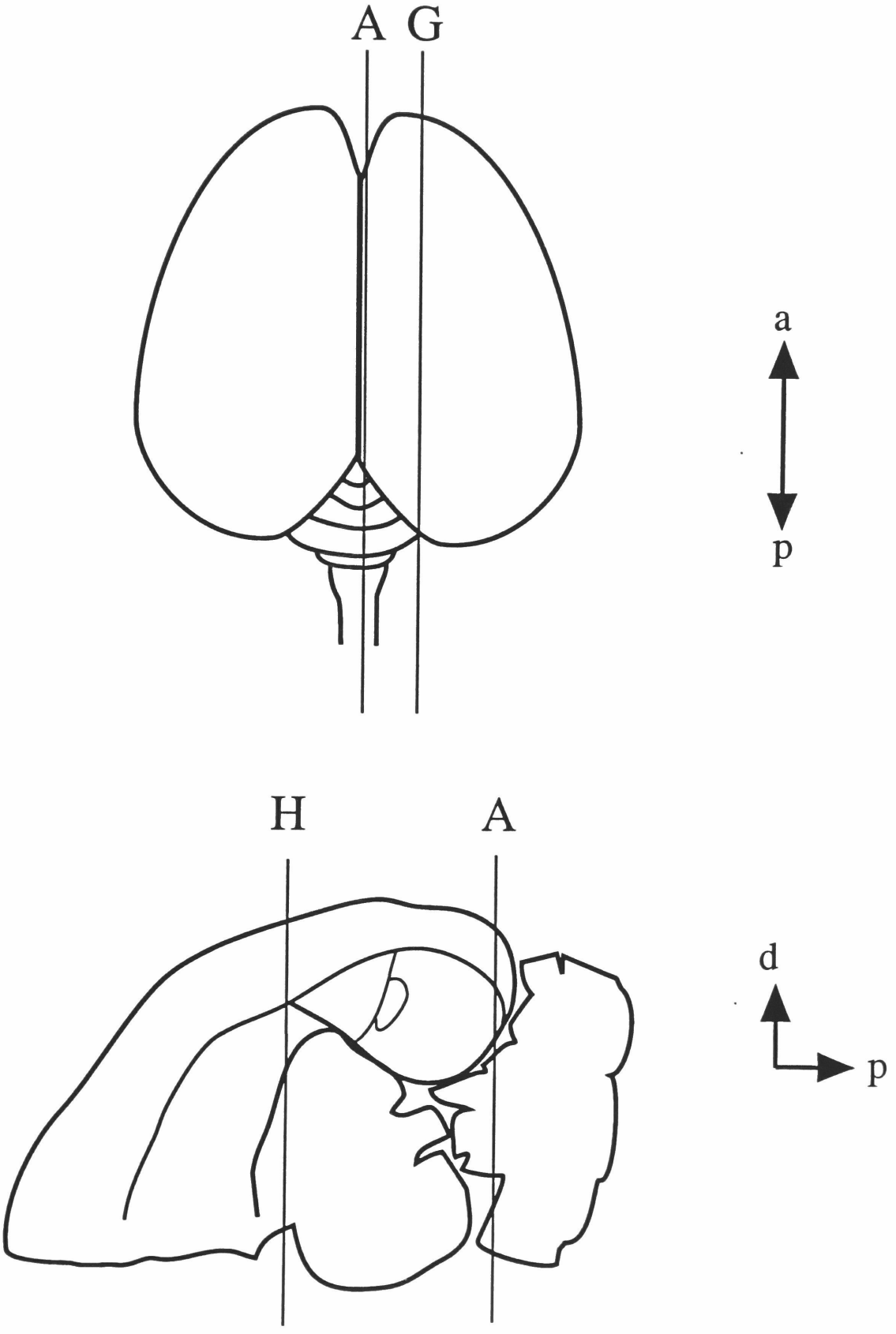
A G
a
p
H A
d
p

FIGURE 4.2 - ZENK induction in the zebra finch brain following exposure to song. A to G represents a series of parasagittal sections, from 0.25mm (A) to 2.2mm (G) lateral to the midline, as shown in figure 1. Left column: diagrams of camera lucida drawings of the sections whose autoradiograms are shown in the middle column. Other columns: in situ hybridization autoradiograms at levels corresponding to the diagrams on the left for a song-stimulated (middle column) and an unstimulated control (right column) bird. Abbreviations: A, Archistriatum; BS, Brain stem; Cb, Cerebellum; H, Hyperstriatum; Hp, Hippocampus and parahippocampal area; Hv, Hyperstriatum ventrale; HVC, High Vocal Center; L2a, subfield L2a of Field L; L2, subfield L2 of Field L; LPO, Lobus paraolfactorius; M, midbrain; MAN, lateral nucleus Magnocellularis of the Anterior Neostriatum; N, Neostriatum; NC, Neostriatum caudale; P, Paleostriatum; PA, Paleostriatum augmentatum; PP, Paleostriatum primitivum; RA, nucleus Robustus Archistriatalis; T, Thalamus; X, Area X. Orientation: dorsal is up and anterior is to the left. Line size: 2mm.

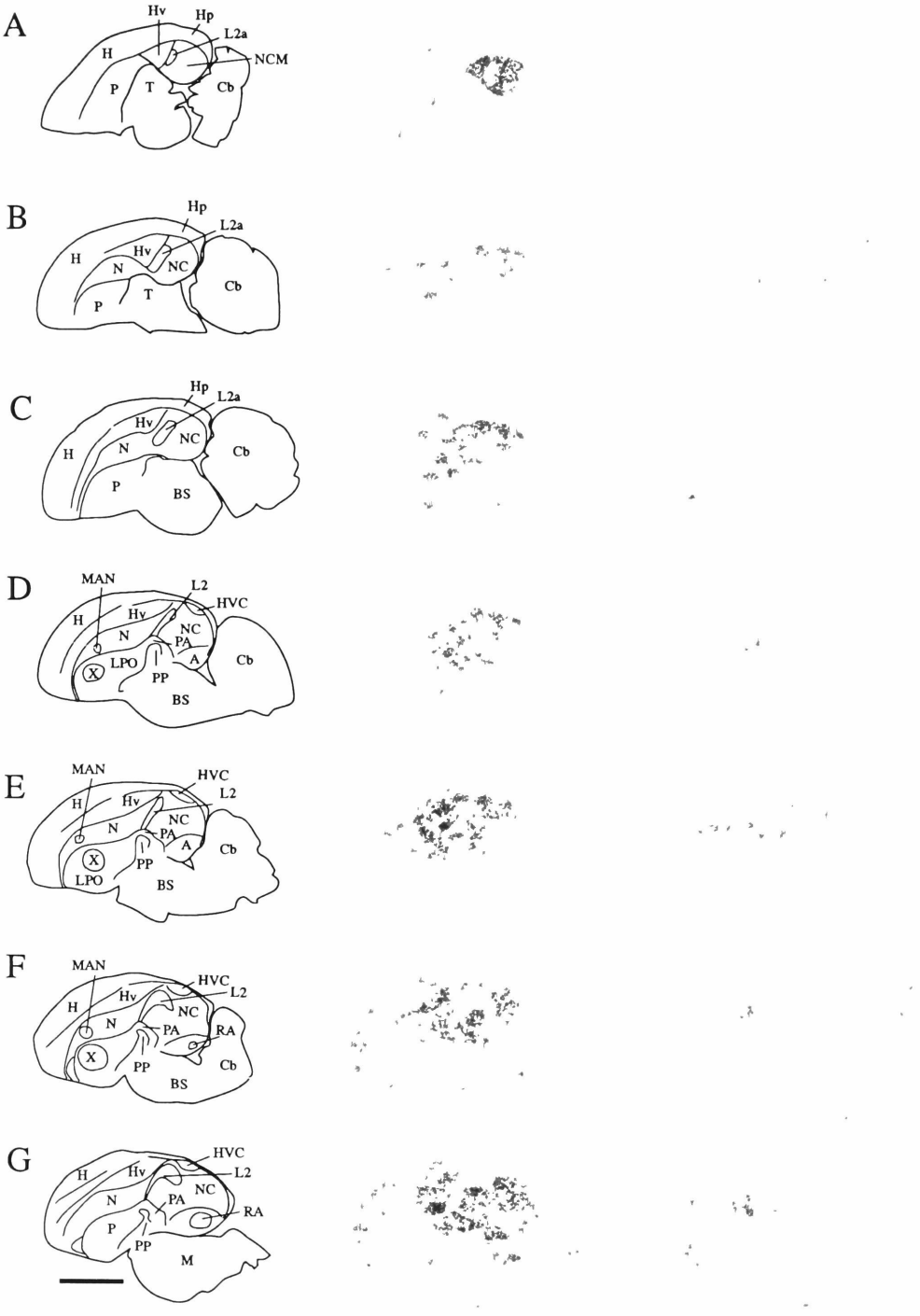
A
Hv
Hp
L2a
NCM
H
P
T
Cb
B
Hp
L2a
Hv
H
N
NC
Cb
P
T
C
Hp
L2a
Hv
NC
H
N
Cb
P
BS
D
MAN
L2
HVC
H
Hv
NC
N
PA
A
Cb
X
LPO
PP
BS
E
MAN
HVC
L2
H
Hv
NC
N
PA
A
Cb
X
LPO
PP
BS
F
MAN
HVC
L2
H
Hv
NC
N
PA
RA
X
PP
Cb
BS
G
HVC
H
Hv
L2
NC
N
PA
RA
P
PP
M

FIGURE 4.3 - ZENK mRNA induction in the zebra finch brain following exposure to song. A to H represents a series of coronal sections, from +0.25 (A) to +2.5mm (H) in the antero-posterior axis, as indicated in figure 1. Left column: diagrams of camera lucida drawings of the sections whose autoradiograms are shown in the middle column. Other columns: in situ hybridization autoradiograms at levels corresponding to the diagrams on the left for a song-stimulated (middle column) and an unstimulated control (right column) bird. Abbreviations: A, Archistriatum; Cb, Cerebellum; E, ectostriatum; H, Hyperstriatum; Hp, Hippocampus and parahippocampal area; Hv, Hyperstriatum ventrale; HVC, High Vocal Center; L2, subfield L2 of Field L; N, Neostriatum; PA, Paleostriatum augmentatum; PP, Paleostriatum primitivum; RA, nucleus Robustus Archistriatalis. Bar size: 2mm.

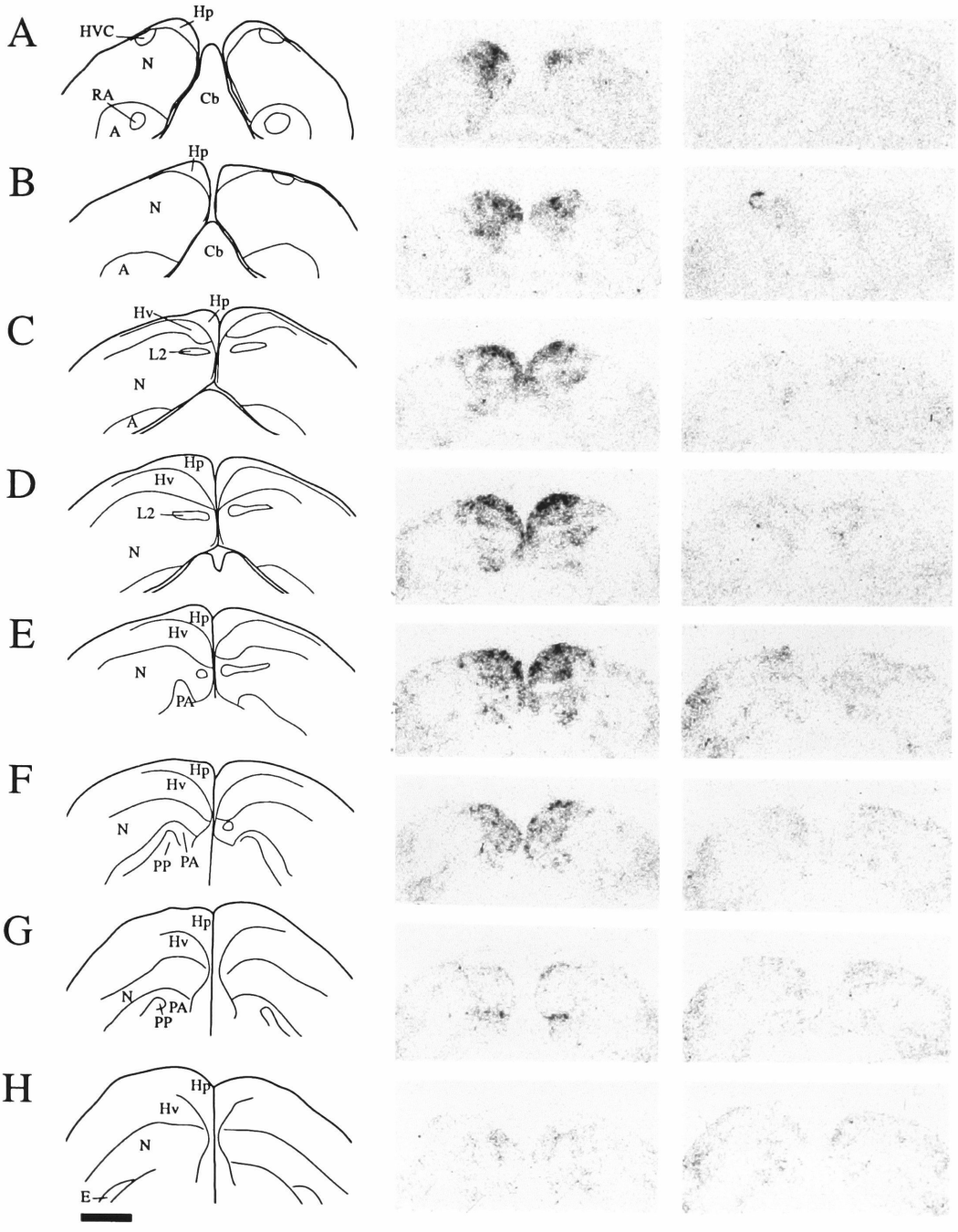
A
HVC
Hp
N
RA
Cb
A
B
Hp
N
Cb
A
C
Hv
Hp
L2
N
A
D
Hp
Hv
L2
N
E
Hp
Hv
N
PA
F
Hp
Hv
N
PP
PA
G
Hp
Hv
N
PA
PP
H
Hp
Hv
N
E

(figures 4.2D and E), taking a caudo-dorsal course that gradually becomes parallel with the lamina hyperstriatica (LH) and ending in the dorsal neostriatum (figure 4.2B to E); in more lateral sections, this area assumes a boomerang or inverted-v shape (figure 4.2F and G). Areas with high ZENK signal in general surround this negative core and occasionally assume a more localized or nuclear aspect (as in figure 4.2G); fold-induction in these areas is probably not as high as in NCM, since ZENK levels are relatively high in the control (for instance, 4.2G). The signal decreases sharply at more lateral levels in the parasagittal series (not shown, but see coronal series below).

This general pattern of ZENK mRNA distribution is confirmed in a series of coronal sections (figure 4.3). It can be seen that ZENK induction is bilateral and restricted to the medial portions of the caudal telencephalon. The area of high ZENK signal includes the caudo-medial neo- and hyperstriatum (see below) and resembles a lobular structure that bulges towards the midline; this lobule is bound dorso-medially by the hippocampus and lies over the cerebellum caudally (figures 4.3A and B) and over caudal diencephalic structures more rostrally (figure 4.3D, compare with 4.2A). There seems to be no gross interhemispheric differences, although no systematic quantitative analysis was performed (the difference seen in panel A of figure 4.3 is most probably the result of the plane of sectioning, which was not exactly orthogonal to the sagittal plane). A central or core negative area surrounded by areas showing significant ZENK induction can also be seen in the coronal series. In general, ZENK signal tends to be denser in more medial areas and more diffuse laterally. The lateral boundaries of areas

showing high ZENK signal can be clearly seen in the coronal series (figure 4.3A to F). No obvious natural boundaries such as laminae or differences in cell number or density are seen between the medial and the lateral neo- or hyperstriatum when cresyl-violet stained sections are examined, that could correspond to the borders of the high ZENK regions, although a more detailed analysis is necessary (especially in thicker sections).

B - Caudo-medial neostriatum (NCM)

The area showing the most marked induction has well-defined boundaries in parasagittal sections and corresponds to the most medial part of the caudal neostriatum; this general area was named NCM (figure 4.2A, seen in more detail in figure 4.4). Note that ZENK levels are particularly low in this area in the unstimulated control (figures 4.2A and 4.4B). In parasagittal sections at more medial levels than that shown in figures 4.2A and 4.4A (for example, see figure 4.16), NCM appears as a small circular or ovoid area of homogeneously high ZENK induction levels, which is separated from the rest of the telencephalon. In more lateral sections, the caudal neostriatum becomes gradually larger, assuming a drop-like shape together with the caudo-medial HV (figure 4.2A), and eventually becoming continuous with the rostral parts of the neostriatum (figures 4.2B, C and D). At these levels, ZENK signal is more diffuse and a stripe-shaped area negative for ZENK appears within the neostriatum (figures 4.2A to D); this corresponds to portions of the auditory thalamo-recipient zone (see below under Field L) and is excluded from NCM, according to the definition above. In medial parasagittal sections, NCM is easily defined by its natural boundaries:

FIGURE 4.4 - Induction of ZENK mRNA in the songbird forebrain following exposure to song. In situ hybridization autoradiograms of sections corresponding to the parasagittal plane 250μm lateral to the medial surface of the brain are shown. (a) Adult male zebra finch exposed for 45 minutes to recorded conspecific song. (b) Unstimulated control. (c) Cresyl violet staining of the section whose autoradiogram is shown in (a). (d) Camera lucida drawing of the section shown in (c). The arrows in all panels point to the area of high ZENK induction that includes NCM and a portion of HV. Cb - cerebellum, H - hyperstriatum, HV - hyperstriatum ventrale, Hp - hippocampus, LPO - paraolfactory lobe, NCM - caudo-medial portion of neostriatum. Orientation: dorsal is up and anterior is to the right. Line size : 4 mm.

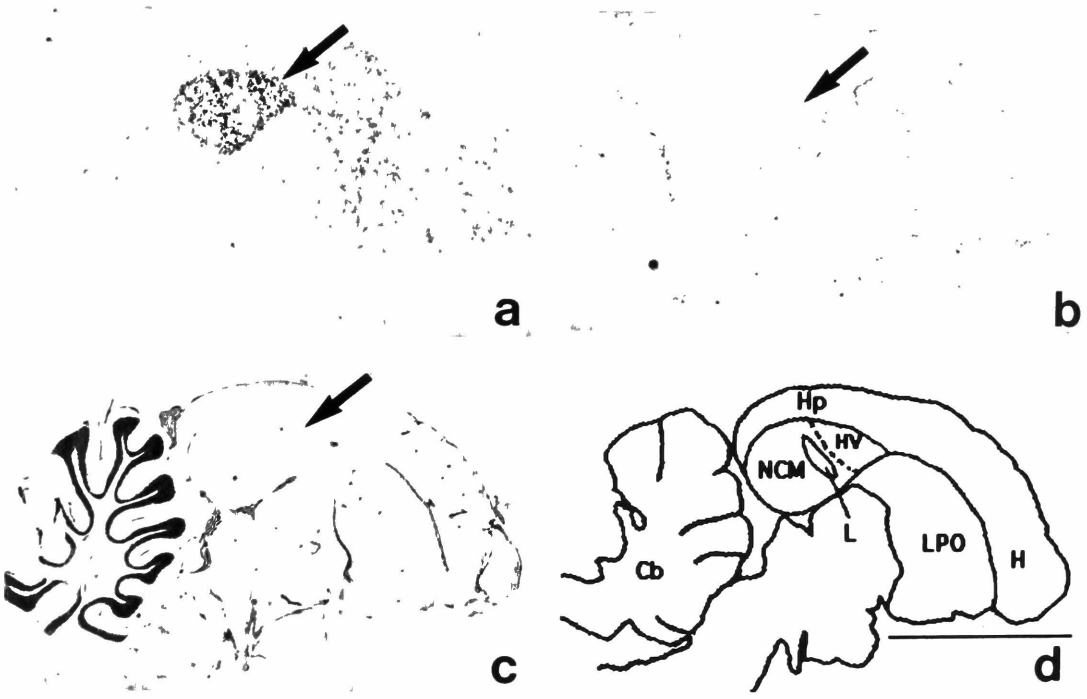
a
b
c
Hp
HV
NCM
L
LPO
H
Cb
d

the ventricular zone dorsally, ventrally and caudally; rostro-dorsally, it is separated from HV by the lamina hyperstriatica and medial portions of Field L (figure 4.4). In even more medial sections (see figure 4.17, for example, Field L and HV are absent, and NCM is surrounded on all sides by ventricular zone.

In coronal sections, a thin neostriatal layer of high ZENK signal separates the core negative region from the midline (figures 4.3C, D and E). This thin layer corresponds to a transverse view of the circular area of high ZENK expression in figure 4.16. The negative core is no longer present more caudally (figures 4.3B and A), whereas neostriatal areas showing high ZENK signal become thicker at this level (this corresponds to a transverse view of the caudal portions of NCM in figures 4.2A or 4.16).

To investigate the induction in NCM at the cellular level, hybridized sections were also prepared for emulsion autoradiography (figure 4.5). Within the NCM of song-stimulated birds, a large number of cells with neuronal appearance (larger, with paler staining nuclei) are labeled with high concentrations of autoradiographic silver grains (figures 4.5A and B). This high level of induction is confined to NCM and adjacent HV and respects the boundaries with the overlying hippocampus and parahippocampal area (figure 4.5A). In the NCM of unstimulated birds, most of the cells are unlabeled (figure 4.5C). However, even in these brains a few cells in NCM (<5%) are labeled as highly as most cells in the song-stimulated brain (figure 4.5C, arrow). Thus some expression of the ZENK gene occurs in NCM of birds not exposed to song, and the difference in overall RNA levels between the control and

FIGURE 4.5 - High-power bright-field view of NCM in sections dipped with autoradiographic emulsion. (a) Conspecific song-stimulated zebra finch, boundary between HP and NCM. Large numbers of silver grains are seen on cells in NCM but not HP. The boundary between NCM and HP is defined by the darkly-staining tightly-packed cells of the ventricular zone. (b) and (c) Comparison of NCM between conspecific song-stimulated (b) and unstimulated (c) birds. Arrow indicates labeled cell in control NCM. HP, hippocampus; NCM, medial portion of caudal neostriatum. Bar size: 25μm.

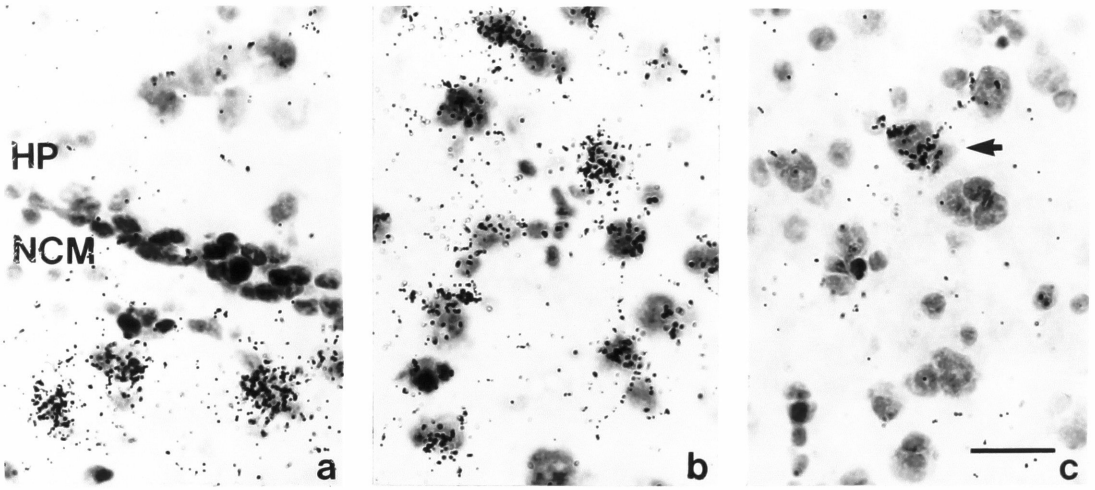
HP
NCM
a
b
c

experimental animals appears to be due primarily to an increase in the number of cells expressing the gene at high levels.

C - Caudo-medial HV

A high ZENK induction is also seen in the most medial part of the caudal hyperstriatum ventrale (HV), immediately adjacent to Field L and NCM (figures 4.2, 4.3 and 4.4). The caudo-medial HV is seen in coronal sections extending medially and ventrally towards the midline, between the hippocampus and the caudo-medial neostriatum; it constitutes most of the dorsal area of high ZENK expression on figures 4.3C to F. On medial parasagittal sections, HV constitutes the rostro-dorsal portions of the drop-shaped area separated from the rest of the telencephalon and which shows high ZENK induction (figures 4.2A and 4.4A). At more lateral levels, the caudal HV extends rostrally, and eventually becomes continuous with the more rostral portions of HV; high ZENK levels are restricted to the caudal portions, closely adjacent to Field L (figures 4.2C to F).

D - Field L

A considerable portion of the areas highlighted in figures 4.2 and 4.3 corresponds to the primary auditory region of the forebrain, Field L. Based on the shapes of dense areas in the autoradiograms and their localization relative to other structures, the following observations are made (see figures 4.2 and 4.6): a- the core or central area of negative signal corresponds to subfields L2a (thin stripe oriented obliquely from the dorso-caudal tip of the paleostriatum towards the dorso-caudal neostriatum), L2b (the apex of the boomerang or inverted-V negative core region in figures 4.2F and 4.G) and the lateral portions of Field L of Rose (the caudal leg of

Figure 4.6 - ZENK mRNA induction after song presentation in the zebra finch Field L complex. The area enclosed by the hatched rectangle in the diagram on the top left is shown in detail in (A), (B) and (C). (A) Bright-field view of an emulsion-dipped section stained with cresyl-violet; hatched lines are drawn over the laminae that separate L subdivisions and the paleostriatum (see top diagram). (B) and (C) Dark-field view of the same area as shown in (A) in a song-stimulated and a control bird respectively. (D) High-power view of the area enclosed by the small rectangle in (A); hatched line is drawn over the lamina that separates L2a (left) and L1 (right) and arrow indicates ZENK-positive cluster in L1. (E) High-power view of the area enclosed by the large rectangle in (A); hatched line is drawn over lamina that separates L3 and PA. Bar sizes: (A), (B) and (C), 200μm; (D) and (E), 50μm.

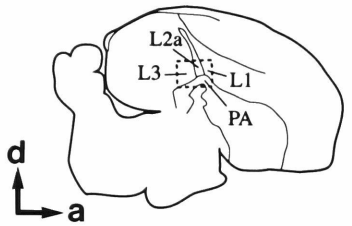
L2a
L3
L1
PA
d
a

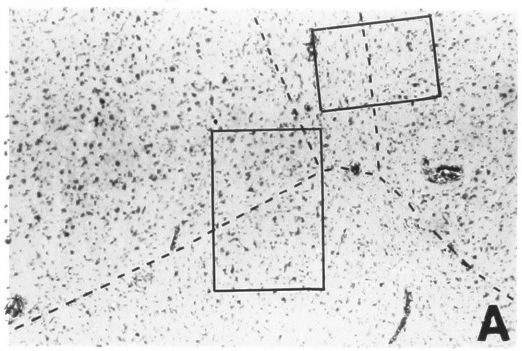
A

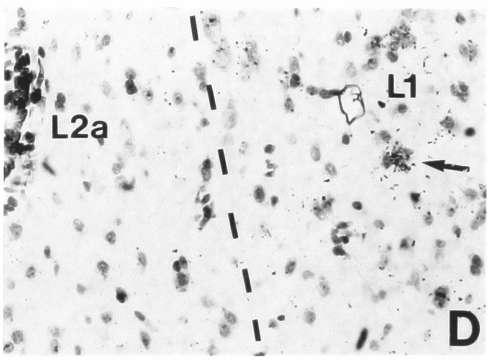
L2a
L1
D

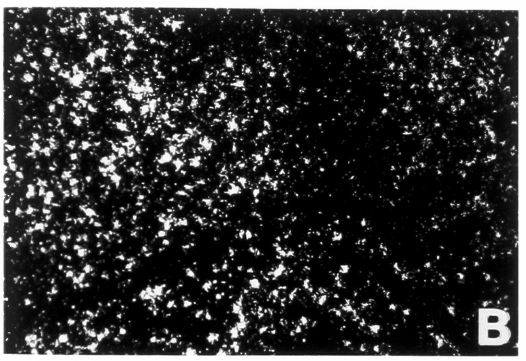
B

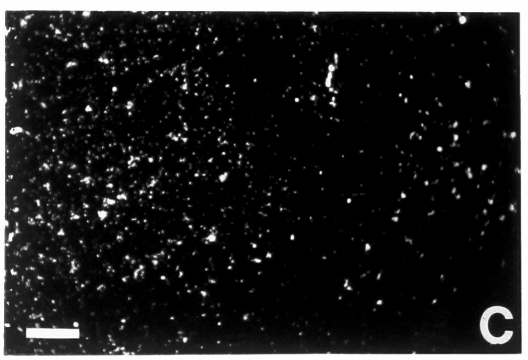
C

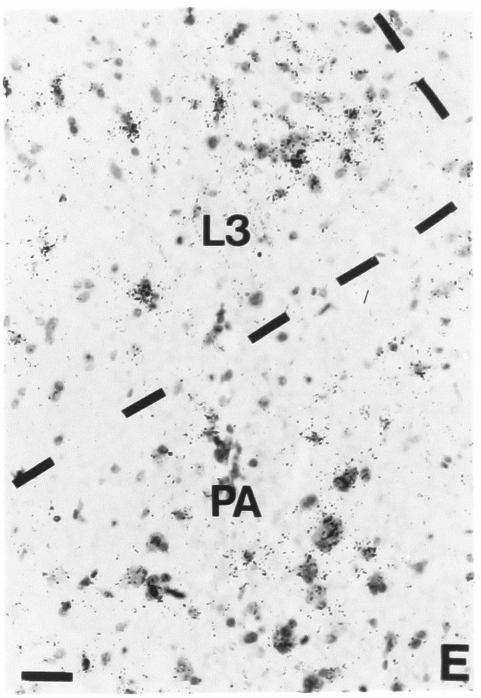
L3
PA
E

the inverted-V in figure 2G, compare with definition by Fortune and Margoliash, 1992); b- one of the patches showing high ZENK induction lies ventro-caudally to the stripe-shaped negative core and dorso-caudally to the paleostriatum and occupies the concavity of the boomerang or inverted-V (figures 4.2F and G and figure 4.6); it thus closely matches L3 (Fortune and Margoliash, 1992); c- a significant induction is also seen in the region antero-dorsal to the negative core, an area which probably corresponds to L1 (figures 4.2D and E and figure 4.6; compare with Fortune and Margoliash, 1992).

In coronal sections, the negative core region (L2) appears as a horizontal stripe (figure 4.E) that gradually moves dorsally as one progresses rostro-caudally (figures 4.3E, D and C, in this sequence). Some portions of the areas of high ZENK signal immediately surrounding this negative core correspond to other L subfields. For example, the area between L2 and the lamina separating HV and N (figures 4.3C, D and E) corresponds to L1; the boundaries between other Field L subdivisions are not clear in thin cresyl-stained coronal sections.

The relationships between Field L subfields are observed in closer detail in figure 4.6. The diagram on the upper left corner represents a camera lucida drawing of a parasagittal section at the same level as the autoradiogram in figure 4.2F (notice the reverse orientation of the figures). L2a is easily defined in cresyl-violet stained sections as a field that extends from the caudo-dorsal tip of the paleostriatum towards the dorsal neostriatum, running parallel to the lamina hyperstriatica. L2a contains small and darkly staining cells, typically organized in short rows or columns aligned with the major axis of

L2a. Caudal to the angle between L2a and the caudal paleostriatum is L3 and immediately rostral to L2a is L1, whose rostral boundaries are not well-defined. The area enclosed by the hatched rectangle in the diagram is represented in detail in figures 4.6A and B (bright- and dark-field views respectively of a section from a song stimulated bird) and 4.6C (dark-field view of a section from an unstimulated control). Some signal is seen in the unstimulated L1 and L3 (figure 4.6C) but a dramatic increase in the number of positive cells occurs in both fields after song presentation (figure 4.6B), but not in L2a. High power views demonstrate positive cells in L1 (figure 4.6D, right, arrow points to a positive cluster) and L3 (figure 4.6E, upper half, positive cells in clusters or in isolation) but not in L2a (see the left half of figure 4.6D) after song presentation.

E - HVC shelf

A marked induction can be seen in the caudo-dorsal neostriatum, most prominently in the area immediately adjacent to HVC (figure 4.7). This area underlying HVC receives a direct input from Field L (possibly from subfields L1 and L3, as discussed in chapter 5) and has been called the shelf region (Kelley and Nottebohm, 1979). As can be seen from the dark-field images, the shelf in unstimulated controls contain a few ZENK positive cells (figure 4.7B) but the number of these cells is dramatically increased in song-stimulated animals (figure 4.7A). The exact shape of this area as well as the number of cells that are activated in response to song varies from animal to animal and in some cases the distribution of positive cells under HVC is more homogeneous than that shown in figure 4.7A. ZENK induction in the HVC shelf is shown in further detail in figures

FIGURE 4.7 - ZENK mRNA induction in the HVC shelf and RA cup after song presentation; dark-field views of emulsion-coated zebra finch brain sections after in situ hybridization with riboprobes for ZENK are shown. The area enclosed by the upper rectangle in the diagram on the upper right contains HVC and surrounding tissue and is shown in detail in the panels on the left: (A) song stimulation; (B) unstimulated control; and (C) hybridization of a section adjacent to (A) with sense-strand probe. The area enclosed by the lower rectangle in the diagram contains the rostro-ventral part of RA and surrounding tissue and is shown in the panels on the right: (D) song-stimulation; (E) unstimulated control. Bar size: 200μm.

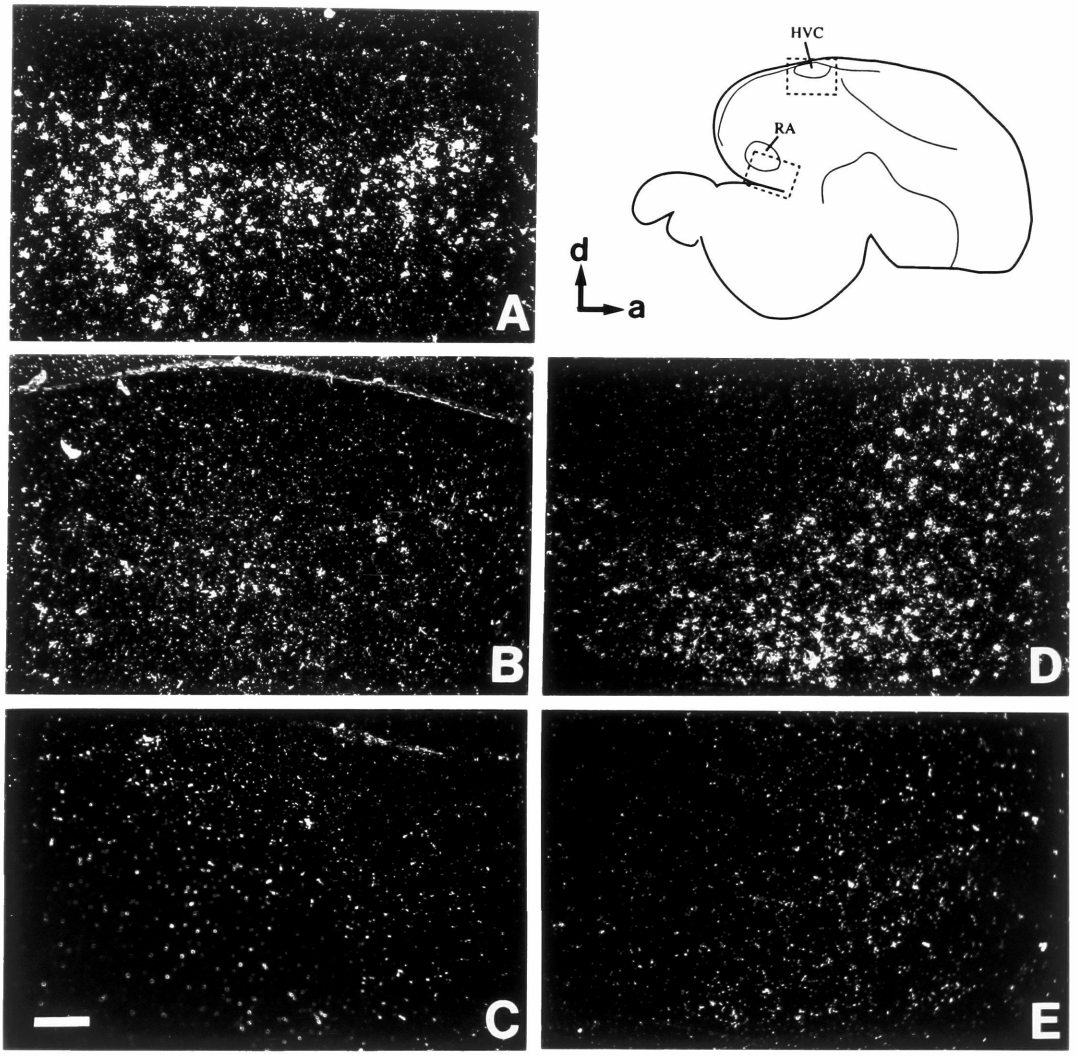
HVC
RA
d
a
A
B
C
D
E

4.8A and C. It can be clearly seen that ZENK positive cells occur immediately adjacent to HVC and respect its boundaries, although a few cells are localized right at the transition between HVC and its surrounding fibrous layer (figure 4.8C, arrow); positive cells in the shelf are relatively small, compared with the large negative cells within HVC (for instance, the neuronal cluster within HVC depicted by the arrowhead in figure 4.8C).

F - RA cup

ZENK is markedly higher in the archistriatal area surrounding RA after song presentation compared to the control (figure 4.7D and E). Here, again, although few positive cells seem to be present in this area in unstimulated controls (figure 4.7E), the number of these cells rises drastically after song presentation (figure 4.7D). The majority of ZENK positive cells tend to be in clusters that localize rostro-ventrally to RA, in contrast to the large negative cells within RA; some positive cells are present within the capsule that surrounds RA and assume an elongated form in a direction tangential to RA (figure 4.8D). This general area surrounding RA seems to colocalize at least partly with a projection area from the auditory Field L which has been named the RA cup (Kelley and Nottebohm, 1979). The archistriatum next to RA also receives an input from the dorsal neostriatum (HVC shelf) and originates descending projections to lower auditory centers (discussed in chapter 6).

G - Paleostriatal complex

Another area that shows an increase in ZENK mRNA levels is the caudo-dorsal portion of the paleostriatal complex, more specifically within the paleostriatum augmentatum (PA, figures 4.2E to G, 4.3F

FIGURE 4.8 - ZENK mRNA induction in the HVC shelf and RA cup after song presentation; emulsion-coated zebra finch brain sections hybridized with riboprobes for ZENK and counterstained with cresyl-violet are shown. (A) and (B) are bright-field view of the same sections as shown in figure 4.7A and D respectively; hatched lines are drawn over the boundaries between HVC and RA and surrounding tissues. (C) High-power view of the area enclosed by the rectangle in (A); arrow indicates labeled cell in the transition zone between HVC and surrounding N and arrowhead points to an unlabeled neuronal cluster within HVC. (D) High- power view of the area enclosed by the rectangle in (B). Bar sizes: (A) and (B), 200μm; (C) and (D), 30μm.

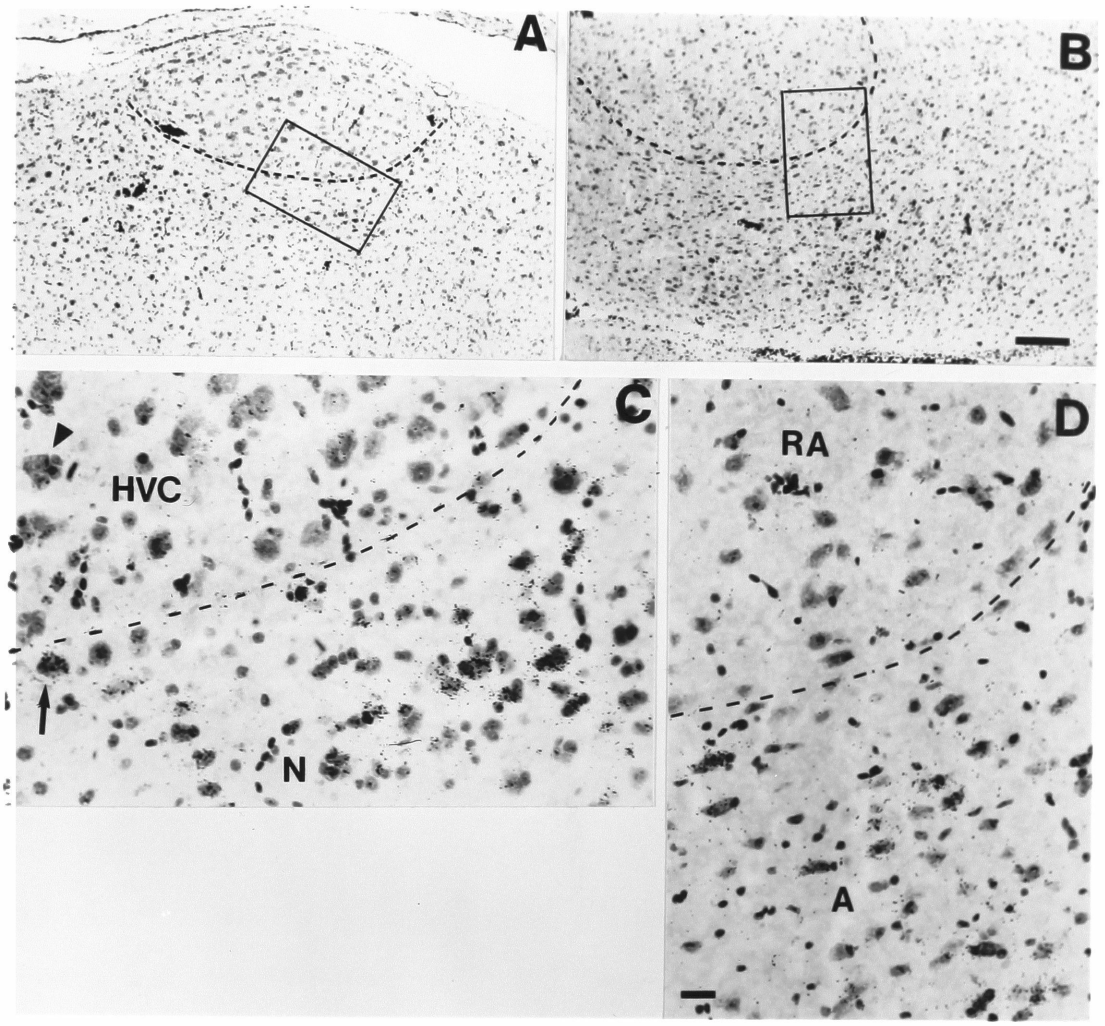
A
B
C
HVC
N
D
RA
A

and G and 4.6B and E). This area receives a direct projection from the thalamic relay nucleus ovoidalis (Kelley and Nottebohm, 1979) and seems to be reciprocally connected with some parts of the auditory forebrain (see chapter 5).

H - Intermediate neostriatum

A marked induction occurs in a discrete circular spot in the neostriatum adjacent to and anterior to Field L (L1) and NIf (figure 4.2G); its appearance and shape in the autoradiograms suggest that it could correspond to a discrete nucleus within the neostriatum; it is not obvious, however, in cresyl-violet stained sections.

I - Brain stem

The only area outside the forebrain where a significant ZENK induction is observed is the nucleus mesencephalicus lateralis, pars dorsalis, or MLd (figure 4.9), a subdivision of the avian midbrain that relays ascending auditory information to thalamic centers and is thought to be homologous to the mamalian inferior colliculus (Karten, 1967); MLd's connections are further discussed in chapter 6.

J - Song control circuit

ZENK induction is not observed in the nuclei that comprise the song control circuit, including HVC (figures 4.2, 4.3, 4.7 and 4.8), RA (figures 4.2, 4.3, 4.7 and 4.8), NIf (not shown), Area X (figure 4.2), DLM (not shown) and lMAN (figure 4.2). ZENK induction occurs in areas in close apposition to NIf (Field L1). To test whether ZENK induction occurs in NIf, cells were retrogradely labeled in this nucleus with injections of fluorogold in HVC in two animals; backfilled cells were restricted to the area of low ZENK induction in the negative core of Field L (not shown). In one case, NIf (a nucleus

FIGURE 4.9 - ZENK mRNA induction in MLd after song presentation; emulsion-coated brain sections hybridized with riboprobes for ZENK and counterstained with cresyl-violet are shown. (A) and (B) Dark-field view of sections containing MLd and surrounding areas in song-stimulated and unstimulated zebra finches respectively. (C) Brightfield view of (A). Bar size: 230µm.

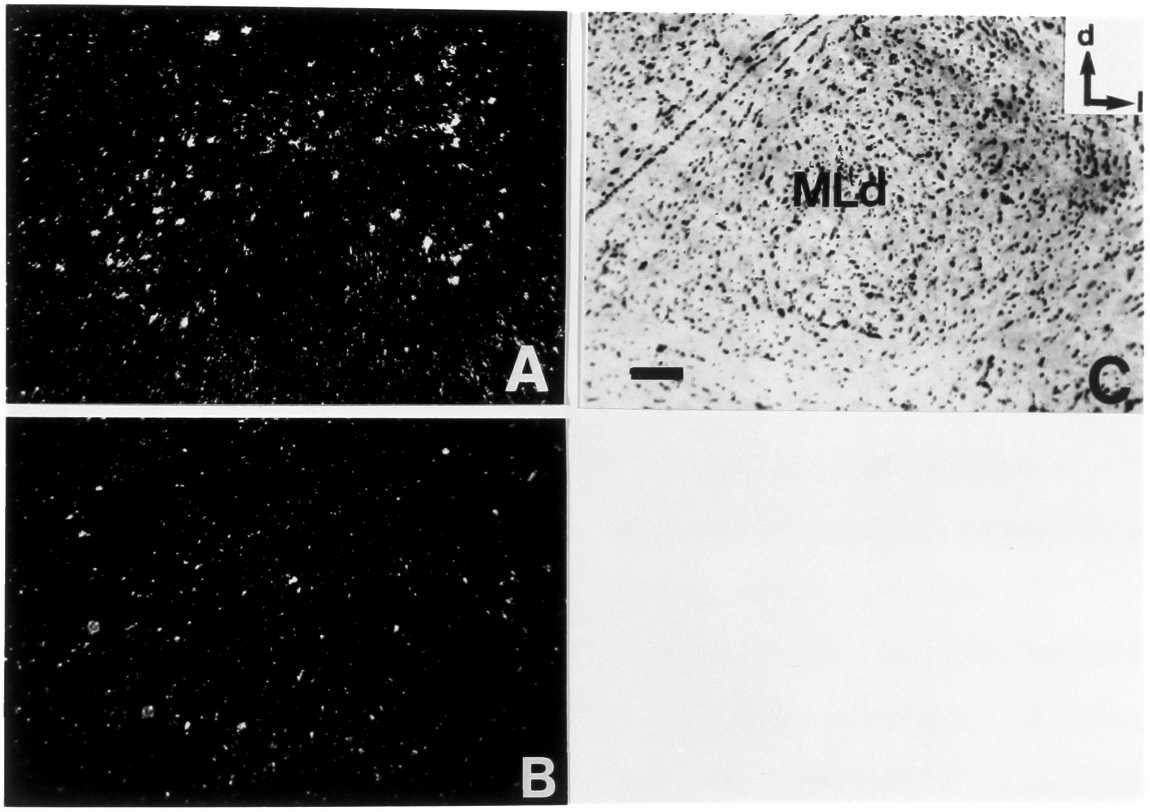
A
B
MLd
d
l
C

of difficult visualization in thin cresyl-stained sections) could be directly identified in emulsion-dipped sections and absence of grains on Nif cells was confirmed.

K - Other areas

Telencephalic regions where very little or no apparent ZENK induction occurs include the anterior and lateral N, as well as some of its dorsal portions, the anterior and lateral portions of all subdivisions of the hyperstriatum (H), the anterior paleostriatal complex (LPO and PA), the paleostriatum primitivum (PP), primary recipient zones other than Field L (N. basalis, ectostriatum), the hippocampus and parahippocampal areas and most of the archistriatum (figures 4.2 and 4.3). In addition, no ZENK induction is seen in the auditory thalamus (nucleus ovoidalis); hypothalamic structures were not examined in detail.

L- Summary and discussion of anatomical analysis

To summarize the anatomical analysis of ZENK induction in response to song presentation, two general effects are seen:

1) induction in the caudomedial telencephalon, in areas adjacent to or closely related with primary auditory structures, including some subfields of Field L (L1 and L3), the caudomedial neostriatum (NCM), the caudo-medial hyperstriatum ventrale anterior to Field L, the caudal paleostriatum, and two Field L targets, HVC shelf and RA cup (note that these two areas are also closely apposed to two song control nuclei); some of these areas, in particular NCM, were not described by earlier workers as directly related to either song production or perceptual processes;

2) a lack of induction in some areas known to be activated by song and where induction was thus expected; these include: a) the direct thalamo-recipient Field L subfield, L2; b) the nuclei of the song system involved in the acquisition and production of learned song.

Among ZENK positive areas, attention is initially drawn to the most caudo-medial portions of N (NCM) and HV (HVCM) for the following reasons: **a**- the most marked ZENK induction seems to occur in these areas; the fact that basal levels are very low in the unstimulated controls may contribute significantly to that effect; **b**- the close proximity to the primary auditory area suggested that they could receive auditory input (discussed in chapter 5) and be related to auditory processing; **c**- these areas are clearly defined by natural boundaries which are easily identified in cresyl-stained sections; this fact allowed for precise delineation of discrete areas for densitometric measurements in the evaluation of the time-course and specificity of the ZENK response (see below); **d**- these areas had not been previously described as directly involved in song production or perception (although there have been some reports on responses to species-specific vocalizations in the vicinity of Field L, including HV and portions of the medial N - see Leppelsack and Vogt, 1976, and Müller and Leppelsack, 1985 - , it is unclear whether this corresponds to NCM as defined above).

Many of the other areas where ZENK induction is observed posed initially a difficult problem: the induction pattern had a patchy appearance and there did not seem to be a correspondence of these patches to anatomically defined regions or subregions of the forebrain. However, recent studies on the organization of the avian

brain have helped shed some light on the meaning of the patterns observed. Fortune and Margoliash (1992) have done a detailed cytoarchitectonic study of Field L in the zebra finch in both the parasagittal and coronal planes of section; in their study, this complex area is further divided, according to the distribution of cell types as seen in Golgi staining, into 5 subregions: L1, L2a, L2b, L3 and L (or L of Rose). The detailed differences in cytoarchitectonic organization described in that work are not easily seen in thin sections after in situ hybridization. L2a, however, is readily identified; the localization of the remaining subdivisions is inferred with reference to L2a, as well as to the laminae LH (which separates HV from N) and LMD (which separates P from N). By comparing the dark- and bright-field views of figure 2 with the diagrams in figure 2 of their paper, it became clear that the patchy pattern observed could be at least partly explained by differential degrees of ZENK induction in various subregions of Field L. For example, the parasagittal section shown in figure 4.2F corresponds approximately to the diagrams shown in panels B and C of their figure 2; this same region is shown in further detail in figure 4.6. ZENK induction is observed in subfields L3 and L1, whereas ZENK levels remained low in L2a, L2b and L of Rose (according to Fortune's definition). These results demonstrate that the various Field L subdivisions are composed of cells with different properties in terms of gene expression in response to stimulation and lend further support to Fortune and Margoliash's classification.

Other brain areas showing high ZENK induction in response to song have been described as intimately related to auditory pathways,

receiving a projection either directly from Field L or from some immediately adjacent area, as is the case of the HVC shelf and the RA cup (Kelley and Nottebohm, 1979), or a direct projection from the thalamic relay nucleus ovoidalis, as occurs in the caudal portions of the paleostriatal complex (Kelley and Nottebohm, 1979). As further discussed in chapters 5 and 6, the shelf and cup probably represent sites of converging auditory inputs; their close proximity to song control nuclei suggest that they could then contribute to the song-selective auditory responses seen within the song control circuit (see below). MLd, on the other hand, is a central component of the ascending auditory pathway and is part of the avian homologue of the mammalian inferior colliculus. ZENK induction in response to song thus seems to occur in specific subregions of the brain that are closely related to auditory structures and could thus be involved in various aspects of auditory processing. It would be very interesting to examine in detail the response properties of these areas to complex auditory stimuli and whether and how these responses can be modified.

The auditory responses recorded in nuclei of the song system in response to song playbacks are highly selective, with preferences for conspecific songs and for the bird's own song, which has led investigators to implicate this circuit in aspects of song processing. ZENK induction patterns, however, draw attention to larger brain regions that are intimately related with the primary auditory area and may process song information before it reaches the song system. Together with data derived from anatomical studies (see chapters 5 and 6), these results suggest that complex circuits may be involved

in the neural processing of complex auditory stimuli such as song; it is, thus, possible that the selectivity to song playbacks observed by neurophysiological recording within nuclei of the song system results partly from auditory processing occurring in these areas.

Field L is the primary forebrain thalamo-recipient zone for auditory stimuli (Karten, 1968; Bonke et al., 1979a; Kelley and Nottebohm, 1979). The heaviest telencephalic termination of the auditory thalamus corresponds to L2a, which then projects to surrounding fields, L1 and L3 (Karten, 1968; Bonke et al., 1979a; Saini and Leppelsack, 1981); these L2a-flanking areas receive a much sparser thalamic projection, if any (Bonke et al., 1979a). Cells in L2a are characterized by very low response selectivity and respond readily, both electrophysiologically and metabolically, to various classes of auditory stimuli, from simple to complex (including species-specific vocalizations), as is expected of an area thought to function primarily as a relay to higher-order auditory regions (Bonke et al., 1979b; Scheich et al, 1979; Braun et al., 1985; Müller and Scheich, 1985). Nevertheless, no ZENK induction was observed in L2a (or in L2b, a subdivision of L2 that specifically receives input from nucleus semilunaris paraovoidalis, or SPO, a subdivision of the auditory thalamus closely related with ovoidalis; see Wild, 1987). Similarly, ZENK induction was notably absent in the nuclei of the song control circuit, where auditory and metabolic responses to auditory stimulation are also well-documented (Katz and Gurney, 1981; Margoliash, 1983 and 1986; Braun et al., 1985; Williams and Nottebohm, 1985). L2a and the song control nuclei constitute, thus, clear examples of areas where no gene induction is detected in spite

of the fact that stimulation from song playbacks is known to reach these regions. It remains to be seen whether other classes of genes responsive to depolarization can be activated in areas that lack a ZENK response.

4.2 - PREFERRED STIMULI

A more complete characterization of ZENK induction in NCM, the area that shows the most robust and consistent induction response, is presented in this and the following sections. In the first experiment, which will be referred to as Exp. #1, the specificity of the response was tested by comparing the effect of conspecific and heterospecific songs and tone-bursts. The conspecific song tapes consisted of recorded bouts of song from three different individuals of the same species, including the bird to which the stimulus was presented. For heterospecific song, canaries heard zebra finch song and vice-versa. The duration of the recorded canary songs was approximately 20-30 seconds; the bouts of zebra finch song were repeated to match for duration in the two groups. Densitometric analysis of ZENK levels in NCM revealed that both classes of song (conspecific and heterospecific) caused an increase in ZENK above control levels in both species (figure 4.10); no induction was observed following stimulation with tone bursts. ZENK induction above levels found in unstimulated birds were 4.5-9x in canaries and 5-10x in zebra finches for conspecific song and 2-4x in canaries and 3-4x in zebra finches for heterospecific song (standard errors calculated from the data are shown in figure 4.10). For a conservative statistical test of

FIGURE 4.10 - Relative ZENK mRNA induction in NCM in zebra finches presented with various auditory stimuli: conspecific song, heterospecific song, tone bursts or no auditory stimulus for 30 minutes (animals sacrificed at the end of playbacks). Optical density measurements were taken from autoradiograms in an area corresponding to NCM (as depicted in figure 4.4) and normalized to levels in unstimulated controls. For each group, the mean (+/- standard error) of the normalized optical densities in NCM is shown.

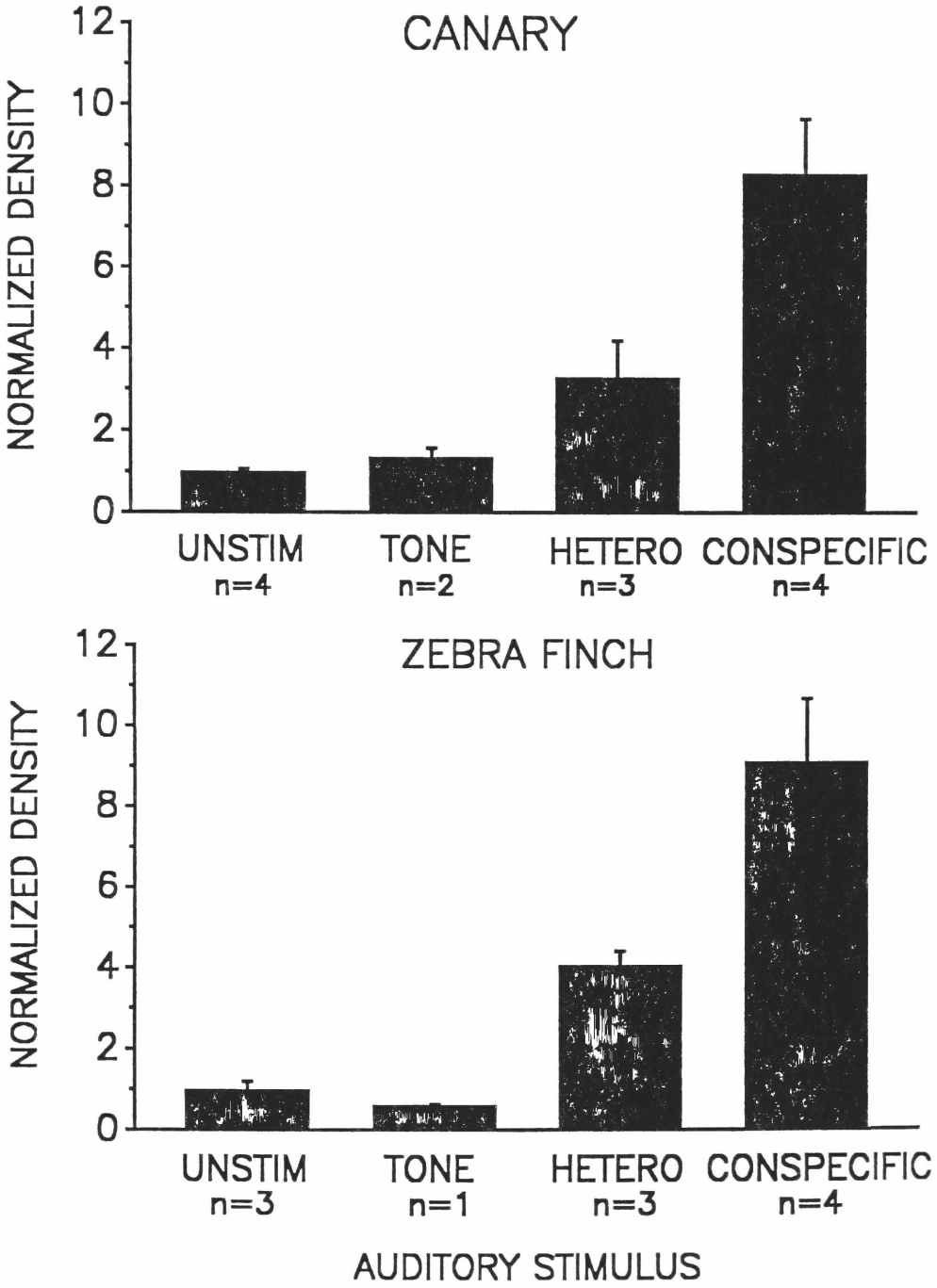
CANARY
NORMALIZED DENSITY
12
10
8
6
4
2
0
UNSTIM
n=4
TONE
n=2
HETERO
n=3
CONSPECIFIC
n=4
ZEBRA FINCH
NORMALIZED DENSITY
12
10
8
6
4
2
0
UNSTIM
n=3
TONE
n=1
HETERO
n=3
CONSPECIFIC
n=4
AUDITORY STIMULUS

these differences, individual normalized density values from combined controls (unstimulated plus tone-stimulated) were compared with individual values from the song stimulated groups and values from the conspecific groups were compared with values from the heterospecific groups (Mann-Whitney U test - as described in Siegel, 1956 - criterion of $p<0.05$, 2-tailed probabilities). In canaries, significant differences were seen both between birds exposed to heterospecific ($n=3$, $U=0$, $p=.024$) and conspecific ($n=4$, $U=0$, $p=.005$) song, compared to combined controls ($n=6$). In zebra finches a significant difference from combined controls ($n=4$) was seen for the birds exposed to conspecific song ($n=4$, $U=0$, $p=.028$), while ZENK induction in the birds exposed to heterospecific song was only suggestive ($n=3$, $U=0$, $p=.056$), perhaps due to the low number of animals. Combining data from both species, differences in induction for birds that heard conspecific vs. heterospecific song were highly significant ($n=8$, $n=6$, $U=0$, $p<.001$).

The interpretation of these results is somewhat complicated by the fact that the conspecific song tapes contained songs from several birds and included BOS (bird's own song, i. e., song of the bird to which the stimulus tape was presented). To test whether the results could be explained by the presence of BOS in the tapes, the effect of playing BOS to 3 male finches was compared with playing the same songs to three other age-matched males. No obvious differences were seen between the two groups (data not shown), suggesting that BOS was not the major factor accounting for the differences seen in Exp. #1 between responses to conspecific and heterospecific song.

In another experiment, which is depicted in figure 4.11 and will be referred to as Exp. #2, the specificity of ZENK response in zebra finches was further studied by comparing the effects of forward song (**FS**, conspecific song played forwards, or in the normal temporal sequence), reverse song (**RS**, the same song played in the reverse temporal orientation, as generated by SoundEdit software), white noise (**WN**) or no stimulus (**S**, for silent controls); the tapes contained song from a single individual, of about 15 seconds of duration, followed by 45 seconds of silence (**WN** was matched for duration) and the total playback duration was 30 minutes for all animals. Differences were significant (criterion of $P<0.05$, two tailed probabilities) when **WN** ($n=4$, $U=1$, $p=0.043$), **RS** ($n=4$, $U=0$, $p=0.029$) and **FS** ($n=5$, $U=0$, $p=0.014$) groups were compared with **S** ($n=4$) and diffeences were also significant when individuals exposed to **RS** ($n=4$, $U=0$, $p=0.029$) were compared with those exposed to **WN** ($n=4$). There were no significant differences in the levels of ZENK induction elicited by playbacks of **FS** and **RS** ($p<0.005$)

Comparing the two experiments, white noise seems to be slightly more effective than the random presentation of tone bursts, probably due to the greater complexity of the stimulus and possibly because the broad band nature of **WN** may be reminiscent of some of the broad band sounds found in zebra finch song. The other intriguing observation is the lack of differences in the response to forward and reverse songs. Even though the latter observation may point to a true lack of difference, some aspects should be emphasized, that may be relevant to these results: 1) conspecific song in Exp. #2 seemed to cause a smaller induction than in the Exp.

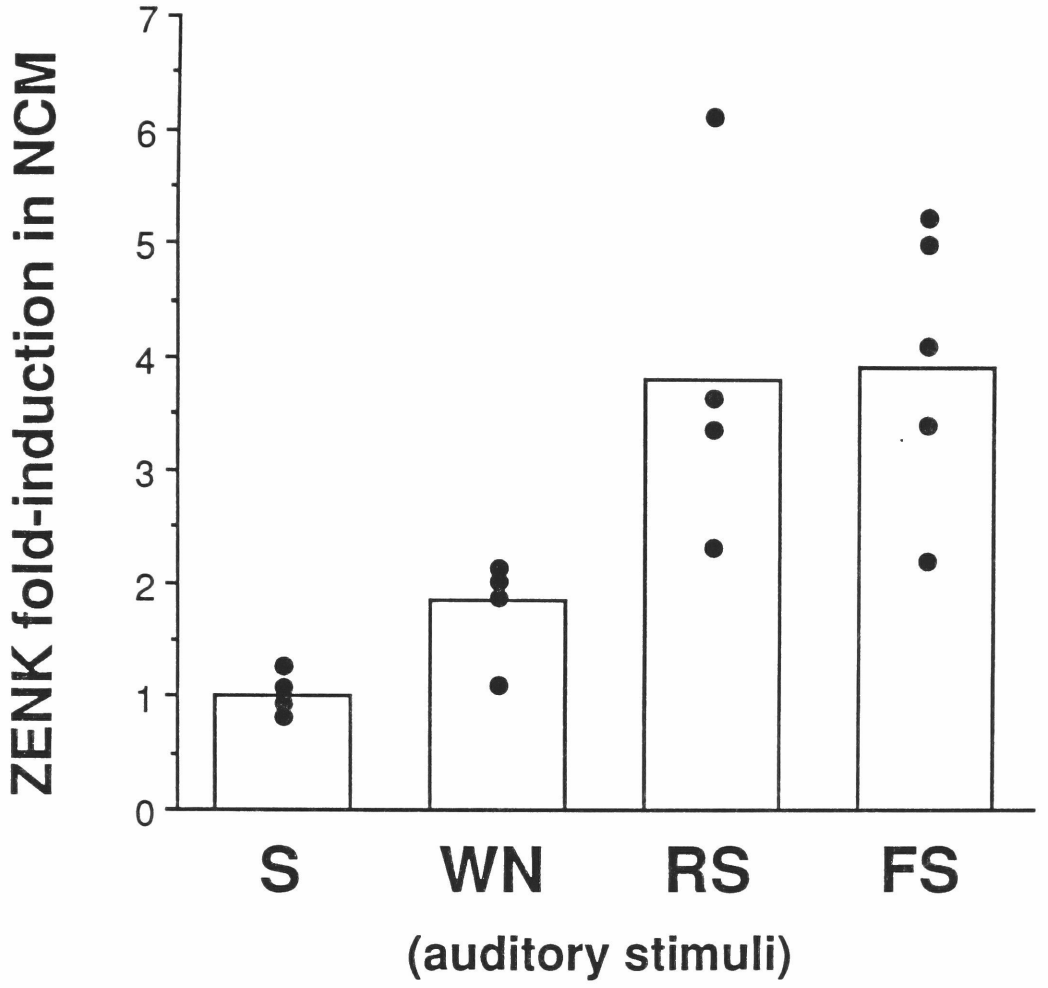

FIGURE 4.11 - Relative ZENK mRNA induction in NCM in zebra finches presented with various auditory stimuli: forward conspecific song (**FS**), reverse conspecific song (**RS**), white noise (**WN**) or no auditory stimulus (**S**) for 30min. (animals sacrificed at the end of playbacks). Optical density measurements were taken from autoradiograms in an area corresponding to NCM (as depicted in figure 4.4) and normalized to levels in unstimulated controls. Open circles represent individuals and columns represent averages (n=4 for **S**, **WN** and **RS**; n=5 for **FS**).

#1; it should be remembered, though, that in Exp. #2 the stimulus tape contained song from a single individual, vs. song from 3 individuals in Exp. #1. It is possible that the total induction is correlated with the complexity of the recorded stimulus; in addition, the particular song used in Exp. #2 may not have been particularly stimulating, or very different from the reverse song; 2) the densitometry covers a large area and does not addresss the behavior of individual cells; thus, nothing can be said about the specificity of the response of single units in NCM to auditory stimuli; 3) it is possible that units in NCM are not particularly interested in temporal patterns but more in the frequency analysis; this could explain the preference for conspecific song but the apparent failure to distinguish between forward and reverse songs.

In summary, whereas the responses to a particular song played in the forward and reverse orientations were not distinguishable, conspecific song elicited a greater response in NCM than heterospecific song. In addition, tone bursts that included the same range of frequencies as is found in conspecific song failed to elicit a significant response, although some effect was seen with white noise. Units within NCM thus seem to be performing tasks related to feature detection of auditory stimuli. This suggests that levels of ZENK induction in NCM may reflect processes of auditory discrimination in the forebrain, and are higher after stimuli that are of greater behavioral significance to the bird. Using electrophysiological techniques, a preference for neuronal activation by conspecific song, especially the bird's own song, has been described in HVC (High Vocal Center), a main component of the motor

pathway for song production (Margoliash, 1983 and 1986). It is unclear, however, how auditory information processed by primary auditory structures and presumably by areas revealed by ZENK induction (such as NCM, HVC shelf and RA cup) reaches this motor pathway. So as to answer this question, the anatomical connections of areas revealed by ZENK induction was investigated in detail (chapters 5 and 6).

Although the results presented in this section suggest that ZENK induction in NCM is related to auditory processing, other aspects of the bird's behavior which can be triggered by song presentation should also be considered, such as song production or non-specific social arousal. These other possibilities seem unlikely explanations for the gene induction because of the following: 1) most birds didn't sing during the song playbacks under the experimental conditions used; 2) similar ZENK induction in the caudomedial neostriatum was seen in female zebra finches (not shown) who never sing; 3) no appreciable induction was seen in one male zebra finch that was presented with a female and sang vigorously to her during the presentation period but was not exposed to song tapes. This seems to preclude a significant effect of active singing behavior or motivation to sing on ZENK induction in NCM, although an arousal or motivational effect caused by song presentation cannot be excluded.

Another aspect to be discussed is the effect of isolation. For all the quantitative comparisons shown in this chapter, birds were visually and acoustically isolated for at least one day before song presentation. That isolation may not be essential for the induction response is suggested by at least two facts: 1) a similar level of ZENK

induction was observed in NCM in a couple of birds that were not isolated before playback and heard the playback of conspecific song immediately upon being put in a sound isolation box (not shown); this result should be taken with caution, though, since no controls were run to test the levels of ZENK expression before birds were put in the isolation boxes; 2) induction was also observed in wild song sparrows (see below). Isolation, however, by decreasing activity and thus basal levels of ZENK expression, may have been important for decreasing variability among birds in the amount of ZENK induction by sound stimulation.

4.3 - INDUCTION KINETICS

Short playbacks (10 minutes) of tapes containing songs of three conspecifics (BOS not included) were used to determine the time course of ZENK induction by song and the survival time from the beginning of the stimulation was varied (0, 10, 20, 30, 40 and 60 minutes, figure 4.12). The results show that 10 minutes of playback is sufficient for a small but detectable increase in ZENK mRNA levels, and that there is a build-up of mRNA amounts that continues until 20 minutes after the end of the stimulation period (30 minutes after the beginning of the stimulation), when the response peaks. This indicates that the response is transient and that there is a latency for the response to be fully expressed. After 30 minutes, ZENK mRNA levels declined rapidly, and by one hour they were again comparable to basal levels. These kinetics are very similar to what has been generally described for IEG induction in other systems and probably

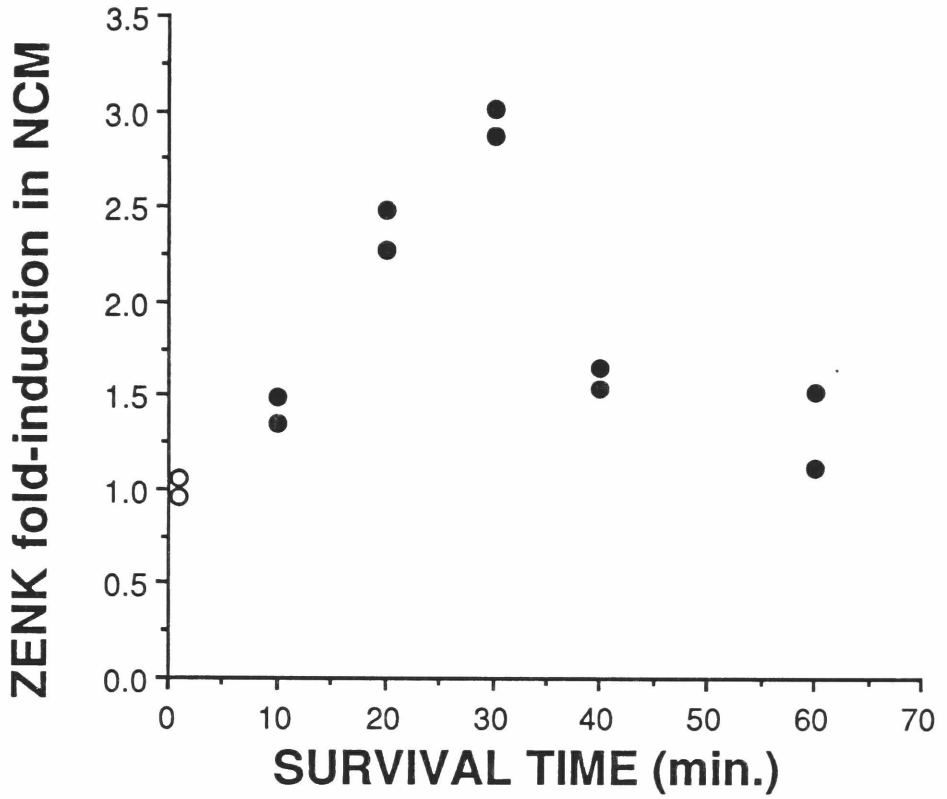

FIGURE 4.12 - Time-course of ZENK mRNA induction after short playback. ZENK fold-induction in NCM of zebra finches is plotted as a function of survival time after short-duration (10min.) playback of conspecific song. After sacrifice, frozen brain sections were hybridized with ^{35}S-labeled riboprobes for ZENK and exposed to X-ray films; optical density measurements were taken from autoradiograms in an area corresponding to NCM (as depicted in figure 4.4) and normalized to levels in unstimulated controls. Dots represent individuals (n=2/time point); silent controls are plotted as open circles at time=0.

reflects an interplay between mechanisms leading to mRNA synthesis (transcriptional activation of the gene) which prevail during the first phase, and transcriptional inactivation and RNA degradation mechanisms, which prevail during the decline phase.

In another experiment the survival time was kept constant (40 minutes after the beginning of the stimulus, which was initially thought to correspond to the peak of the response) and the duration of the playback was varied (0, 10, 20, 30 or 40 minutes of the same tape as in the previous experiment, figure 4.13). The results show that there is a cumulative effect of increasing the playback duration. This effect could be due, in part, to the latency for the build-up of mRNA levels observed in figure 4.12; but comparing, for instance, ZENK levels in this and the previous experiment at minutes 30 or 40, it is clear that a higher level was reached when the stimulus duration was longer (30 or 40, as compared to 10 minutes). These results also show that the experience the animals undergo during the last 10 or 20 minutes contributes significantly to ZENK levels at the time of sacrifice. Even though there is a trend, it is unclear whether the difference between 30 and 40 minutes is significant.

In order to investigate both the decline in ZENK mRNA levels and the possibility of a refractory period for ZENK induction, still another experiment was conducted. As described above, ZENK mRNA is short-lived after a short playback - i.e., a playback that stopped long before the induction reached its peak. In the present experiment, the playback duration was varied and animals were sacrificed at the end of playback (figure 4.14). At 30 minutes ZENK mRNA levels were high, after which levels declined sharply, and from 1 1/2 hour on

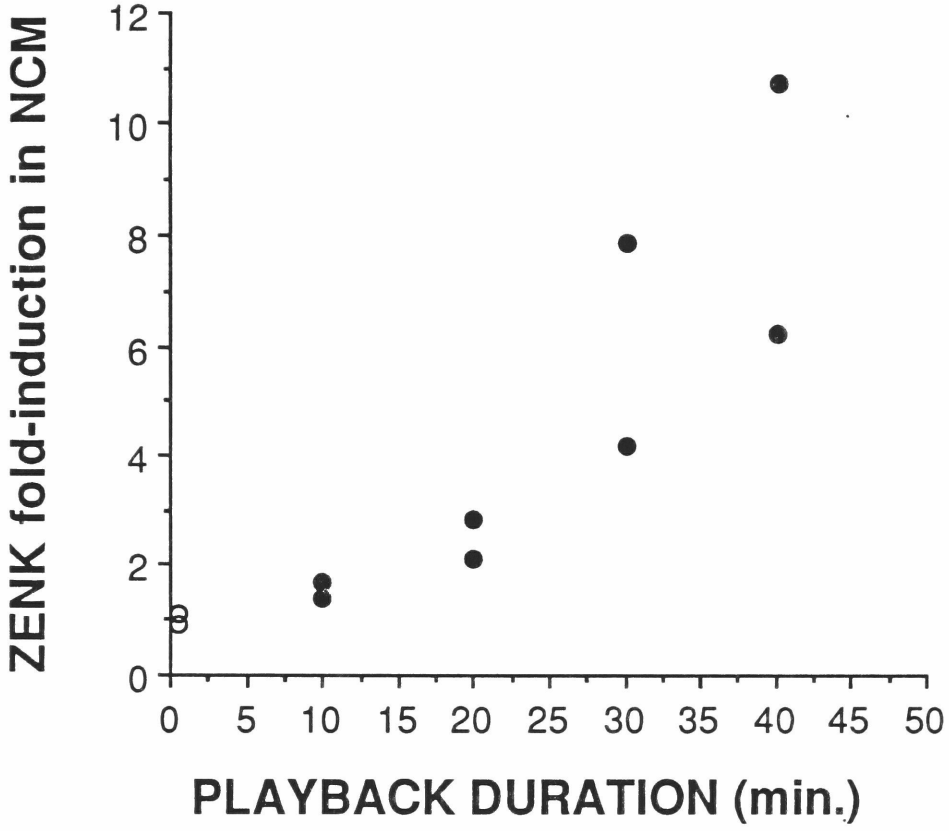

FIGURE 4.13 - Time-course of ZENK mRNA induction: effect of playback duration. ZENK fold-induction in NCM of zebra finches is plotted as a function of playback duration. All animals were sacrificed at time=40min.; frozen brain sections were then hybridized with ^{35}S-labeled riboprobes for ZENK and exposed to X-ray films. Optical density measurements were taken from autoradiograms in an area corresponding to NCM, as depicted in figure 4.4 and normalized to levels in unstimulated controls. Dots represent individuals (n=2/time point); silent controls are plotted as open circles at time=0.

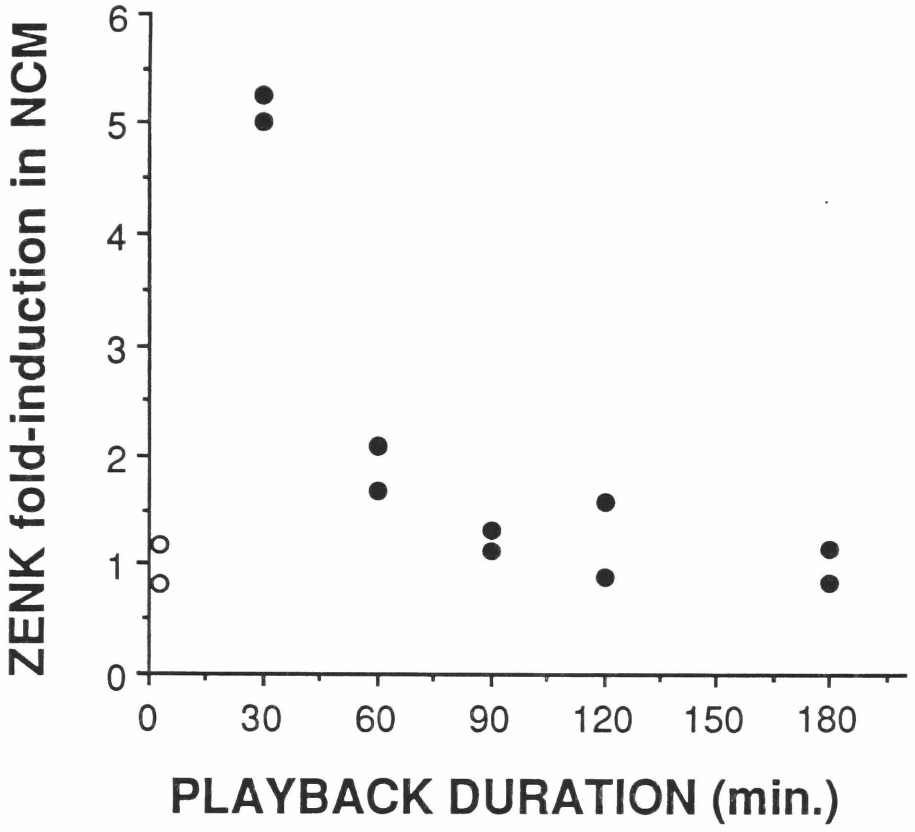

FIGURE 4.14 - Time-course of ZENK mRNA induction: decrease after long continuous playback. ZENK fold-induction in NCM is plotted as a function of playback duration. All animals were sacrificed at the end of playback; frozen brain sections were then hybridized with ^{35}S-labeled riboprobes for ZENK and exposed to X-ray films. Optical density measurements were then taken from autoradiograms in an area corresponding to NCM, as depicted in figure 4.4 and normalized to levels in unstimulated controls. Dots represent individuals (n=2/time point); silent controls (n=4) are plotted as open circles at time=0.

they were indistinguishable from basal levels. This demonstrates that the ZENK response is transitory even when the stimulus is continuously presented and suggests that the system has entered a refractory phase (but see section 4.5 in this chapter).

4.4 - HABITUATION OF THE RESPONSE/ EFFECT OF NOVELTY

In another experiment, the effect of familiarity/novelty of the song on ZENK induction in NCM of zebra finches was tested by studying the effect of previous presentation of one particular song on ZENK induction in response to the same song or to another song. The experiment was divided into three phases (figure 4.15, upper panel): 1- 24-hour isolation in sound-proof chambers (the same for all animals); 2- playbacks of one unfamiliar zebra finch song (S1) for one hour, 3 times a day for 5 days (S1 duration was about 15 seconds, followed by 45 seconds of silence, repeated every minute; birds were thus exposed to a total of 3.7 hours of tape-recorded song during this period); 3- on day 6, either S1 or S2 (another unfamiliar zebra finch song from another individual, matched with S1 for duration) was presented for 30min., and immediately thereafter the bird was killed. Birds were divided into five groups, **A** to **E** (see figure 4.15, upper panel, for diagram), corresponding respectively to birds that heard no stimulus (**A**), heard S1 only on days 1-5 (**B**), heard S1 on days 1-5 and again on day 6 (**C**), heard S1 only on day 6 (**D**) or heard S1 on days 1-5 and S2 on day 6 (**E**). Normalized fold-induction levels in NCM for all groups are shown in figure 4.15, lower

FIGURE 4.15 - Upper panel: Schematic diagram representing the experimental design described in the habituation/novelty section. The horizontal axis represents the time scale (days). The experiment was divided into three phases: 1- 24-hour isolation in sound proof chambers (the same for all animals); 2- repeated playbacks of S1 for five days; 3- playbacks of S1 or S2 for 30 minutes, immediately followed by sacrifice. Birds were divided into five groups, **A** to **E**, corresponding to birds that heard no stimulus (**A**), heard S1 only on days 1-5 (**B**), heard S1 on days 1-5 and on day 6 (**C**), heard S1 only on day 6 (**D**) or heard S1 on days 1-5 and S2 on day 6 (**E**).

Lower panel: Comparison of normalized ZENK fold-induction levels in NCM for the groups described above; open circles represent individuals and the columns represent averages.

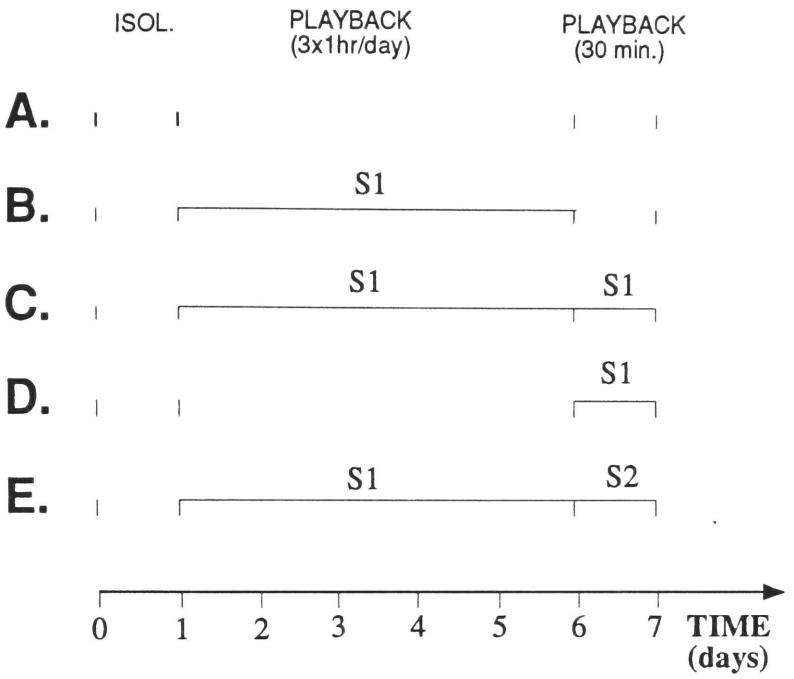
ISOL.
PLAYBACK
(3x1hr/day)
PLAYBACK
(30 min.)
A.
B.
S1
C.
S1
S1
D.
S1
E.
S1
S2
0
1
2
3
4
5
6
7
TIME
(days)

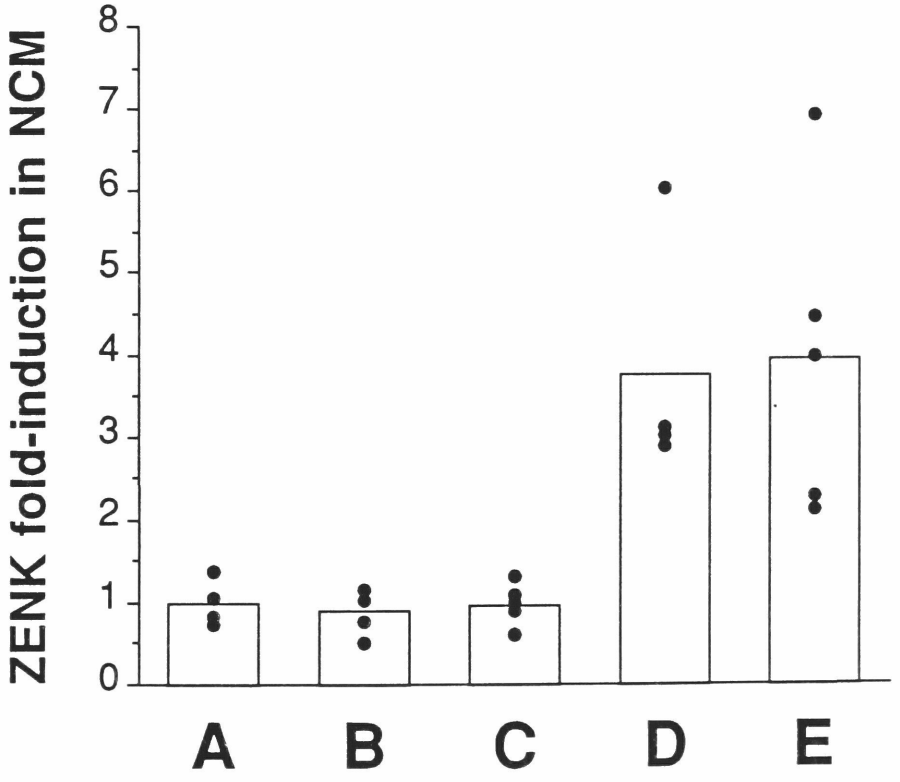
ZENK fold-induction in NCM
0
1
2
3
4
5
6
7
8
A
B
C
D
E

panel. Using the Mann-Whitney U test, no significant differences are seen either for groups **B** or **C** when compared with **A** or between groups **D** and **E**. Differences were significant (criterion of $P<0.05$, two-tailed probabilities) for groups **D** ($n=4$, $U=0$, $p=0.021$) when compared with **A** or **B** ($n=4$) and for **D** ($U=0$, $p=0.014$) and **E** ($U=0$, $p=0.009$) when compared with **C** ($n=5$).

The difference between groups **A** and **D** represents a replication of results obtained previously (ZENK induction in response to song presentation, as shown in the preceding sections). Group **B** served as a control to test for changes in ZENK basal levels due to presentation of S1 during days 1-5 (no effect observed). The first striking effect observed in this experiment is the difference between groups **C** and **D**: the induction response is absent in group **C**, which was previously exposed to the test song (S1) and ZENK levels in this group are indistinguishable from control groups **A** and **B**. The second effect observed is the induction in group **E**, the group that was exposed to S2 on the last day, after previous exposure to S1 during days 1-5.

These results clearly show that ZENK induction is dependent on previous auditory experience. Thus, pre-exposure to a specific song stimulus abolishes the induction response for that same song: this effect seems to be a good candidate for a molecular correlate of habituation to an auditory stimulus. The two groups where a significant induction was observed consist of birds exposed to a novel stimulus, either S1 for birds that had not heard it before (group **D**) or S2 for birds habituated with song 1 (group **E**).

An interesting aspect of these results is the considerable spread of values observed both for groups **D** and **E** in this experiment and for

groups that heard conspecific song in previous experiments (figures 4.10 and 4.11). This spread of values suggested that there might be other variables which were uncontrolled for in these experiments. Although all songs used (with the exception of the first experiment, where the tapes included the BOS) were unfamiliar to the birds (songs from other aviaries), it is possible that part of this variability could reflect the degree to which the presented songs are similar to either songs the birds are familiar with or to their own songs. The habituation results suggest that higher similarity to familiar songs or to BOS (based, for instance, on the occurrence of the same or similar syllables or syllable groups) may result in lower levels of ZENK induction.

4.5 - REFRACTORINESS OF ZENK INDUCTION

IEG induction is usually transient and followed by increases in the levels of the specific proteins these genes encode (Bartel et al, 1989; Sonnenberg et al., 1989a). Proteins are usually detected within 30 minutes after stimulation and elevated levels can persist for as long as 8 to 10 hours, depending on the nature and intensity of the stimulus (Sonnenberg et al., 1989a). Many IEGs encode transcription factors that can bind to their own promoters as well as to the promoters of other IEGs; this binding has been hypothesized to have a negative regulatory effect on transcription in order to explain the rapid decreases in IEG levels following their induction peaks (McMahon and Monroe, 1992). Although data about protein levels in this system is not yet available (no specific binding was detected in

immunocytochemical staining with songbird brain tissue using an antibody raised against the rat form of ZENK), ZENK protein levels are most probably also increased for a certain time following the song stimulus.

To test whether there exists any refractoriness in the ZENK induction response after exposure to a particular song stimulus, and to try to simplify the protocol for the study of song habituation/discrimination as described in the previous section, a similar experiment with a shorter time-scale was performed, the duration of previous exposure to song being 2 1/2 hours. The birds were divided into five basic groups, from **A** to **E** (figure 4.16), representing respectively animals exposed to silence (**A**), S1 (**B**) or S2 (**C**) during the last 30 minutes before sacrifice, S1 for three hours (**D**) or S1 for 2 1/2 hours and then S2 for 30 minutes (**E**); in two additional groups the duration of the playbacks was the same as in groups **D** and **E** but the order of the songs was inverted (**F** and **G**, exposed to S2 and S2/S1 respectively). S1 and S2 are the same as in the previous experiment.

Examples of autoradiographic patterns at the level of NCM from one bird in each of the first five groups (**A** to **E**) are shown in figure 4.17. The results of quantitative analysis in NCM are shown in figure 4.16. S1 (**B**) and S2 (**C**) raised ZENK expression to about the same range of levels. Continuous exposure to the same song stimulus (S1) for three hours (**D**) results in ZENK mRNA levels that are comparable with the unstimulated control group (**A**, also compare this result with figure 4.14, 180 minutes), indicating that ZENK levels have dropped down to basal levels. Group **E**, however, was exposed to a different

FIGURE 4.16 - Comparison of normalized ZENK fold-induction levels in NCM for the experiment described in section 4.5. The experiment was divided into three phases: 1- 24-hour isolation in sound proof chambers (the same for all animals); 2- continuous playback of S1 for three hours; 3- playbacks of S1 or S2 for 30 minutes, immediately followed by sacrifice. The birds were divided into seven groups, from **A** to **E**, representing respectively animals exposed to silence (**A**), S1 (**B**) or S2 (**C**) during the last 30 minutes before sacrifice, S1 (**D**) or S2 (**F**) for three hours or S1 for 2 1/2 hours and then S2 for the last 30 minutes (**E**) or vice-versa (**G**); S1 and S2 are the same as in the previous experiment (section 4.4); open circles represent individuals and the columns represent averages.

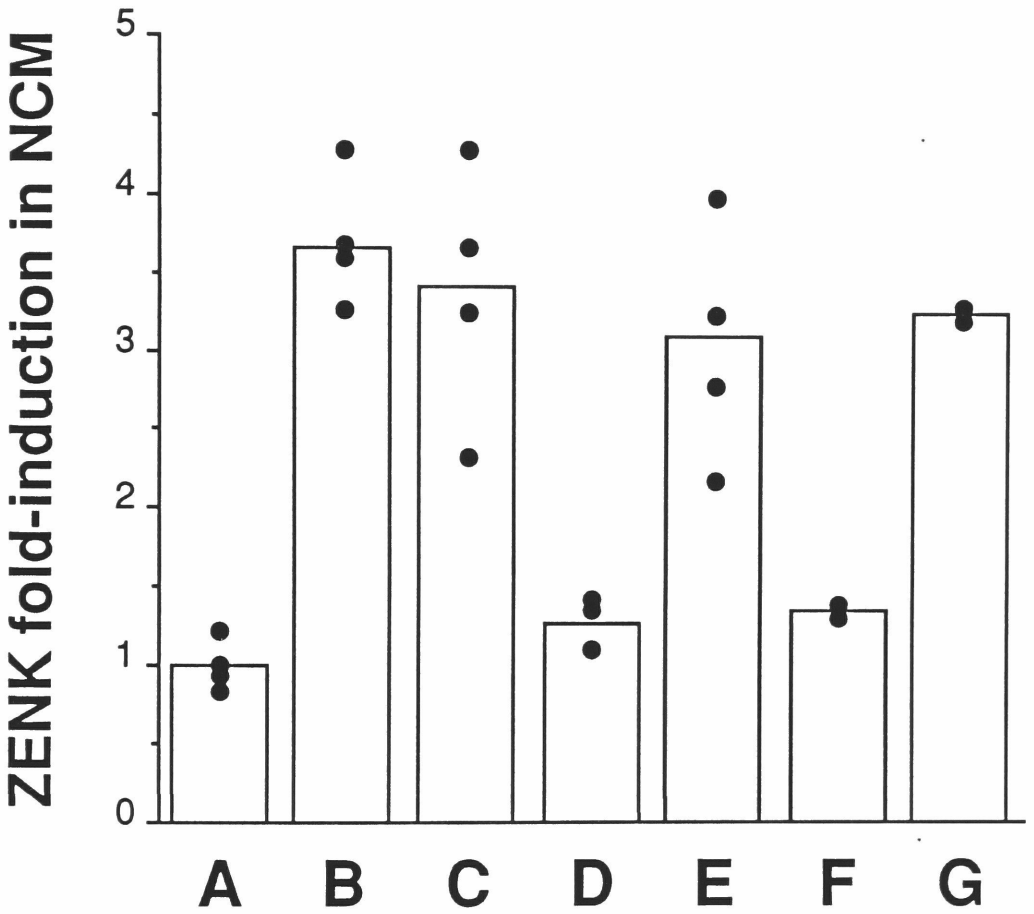
ZENK fold-induction in NCM
5
4
3
2
1
0
A
B
C
D
E
F
G

FIGURE 4.17 - ZENK mRNA induction in the zebra finch brain following exposure to song; digitized images are shown of in situ autoradiograms of parasagittal sections at a level slightly more medial than the diagram in figure 4.4. Panels A to E correspond to sections from birds in groups **A**, **B**, **D**, **C** and **E** respectively, as described in figure 4.16.

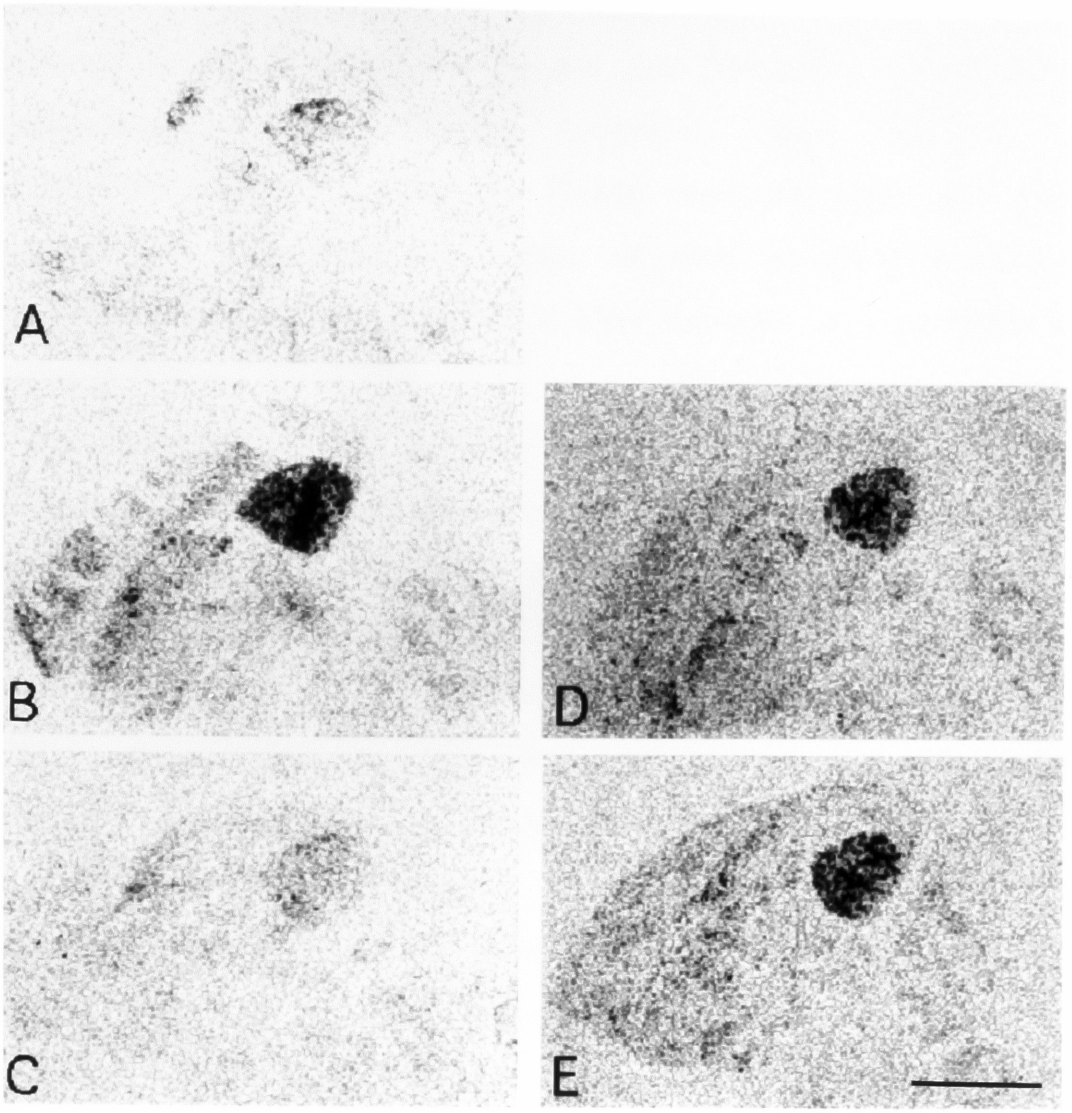
A
B
C
D
E

song, S2, during the last half hour of the stimulation period; ZENK levels in this group are comparable with levels in birds exposed to either song for 30 minutes only (**B** and **C**). The same results are seen in froups **F** and **G**. These results show that: 1- S1 and S2 are equally effective in inducing ZENK; therefore, the results of the experiment described in the last section are not just the result of S2 being a particularly more effective stimulus than S1; 2- the habituation/novelty effect can be further explored using this simpler paradigm; 3- there does not appear to exist an absolute refractory period for ZENK induction in NCM after exposure to a particular song stimulus.

To further clarify the meaning of these results, an analysis at the cellular level was performed by counting the number of labeled cells and comparing with the total number of cells. This analysis is rendered particularly difficult due to the cell clustering typical of the avian brain; in many cases, however, there were clear examples of ZENK induction occurring in a single cell or in a few cells within a cluster, whereas other cells within the same cluster were unlabeled. The results are shown in Table 1. Cell counts were done in two birds from each of the first five groups; numbers represent the sum of cells counted in 5 randomly chosen fields of 87x120μm within NCM. The percentage of labeled cells is similar for birds in groups **A** and **D** (between 5 and 8.5%), or for groups **B**, **C** and **E** (between 42 and 54%).

A very large number of cells (around 50%) is thus activated in NCM by a particular song stimulus. It is interesting to note that estimates of the number of activated cells in the initial experiments,

	Labeled Cells	Total Cells	% Labeled Cells
A	7	128	5.47
(control)	11	133	8.27
B	54	109	49.54
(S1)	70	142	49.30
C	46	108	42.59
(S2)	71	130	54.61
D	6	99	6.06
(S1/S1)	9	111	8.11
E	60	127	47.24
(S1/S2)	52	113	46.02

TABLE I - Percentage of labeled cells in NCM following song presentation as described in section 4.5; values for two birds are shown in each group.

when various song stimuli were presented to each bird, were even higher (on the order of 95%, see figure 4.5). This suggests that the response to various stimuli presented to the same bird represents, in part, the summation of the response to each individual stimulus. It also indicates that some cells may be preferentially or specifically activated by a particular song type or by specific elements such as syllables or combinations of syllables present in particular songs; by simultaneously presenting a large variety of song types, a vast range of such specific elements may be covered, which results in a higher induction response. Individual songs, however, activate a smaller number of cells, as observed.

The percentages seen for groups **B**, **C** and **E** also suggest that there probably are cell populations in NCM that can respond equally well to more than one particular song stimulus (in these experiments, either S1 or S2); in other words, there most probably is an overlap in the cell populations responding to S1 or S2. Furthermore, the population of cells responding to S2 is not affected by previous presentation with S1 (compare groups **C** and **E** in figure 4.16 and Table 1). This indicates that cells that respond to a particular song stimulus do not enter an absolute refractory period after presentation of that particular song; these cells can still show an induction response to a new stimulus to which the bird had not been exposed.

The results presented in this and in the previous section generally show that previous or continuous exposure to a particular song stimulus abolishes the genomic response to that particular stimulus but does not affect the tissue response to another stimulus. One can

hypothesize several different mechanisms leading to this effect and which represent various levels in the pathway from the auditory stimulus to the gene induction event: 1- habituation could occur in the auditory periphery or in the stations of the ascending auditory pathways, by physiological mechanisms that decrease the response of cells to repeated, unreinforced auditory stimuli; the drop in ZENK induction could thus reflect a drop in the levels of stimulation reaching NCM cells (notice that this could not be a generalized decrease but would have to be specific for cells responding to a particular song type; such degree of specificity is not usually thought of as occurring in low auditory centers); 2- habituation could occur in cells within NCM; in this case, it is hypothesized that habituation to one or the other stimulus can occur independently in cells responding to both stimuli (for instance, by spatial segregation of the dendritic branches and/or signalling mechanisms such as receptors or kinases that get activated by each stimulus alone); 3- habituation at the gene promoter level: even though this level of regulation cannot be ruled out, it seems unlikely that recognition of specific songs are tightly coupled with transcriptional mechanims; it seems more likely that differential ZENK expression is a reflection of recognition events that occur at the level of whole neurons or circuits.

4.6 - INDUCTION PATTERNS IN JUVENILES

Experiments with juvenile zebra finches were initiated with the purpose of addressing two main issues:

1) What are the ZENK induction patterns during the time when young songbirds acquire the model that they will imitate later? Of particular interest was the question whether there are any times during development when ZENK might be inducible within the song control nuclei, for instance, at times when song learning occurs. The zebra finch, the reader will recall, is a sensitive period learner and the song learning period is usually thought to extend from day 25 to 60 (Morrison, 1992). Playbacks were performed to birds at various ages during this period (32, 45 and 60 days) and a similar induction pattern as in adults was found, that is, a marked induction in NCM, the HVC shelf and the RA cup, with the following differences: a) basal levels are usually higher in juveniles than in adults, which results in a lower fold-induction and makes the assessment of any effect more difficult; b) the anatomical boundaries of regions in which song playbacks cause ZENK induction are less defined than in adults, possibly covering larger areas of the caudal neostriatum; c) induction was very pronounced in structures like the shelf and the cup, even more so than in adults. No obvious differences in ZENK induction are seen between the song control nuclei of adults and juveniles (ZENK induction is absent in both cases), at least at those ages when these nuclei are recognizable by cresyl-violet staining.

These results are thus comparable with results from metrazole experiments, where no differences in the induction patterns between adult and juvenile zebra finches was observed. The possibility still remains that a combination of stimuli of various sensory modalities may be necessary for ZENK induction in a nucleus like HVC. Indeed, song learning in finches seems to be critically dependent on social

interactions and there is no evidence that imitation can occur solely as a result of exposure to tape-recorded song; other cues such as visual or tactile, which are present in the natural interactions between juveniles and parents or tutors, may be essential for both song learning and ZENK expression in the song control circuit.

Another possibility is that ZENK repression is a distinctive feature of these brain areas, irrespective of age or hormonal status, which is developmentally regulated by some very early process or event. It would be interesting to investigate whether young brain cells express the gene at an earlier age, before they become committed to or enter the differentiation pathway that turns them into cells of the song control circuit - i. e., before they become recognized by morphological or connection criteria as HVC cells, for instance. Nevertheless, it is also possible that a particular - and as yet unidentified set of genes - may be induced in these areas in response to depolarization.

Taking into account the hypothesis that ZENK induction may correlate with plastic changes affecting circuit performance and possibly underlying the formation of memories, an interesting interpretation of these initial findings in juveniles is that the critical events related to the formation of memories related to song do not occur at the level of the song circuit but at levels that precede it. In that case, a shift of emphasis towards areas more closely related to perceptual processes and auditory discrimination might be extremely informative.

2) Another important aspect of the work in juveniles which we have not yet addressed is whether the preference for conspecific

song (as expressed by levels of ZENK induction in NCM) is innate or dependent upon previous auditory experience.

4.7 - SEASONAL COMPARISON IN CANARIES

In order to test whether ZENK levels after song presentation are seasonally regulated within the song control circuit, ZENK expression patterns were studied in canaries in the Spring and in the Fall (n=6 for each group), with particular attention to HVC, where seasonal and hormonal effects on cell size and shape are well documented (Nottebohm, 1981 and 1989). No significant differences are seen between the two groups by visual examination of autoradiograms; for instance, in both groups HVC is negative for ZENK, although signal can be seen in the surrounding tissue or shelf. This reinforces the idea that ZENK is repressed in HVC, irrespective of age or season.

Seasonal regulation of HVC size, as seen in cresyl-violet stained sections in canaries, may be achieved in part by incorporation of adjacent or shelf cells into HVC and the motor pathway circuitry (Gahr, 1990). In this case, the area in the dorso-caudal neostriatum that shows low ZENK signal after song (corresponding to the area where the large HVC cells and clusters are seen in cresyl staining, as in figure 4.8) may also show seasonal fluctuation in size, but this awaits a finer anatomical analysis.

4.8 - EXPERIMENTS WITH SONG SPARROWS

In order to test whether ZENK induction in response to song also occurs in a natural situation and is not just the result of the use of artificial conditions such as isolation or stress due to confinement, some field experiments were performed. Song sparrows were chosen, for the following reasons: 1) it is a common species and a few specimens could be collected without any ecological danger; 2) male song sparrows are very territorial during the breeding season and show a well-defined behavioral response to the presence of unfamiliar conspecifics: the bird approaches the source of an unfamiliar sound (another singing male who invades his territory) and attacks in an attempt to scare away the intruder; this response can also be obtained when playbacks of conspecific songs are used (Wingfield and Wada, 1989); 3) a hormonal response indicating activation of the hypothalamo-pituitary axis and represented by a sharp increase in blood testosterone levels is seen within 20 minutes after beginning of playbacks (Wingfield and Wada, 1989).

Two males were captured within their natural territories after playbacks of tape-recorded song from three different individuals for thirty minutes. During the playback, the birds presented the stereotypical behavior of localizing the sound source, approaching and then actively searching for an intruder male; this behavior did not show any signs of habituation during the whole duration of the playback. The birds were sacrificed immediately upon capture (which occurred within five minutes after the end of playbacks) and the brains were dissected and frozen. Two control birds that did not

hear any playbacks were captured within their natural territories. All birds were uncontrolled for the experience previous to the playbacks, which were performed between 10am and 1pm.

The playbacks resulted in about a two-fold induction of ZENK within NCM. This value may still be an underestimate of ZENK fold-induction, since one of the control birds had particularly high ZENK levels within NCM and one experimental had high levels in the hippocampus, which was used for normalization; the values did not overlap, though. This spread of ZENK values could represent differences due to variation in recent experience (for instance, birds could have just been engaged in territorial defense or mating behavior) but that awaits further experiments with more birds under various conditions. Nevertheless, the results indicate that ZENK induction in response to song presentation can occur in the life of a freely ranging and behaving animal; this is the first step to determine whether it could play any role in the regulation of natural behaviors.

4.9 - OTHER GENES

Expression of other inducible genes such as c-jun, n-myc and c-myc, for which a canary probe is available, were also analysed. Of these, a significant increase was detected only in c-jun levels whereas the other genes seemed not to respond to song presentation (data not shown). The increase in c-jun expression was small, though, and more prominent in canaries than in zebra finches (not shown). The anatomical pattern of expression is very similar to ZENK at the

NCM level, although a more extensive anatomical characterization is still needed.

Induction of GAP-43 was tested both after 30 minutes or after three hours of continuous song presentation, but no increase was detected. It should be noted that the GAP-43 gene is considered a late response gene and is characterized by a delayed induction response in paradigms such as kindling or treatment of PC-12 cells with nerve growth factor and may indeed be a target for some IEGs (Karns et al, 1987; Milbrandt, 1987). It remains to be determined whether a gene like GAP-43 can be induced at later time points following song presentation.

4.10 - SUMMARY AND CONCLUSIONS

In this chapter, birdsong, a natural stimulus of known physiological and behavioral relevance, is shown to induce ZENK expression to high levels in the intact songbird telencephalon, without the need for electrical or noxious stimulation or pharmacological manipulation. Using ZENK induction as a mapping tool for areas activated by song presentation, a marked and transient induction is demonstrated in caudo-medial parts of the songbird telencephalon. ZENK induction is notably absent in the primary auditory zone and in the nuclei of the motor pathway for learned vocalization but occurs in regions closely adjacent to these and which may represent higher-order auditory processing areas and/or an interface between the auditory and motor systems.

A detailed analysis of specificity, induction kinetics and habituation/novelty effects is described for one particular area, NCM, where the most robust and consistent response occurs. The best stimulus was conspecific song, compared with heterospecific song or artificial stimuli and the response depended on previous auditory experience, being higher for unfamiliar songs and showing habituation after repetitive presentations of the same song. Cells expressing ZENK in response to a particular song do not seem to enter an absolute refractory period, and can still show a genomic response to another song.

ZENK induction occurs in a subset of depolarized areas, and cellular activation does not seem to be sufficient; rather, a combination of auditory stimulation and other factors such as the simultaneous activation of other sensory modalities or more general mechanisms such attention, arousal or even stress (triggered by novelty) may be necessary. This could be translated physiologically by the simultaneous activation of multiple pathways representing various aspects of the stimulus presentation that somehow converge onto those areas showing ZENK induction in this paradigm.

Together with the metrazole experiment (chapter 3), the results presented here contradict the hypothesis that ZENK induction is part of a general homeostatic or signal-response mechanism that occurs whenever cells are physiologically activated. The fact that many IEGs including ZENK encode transcription factors which may be actively engaged in the transcriptional regulation of other genes, has led investigators to postulate that IEGs could be mediators of long-lasting changes in response to extracelular stimuli. If this is the case, areas

revealed by ZENK induction could specifically correspond to areas where plastic changes occur in response to external stimulation. This can now be tested by examining whether physiological modulation (potentiation/depression) of auditory responses and/or morphological changes (in dendrites, synaptic density and size, etc.) also occur in response to song in areas showing a high ZENK induction, as opposed to areas negative for ZENK.

The studies described above have raised an essential question that is addressed in the next two chapters, namely, what are the connections of areas showing ZENK induction in response to song, and how do they relate to primary auditory and motor areas.

CHAPTER 5: ANATOMICAL CONNECTIVITY OF AREAS REVEALED BY ZENK INDUCTION: NCM

INTRODUCTION

As described in the preceding chapter, song presentation leads to ZENK induction in the songbird forebrain. The most marked effect is observed in the medial portions of the caudal neostriatum, which has been called NCM. This came initially as a surprise, because NCM is not part of the song control pathway or of Field L, the primary forebrain target area of the auditory thalamus, both of which have been shown to respond to song stimuli (Katz and Gurney, 1981; Margoliash, 1983 and 1986; Margoliash and Konishi, 1985, Williams and Nottebohm, 1985). NCM, defined according to ZENK expression patterns, includes a relatively large area of the caudal forebrain and does not correspond to a particular or discrete nucleus; this region could indeed be composed of several smaller nuclei or subfields, as occurs in the adjacent Field L.

In the present chapter are described studies using neuroanatomical tract-tracing methods to establish the connectivity of NCM, defined as the high density region in the ZENK mapping experiments (as described in chapter 4). The main purposes of this analysis are: 1) to investigate whether NCM has any connections with auditory areas which could explain its activation by song stimuli; 2) to verify whether NCM somehow contributes an input to the song control circuit and could thus be part of an interface between the sensory and motor systems for song.

METHODS

Animals and surgery.

A total of 22 adult zebra finches of both sexes (older than 90 days, 12 males, 10 females) was used. All intracranial tracer injections were made in birds that had been deprived of food for 30 minutes, then deeply anesthetized with intramuscular injections of Ketamine (30mg/kg) and Xylazine (40mg/kg). The head of the animal was held in a stereotaxic instrument while injections were made. A scalp incision exposed the skull and small openings in the skull revealed the surface of the brain at the desired point of entry. Stereotaxic coordinates used for NCM were: +0.5 to +1.5 AP, 0.5 to 2.0 DV and 0.1 to 0.4 ML on either side; coordinates for area X were: +3.3 to +4.2 AP, 3.8 to 4.2 DV and 1.4 ML. Following tracer injection, the lips of the scalp were closed using Collodion (Merck). Birds were placed by a heat source during the recovery period, until they had fully regained their vigor. After the adequate survival, birds were killed by an overdose of anesthesia and perfused transcardially with 0.1M PBS, followed by the appropriate fixative.

Tracers.

Anterograde projections were traced using either of two substances, Phaseolus vulgaris leucoagglutinin (PHA-L) (Gerfen and Sawchenko, 1984) or biocytin (King et al., 1989; Izzo, 1991), both injected by iontophoresis using micropipette tips of 10-20μm. It proved easier to make very small injections of biocytin - e.g. with a spread of approximately 100μm in diameter - than of PHA-L; consequently, PHA-L injections were used when the intention was to

cover larger areas. Injections of PHA-L lasted from 5-15 minutes and used 3-5μA of cathodal current in 7s-on-7s-off cycles. Biocytin (5% in sodium methyl-sulphate) injections varied from 10-30 minutes using 3-5μA with the same pulsing cycle as for PHA-L. These parameters were chosen to minimize transport by fibers of passage (Gerfen and Sawchenko, 1984). Survival times were 22-26 hours (biocytin) or 7-10 days (PHA-L). In some cases, for very large or odd-shaped targets, a few small injections were made.

Processing of tissue for PHA-L was performed essentially as described in Simpson and Vicario (1991). Brains were fixed by perfusion with periodate/lysine/paraformaldehyde (McLean and Nakane, 1974), removed from skull and placed in the same fix overnight at 4°C. The next day, 50μm sections were cut on a vibratome and collected in 0.1M PBS, pH 7.4. After several changes of buffer, sections were soaked for 2 hours in 0.1% TritonX-100/3% skim milk/0.1M PBS (TrisX/SM/PB); they were then incubated for 18 hours at room temperature under agitation in a 1:2000 dilution of goat anti-PHA-E+L (Vector) in TrisX/SM/PB. After 30 minutes of rinsing with SM/PBS, sections were incubated for 2 hours in a 1:300 dilution of anti-goat IgG (Vector) in TrisX/SM/PB. After 30 minutes of rinsing with SM/PBS (last wash only PBS), sections were incubated for 2 hours in either the Vectastain ABC reagent (Vector) or streptavidin-peroxidase complex (Amersham), 1:300 dilution. After 30 minutes of rinsing with PBS, sections were incubated for 5-30 minutes in 30ml of PB containing 0.2mg/ml of diaminobenzidine (DAB), 100μl of 0.3% hydrogen peroxyde and 1.33mg/ml of

Nickelous Ammonium Sulfate to intensify the DAB reaction product of the peroxidase reaction.

Brains injected with biocytin were fixed by perfusion with 4% paraformaldehyde/1% glutaraldehyde, removed from the skull, post-fixed in the same fixative for a few hours at room temperature and cut on a vibratome or stored in 0.1M PBS at 4°C. 50µm sections were incubated with 1% Triton-X in 0.1M PBS for two hours and then incubated with ABC reagent (Vector) or streptavidin-peroxidase complex (Amersham), 1:300 dilution, for 2 hours to overnight. This was followed by 3 washes of 10 minutes with PBS and incubation with DAB, intensified with Nickelous Ammonium Sulfate (as above). After rinsing for 30 minutes in PBS, all sections were mounted onto chromalum slides, dehydrated in alcohol, delipidized in xylene and coverslipped. When necessary, sections were counterstained with cresyl-violet; in some cases, adjacent sections were also stained.

Pathways were traced <u>retrogradely</u> by using pressure injections of either the fluorescent retrograde tracer fluorogold (Schmued and Fallon, 1986) or fluorescent latex microspheres (Luma Fluor Inc., Katz at al. 1984). The latex microspheres or beads show the least spread from the point of injection and therefore are particularly adequate for backfilling projections that end in small nuclei. Pressure injections used micropipette tips of 20-30µm (fluorogold) or 25-40 (beads) and injected volumes varied from 10-50nl. To minimize leakage of beads along the injection tract, a "sandwich" technique was often used, in which the exact volume to be injected is aspirated between two layers of mineral oil, taking care to avoid air bubbles in the interfaces; micropipettes were slowly withdrawn 5-10 minutes

after injection. Survivals were of 4-7 days and brains were fixed in 4% paraformaldehyde and sectioned (30 μm) with a vibratome or a freezing microtome after cryoprotection (by equilibration with 30% sucrose in fixative). Mounted sections were inspected using filters of the appropriate wavelength.

RESULTS

Injections into NCM were done bilaterally in most birds and criterion for targetting was based on examination of parasagittal sections. Since no stereotaxic data were previously available, a large range of coordinates had to be gradually adjusted for centering injections in the most caudal parts of NCM, avoiding Field L and HV, as seen in figure 5.1.

Injections of retrograde tracers

Two in six injections of fluorogold were restricted to the caudal portion of NCM and completely respected Field L (as shown in figure 5.1. In these brains, backfilled cells are seen in the thalamus, in the periphery of nucleus ovoidalis, as a rim of cells that seem to respect the central portions of this nucleus (figure 5.2A, B and D). Cells are also seen along the tractus ovoidalis, antero-ventrally to nucleus ovoidalis (figure 5.2C). This is in sharp contrast to injections including or centered in L2, which result in backfilled cells within nucleus ovoidalis (figure 5.2E).

After injections restricted to NCM, numerous backfilled cells are also seen in the HV that is closely adjacent to LH and NCM (figure 5.2F); these cells were restricted to the caudal portions of HV. Backfilled cells are also seen in the caudal portions of the paleostriatal complex, predominantly PA, where it is in close apposition to the Field L complex (not shown); other labeled cells are seen within portions of Field L, but the analysis of these cells is complicated by the proximity to the injection site, due to radial

FIGURE 5.1 - Schematic diagrams of parasagittal sections at the level of NCM showing sites of injections of anatomical tracers centered in Field L2a (shadowed area on the left in the lower diagram) or in the caudal portion of NCM (shadowed area on the right in the lower diagram). Cb, Cerebellum; Hp, Hippocampus; Hv, Hyperstriatum ventrale; L2a, subfield L2a of Field L complex; NCM, caudo-medial Neostriatum; P, Paleostriatum; T, Thalamus. Orientation: dorsal is up and anterior is to the left.

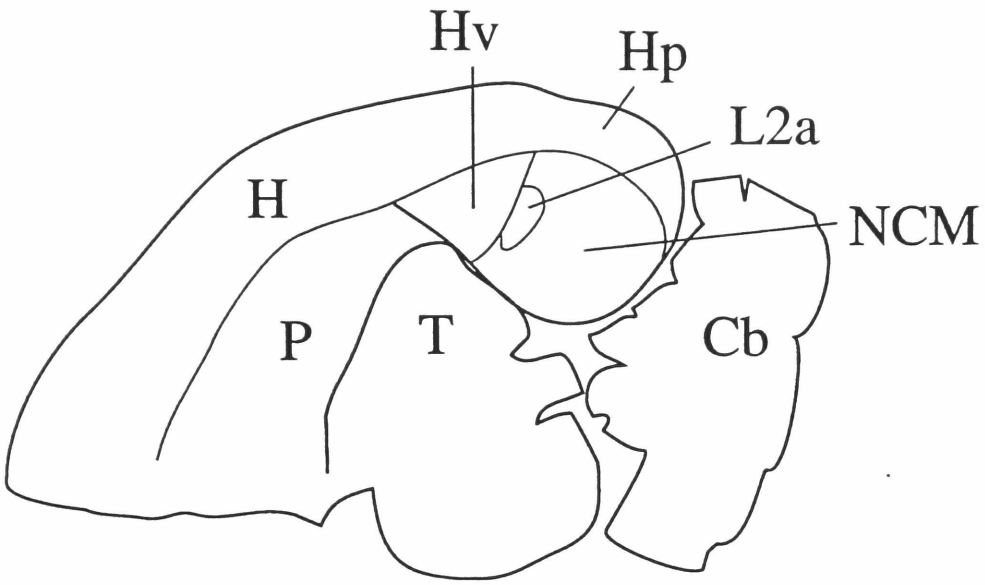
Hv
Hp
L2a
H
NCM
P
T
Cb

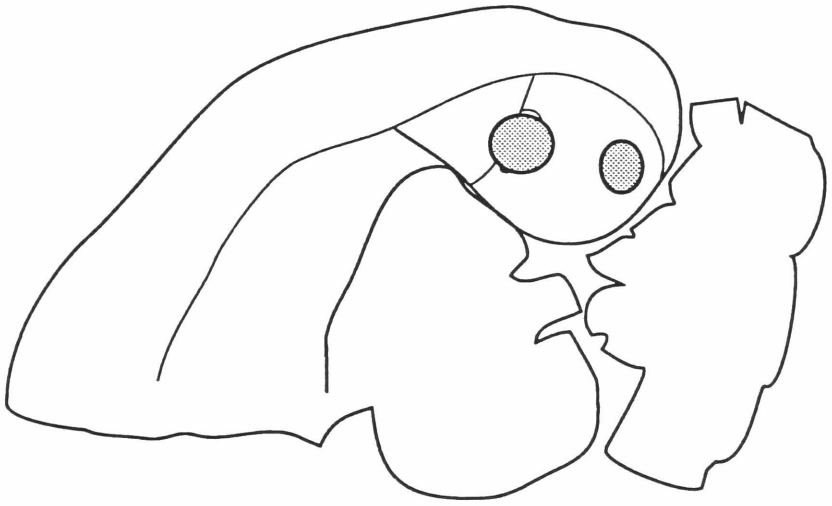

FIGURE 5.2 - Retrogradely-labeled cells after injections of fluorogold in NCM. (A) to (C) Series of parasagittal sections demonstrating backfilled cells in close relation with nucleus ovoidalis (Ov) and the tractus ovoidalis. (D) and (E) Comparison of patterns of backfilled cells in ovoidalis after injections of fluorogold centered in NCM (D) or in Field L (E). (F) Backfilled cells in caudal HV after injection of fluorogold centered in NCM. Bar sizes: (A) and (B), 100μm; (C) and (F), 100μm; (D) and (E), 80μm.

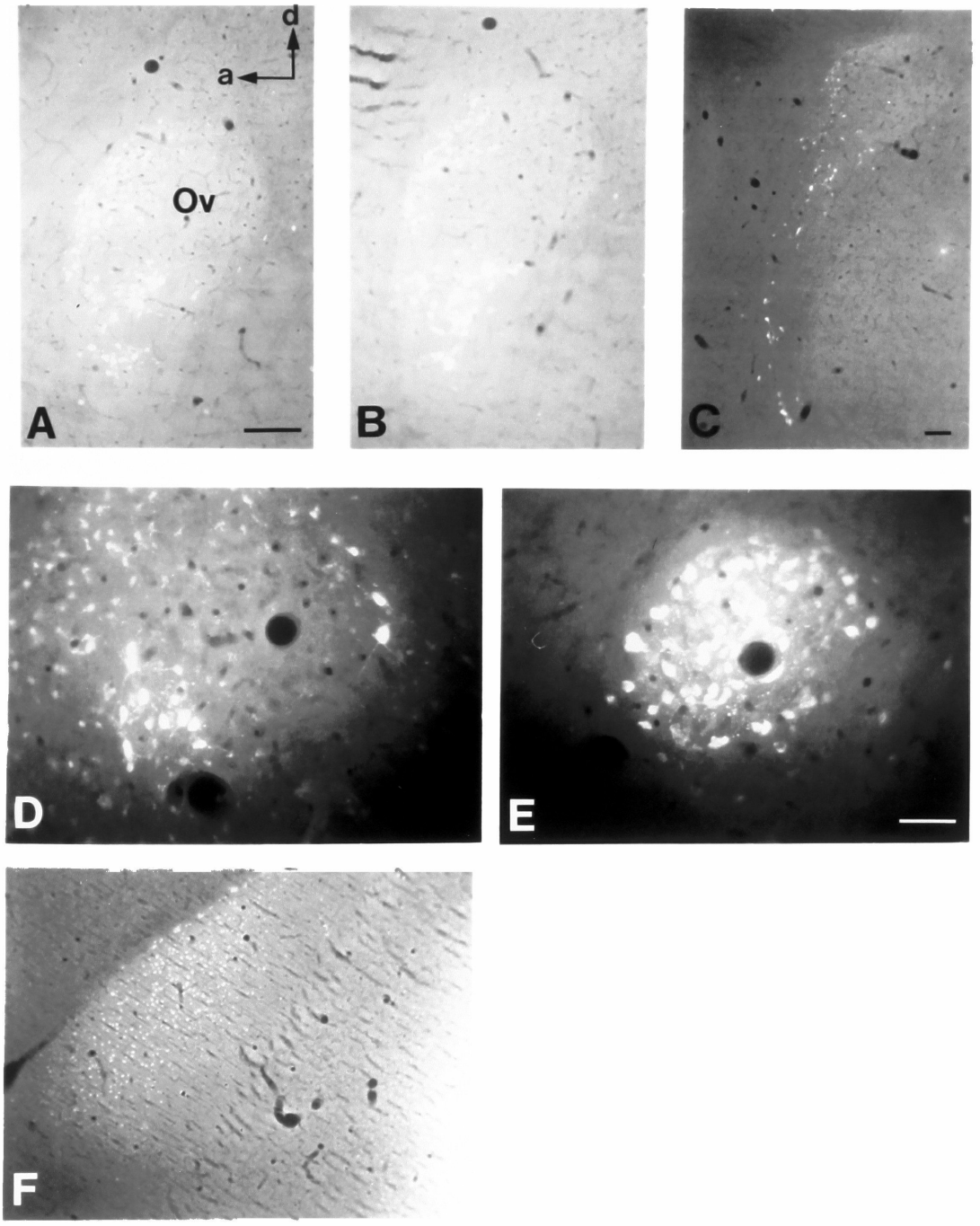
d
a
Ov
A
B
C
D
E
F

diffusion of fluorogold. Indeed, labeled cells are also seen in progressively more lateral parts of the caudal neostriatum, but they form a continuum with the injection site and the diffusion circle, and it is hard to decide whether they are the result of specific label by retrograde transport.

In some cases, labeled cells reach as far laterally as HVC and its surroundings. To investigate whether this could represent a specific population of HVC cells projecting to the medial N, two birds were bilaterally injected with beads in area X (multiple large injections) and fluorogold in NCM; in these cases, the vast majority of fluorogold-labeled cells within HVC were also labeled with beads. In general, a very similar pattern of backfilled cells was obtained when beads were injected in NCM (3 cases), but no backfilled cells were seen inside HVC. This suggests that backfilled cells seen in HVC after placing fluorogold in NCM may have been a result of labeling fibers of passage.

Injections of anterograde tracers

NCM was targeted in 11 birds with either PHA-L or biocytin. Of these, 6 injections (4 females, 2 males) hit the medial portions of the Field L complex (L2a and Field L of Rose) and a brief description of these is presented first. Two birds had stained fibers going into NCM; in one particular bird, a double PHA-L injection centered in L2 showed a rich pattern of stained fibers and terminations in NCM (figure 5.3A and C). In all birds, stained fibers and terminal arborizations are also seen in the caudo-medial HV (figure 5.3A and B). In two birds injected with PHA-L, backfilled cells are seen in

FIGURE 5.3 - Injection of PHA-L centered in the medial Field L2 of the zebra finch. (A) Parasagittal brain section at 500µm from the midline (comparable with figure 4.2B); (B) enlargement of the upper rectangle in (A). (C) enlargement of the double rectangle in (A). Bar sizes: (A), 300µm; (B) and (C), 100µm.

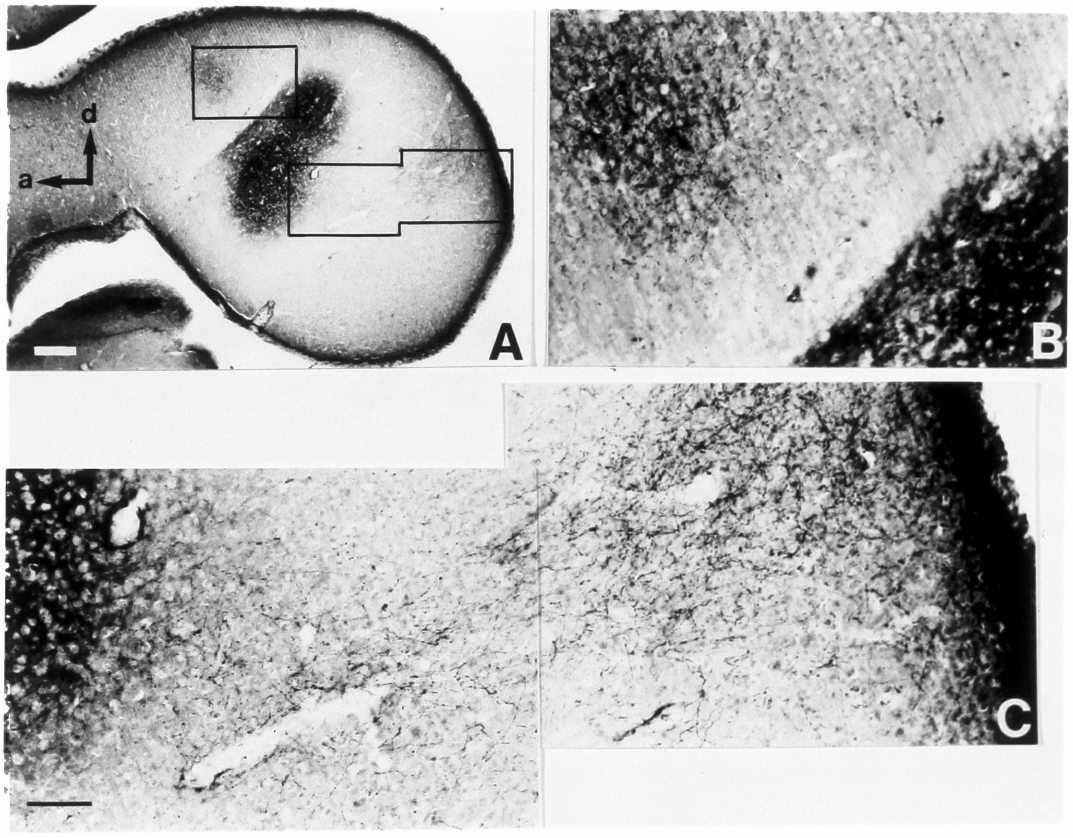
d
a
A
B
C

caudo-medial HV, suggesting a reciprocal connection. Injections into medial Field L and adjacent N (3 birds) yielded projections to caudal PA. Injections into dorso-medial L2a (2 birds) showed stained fibers into L1 and L3, which flanked L2a rostrally and caudally, respectively. Two birds with injections into medial L or L2a had stained fibers in dorsocaudal neostriatum, in close relationship with the shelf area under HVC.

In another 5 birds (3 females, 2 males), biocytin injectons were centered in the caudal NCM and did not involve Field L. One example is shown in figure 5.4. The greatest number of stained fibers is seen within and throughout NCM, suggesting a rich interconnectivity between all regions of NCM. In a parasagittal series, these fibers are seen extending both medially and laterally to the injection site for a few hundred microns (figure 5.4B, C and D). Some fibers run close to the ventricular surface and then divide out into thinner branches and finer terminal arborizations and boutons within NCM (figure 5.4E).

4 birds in this group have stained fibers ending in the caudo-medial HV (not shown) and all birds had fibers in the caudal P, with fine terminal arborizations seen in PA (figure 5.5E) and PP (figure 5.5C and D). In addition, fibers were seen running towards the caudo-dorsal N. In the males, these fibers reached the HVC shelf, where many of them seem to terminate, especially in the more caudal portions (figure 5.5A and B); stained fibers are also seen in the fiber-rich zone between HVC and the ventricular zone, where some fine fibers run along the antero-posterior axis, although it is not clear whether these terminate in the area or not. The exact

FIGURE 5.4 - Injection of biocytin centered in the caudal portion of NCM. (A) Parasagittal brain section at 500μm from the midline (comparable with figure 4.2B); (C) enlargement of the rectangle in (A); areas comparable with (C) in sections immediately lateral and medial to (A) are shown in (B) and (D) respectively; (E) enlargement of the rectangle in (D). Bar sizes: (A), 500μm; (B), (C) and (D), 200μm; (E), 70μm.

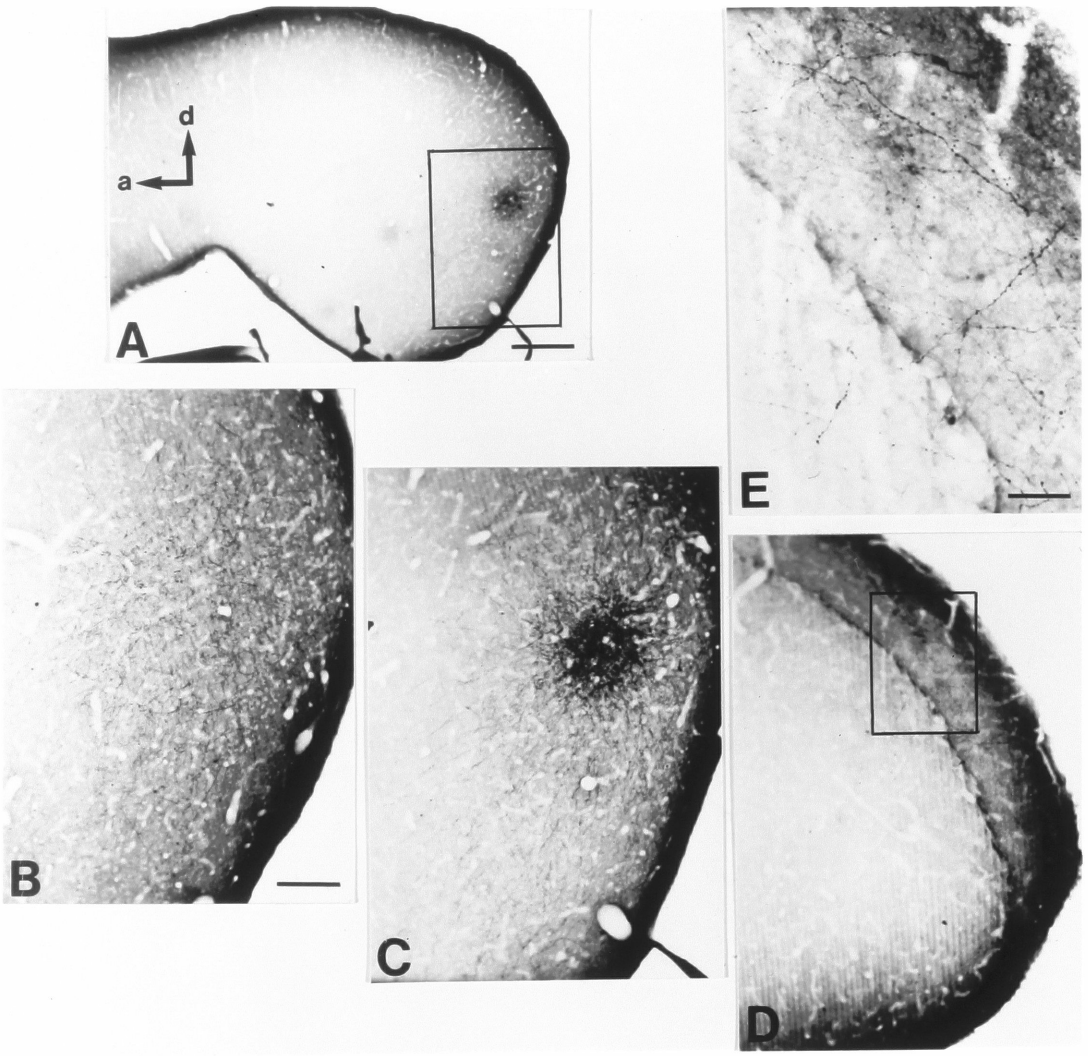
d
a
A
B
C
D
E

FIGURE 5.5 - Anterogradely-labeled fibers after injection of biocytin in the caudal portion of NCM. (A) Detail of parasagittal brain section at the level of HVC; hatched line is drawn over fiber-rich zone that separates HVC from surrounding N; (B) enlargement of rectangle in (A); arrows point to fine branches and boutons in the HVC shelf area; (C) detail of caudal P in parasagittal section; hatched lines are drawn to demarcate separation between PA and PP and PP and N; (D) enlargement of rectangle in (C); (E) detailed view of terminations in PA. Bar sizes: (A) and (C), 200μm; (B), (D), and (E), 100μm.

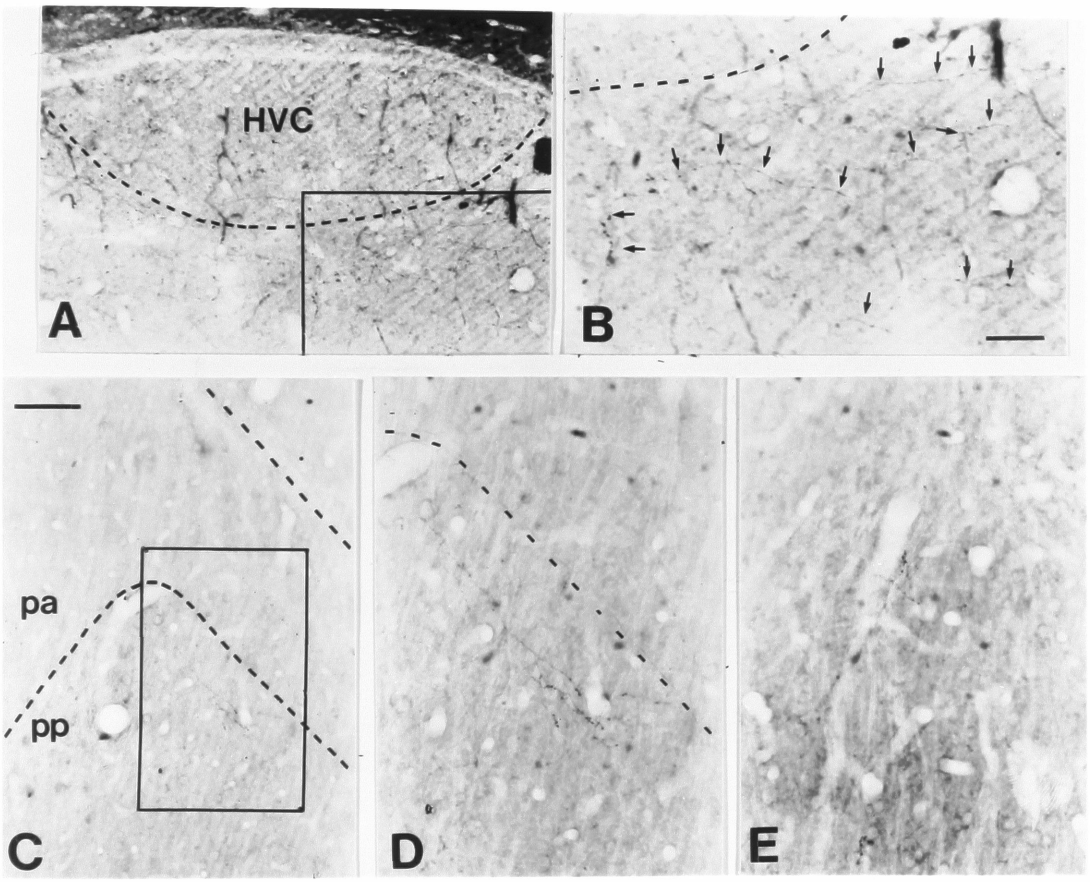
HVC
A
B
pa
pp
C
D
E

pathway taken by fibers that reach the shelf is also unclear; they could take a lateral course and then ascend towards HVC or enter the fiber-rich zone medially and then turn laterally.

DISCUSSION

The results presented in this chapter clearly indicate that NCM is intimately related with auditory pathways. It receives inputs from a specific portion of the auditory thalamus and possibly from the telencephalic Field L and is reciprocally connected with some of Field L targets such as the caudo-dorsal P (Kelley and Nottebohm, 1979) and caudo-medial HV (Bonke et al, 1979). In addition, some fibers reach as far laterally as the neostriatum that surrounds HVC, or HVC shelf, a Field L target that is in close apposition to a nucleus of the motor pathway for song production (Kelley and Nottebohm, 1979).

The auditory input from the ovoidalis periphery could represent a somewhat separate ascending auditory pathway, different from that ascending from nucleus ovoidalis itself. Such a separation has been described recently in the ring-dove, Streptopelia risoria, where neuronal populations in the periphery of ovoidalis have been shown to receive a distinct input from the region that surrounds MLd, and to project to hypothalamic structures presumably involved in regulation of endocrine function (Durand et al., 1992). This area is also the recipient of projections from the telencephalon that may represent a major descending auditory pathway (see discussion in chapter 6).

The caudo-medial HV has been previously shown to be reciprocally connected with Field L (Bonke et al., 1979) in the guinea fowl; in addition, auditory responses have been recorded in this area in starlings, with a high selectivity for complex stimuli (Müller and Leppelsack, 1985). Similar connections have been described for the

caudo-dorsal P (Bonke et al., 1979), which in addition receives a direct input from ovoidalis (Kelley and Nottebohm, 1979). As seen in figures 4.2 and 4.3, both the caudo-medial HV and the caudo-dorsal P show very marked ZENK induction in response to song presentation.

HVC cells backfilled with retrograde tracers injected in NCM are most probably the result of labeling fibers of passage on their way from HVC to Area X, but the possibility cannot be ruled out that a small proportion of fibers branch off from the main trunks and terminate in the vicinity of NCM. It is unclear whether some fibers linking HVC to area X run so close to the midline as to have been disrupted and backfilled by injections centered in NCM. These fibers would be separated from most of the HVC fibers that project to area X, which run in LH.

NCM seems to contribute significant inputs to the shelf under HVC. As discussed in the next chapter, this area then sends fibers that enter HVC and that could represent an important contribution to auditory responses within the song control circuit. These results thus demonstrate that some areas revealed by ZENK induction are closely related with telencephalic auditory pathways and could represent part of the interface between song perception and production systems. NCM is a large area and most of the analysis presented in this chapter was restricted to its more caudal portions, which are clearly distinct from Field L. It remains to be seen whether different portions of NCM have different connectivity patterns. The connections of other areas revealed by ZENK induction is discussed in the next chapter.

CHAPTER 6: ANATOMICAL CONNECTIVITY OF AREAS REVEALED BY ZENK INDUCTION: HVC SHELF AND RA CUP

INTRODUCTION

Oscine songbirds learn their song and some of their calls by reference to auditory information (Thorpe, 1958; Marler and Tamura, 1964; reviewed in Kroodsma, 1982). For vocal learning to occur, auditory information has to reach the vocal control pathways. Even though a fair amount of work has been done on mapping the motor pathway for song production, the anatomical details of the auditory-motor interface remain largely unresolved. The descending motor pathway consists of discrete nuclei and projections (Nottebohm et al., 1976 and 1982; Konishi, 1989; Bottjer et al., 1989). A large nucleus of the dorsocaudal neostriatum, the high vocal center (HVC), projects to the robust nucleus of the archistriatum (RA). RA, in turn, projects to the nucleus dorsalis medialis (DM) of the midbrain's intercollicular complex, and to the hypoglossal motor neurons that innervate the trachea and syrinx (nXIIts).

Electrophysiological recordings within nuclei of the motor pathway have revealed responses to auditory stimulation which are usually characterized by high selectivity towards conspecific song (Margoliash, 1983 and 1986; Williams and Nottebohm, 1985). It is unclear, however, how auditory information reaches this pathway. Selective responses are first seen in HVC and the initial studies on connectivity described three main inputs to HVC: the medial subdivision of the nucleus magnocellularis of the neostriatum

(mMAN), the uvaeformis nucleus of the thalamus (Uva) and the nucleus interfascialis (NIf), which also receives input from Uva (Nottebohm et al., 1982). Afferents to these nuclei are still undefined, as well as their possible contribution to auditory responses in HVC. A fourth possible origin of afferents to HVC is the underlying neostriatum or HVC "shelf" (see below); this is of main interest because this region is a target of the primary telencephalic auditory area (Kelley and Nottebohm, 1979) and could thus convey auditory information into HVC.

The anatomy of the avian central auditory pathway has been described in detail in species like pigeons, owls and songbirds (Karten, 1967 and 1968; Boord, 1968; Kelley and Nottebohm, 1979). The midbrain nucleus mesencephalicus lateralis, pars dorsalis (MLd) and its main projection, the thalamic nucleus ovoidalis (Ov), which in turn projects to the primary auditory area of the forebrain, Field L, are central components of this pathway and have been compared, respectively, to the mammalian inferior colliculus, medial geniculate body and primary auditory cortex (Karten, 1967 and 1968; Bonke et al., 1979a; Kelley and Nottebohm, 1979). Another ascending auditory pathway has been identified in the pigeon, consisting of the thalamic nucleus semilunaris paraovoidalis (SPO, a nucleus adjacent to Ov but whose input includes a direct lemniscal projection) which projects to Field L with a termination pattern distinct from Ov (Wild, 1987). In addition, a "shell' of cells surrounding nucleus ovoidalis has been identified which shares some of its telencephalic terminations; this ovoidalis "shell" connects the auditory thalamus to hypothalamic structures (Durand et al., 1992).

The telencephalic Field L is a complex structure whose cytoarchitectonic organization has been recently studied in detail in adult zebra finches (Fortune and Margoliash, 1992). Five main subdivisions were described, each of which may have its own specific connections. Thus, the main target area for thalamic fibers is a core region named L2, which is further subdivided into L2a and L2b, according to their specific thalamic input: L2a receives input from Ov and L2b from SPO. Areas immediately surrounding L2 (L1 and L3), receive a heavy projection from L2 and a lesser projection from thalamus. Early studies in songbirds using relatively large injections of anterograde tracers revealed a projection from Field L to a layer of tissue medial and ventral to HVC known as the "shelf" (Kelley and Nottebohm, 1979). In addition, an area immediately postero-ventral to Field L (possibly including L3) was shown to project to a "cup" of tissue engulfing the anteroventral half of RA. A projection from Field L to dorsocaudal paleostriatum augmentatum (PA) was also revealed in these injections. Recent experiments by Fortune and Margoliash have confirmed earlier results and further suggested a discrete projection from L1 and L3 directly into HVC which had previously gone unnoticed. Even though its physiological significance is still unclear, this constitutes a fifth projection into HVC and a strong candidate for a source of auditory afferents (Fortune and Margoliash, personal communication) .

No avian descending auditory pathway comparable to the mammalian cortico-thalamic projection has yet been demonstrated. Injections in Field L failed to reveal such a connection (Bonke et al., 1979; Kelley and Nottebohm, 1979). Either this very distinctive

feature of the mammalian cortex has not been evolutionarily conserved in all vertebrates or information about it is still missing in birds. This question prompted us to further investigate the connectivity of the auditory forebrain, focusing on the projections of Field L targets. In addition, areas like the shelf and the cup are closely apposed to song control nuclei and could constitute important sources of auditory information to the song control pathway. Katz and Gurney (1981) showed that some neurons in the shelf send axonal branches into HVC. This observation could help explain the auditory responses given by some of the HVC neurons. On the other hand, projections from RA are clearly distinct from those of its surrounding cup, since injections of retrograde tracers into DM, an RA target, backlabel exclusively cells inside RA.

Finally, as described in chapter 4, a marked ZENK induction in response to song occurs in both the HVC shelf and the RA cup after song presentation. The study described in the present chapter was conducted to learn more about the organization and connections of the "shelf" and "cup" areas and their possible interaction with nuclei of the song control circuit.

METHODS

Surgery, tracer delivery and processing of tissues were performed as described in chapter 5. The definition of coordinates for the shelf was based partly on stereotaxic data and partly on direct visualization of landmarks on the brain's surface. Shortly, stereotaxic coordinates were initially used to broadly define the localization of HVC (AP 0.0 to +1.0 , ML 2.0 to 2.5 and DV 0.3 to 0.7). The dura was then exposed and opened carefully with a sharp object (usually the bent tip of a small-gauge needle). The superficial situation of HVC and adjacent fiber tracts (the descending fibers to RA caudally, lMAN to RA fibers laterally and LH rostrally) allows for its ready identification. Micropipettes were then descended to various dorsoventral levels (inside HVC, at its ventral border or ventral to HVC).

Some attempts were made to hit the cup using stereotaxic coordinates; this proved a hard task and the strategy was abandoned in favor of electrophysiological techniques. Shortly, in collaboration with Soshi Okuhata, a recording electrode was descended into the RA and RA coordinates and approximate boundaries were defined according to patterns of spontaneous activity and responses to auditory stimulation or to stimuli delivered by another electrode placed in HVC. Injections were then made in the areas just rostral or ventral to these defined boundaries; control injections were centered directly inside RA. Electrodes recording auditory responses were also used to locate targets that were small or deep (e.g. nuclei OV and DM) and therefore difficult to reach accurately just using stereotaxic

coordinates. Mapping of retrogradely-labeled cells was performed using a system described in Alvarez-Buylla and Vicario, 1988; brain subdivision boundaries were drawn using dark-field microscopy and confirmed after cresyl-violet staining.

RESULTS

Afferents to the shelf underlying HVC

As opposed to injections of anterograde tracers, it proved extremely difficult to make injections of retrograde tracers that completely respected HVC or the shelf and did not cross the HVC/shelf boundary. Leakage along the injection tract during injections in the shelf resulted in labeling of cells within HVC. By the same token, very small volumes of tracer are necessary to completely restrict injections to HVC, which then makes the identification of backfilled cells difficult if not impossible (with volumes normally used it is almost impossible to determine with certainty whether the shelf was spared). Because of these difficulties, injections are not completely restricted but were predominantly in one or the other structure - HVC or "shelf".

A summary of the results is presented here, based on the comparison of various animals. Injections centered in HVC resulted in strong backfilling of cells in NIf, Uva and mMAN, confirming previous reports. Backfilled cells were also seen in Field L, in the L1 and L3 subdivisions; these cells are much less strongly labelled, with either fluorogold or beads, and less densely packed than cells in NIf. When the center of injection is placed in some part of the shelf, backfilled cells in L1 and L3 are more numerous and more strongly labelled; NIf and Uva are also labelled, although less uniformily. Recently, other investigators have succeded in placing injections of retrograde tracers just in HVC (Fortune, personal communication) and so

retrogradely mapped inputs to HVC will not be discussed further here.

Efferents from the shelf

14 male birds received PHA-L or biocytin injections into the caudal neostriatum underlying HVC. The HVC shelf was originally described as a field of degenerating boutons following lesions in Field L (defined, in turn, as that part of caudal neostriatum that corresponded to a field of degenerating fibers and boutons following lesions of nucleus ovoidalis). The shelf so identified in the original report was thick under medial HVC and then became much thinner laterally. However, that original report did not include a systematic attempt to ensure that this was the full extent of the projection from Field L; this seems especially relevant in light of the new findings on the organization of Field L (Fortune and Margoliash, 1992). In other words, the exact dimensions of the shelf under HVC receiving input from Field L still remain to be established and we cannot say that all the injections presented here were inside this shelf, though they were in the neostriatum under HVC.

Injections with biocytin proved particularly useful, since injection sites of small diameter (~100μm) with virtually no leakeage along the injection tract could be obtained. This was very important since the micropipettes had to go through HVC in order to reach the shelf. The evidence that cells within HVC did not take up the tracer injected into the shelf includes, besides the absence of stained cell bodies within HVC, the fact that for those injections no terminals were seen within RA (this fact also demonstrates that there was very

little or no uptake by fibers of passage, since fibers leaving HVC necessarily have to cross the shelf, especially its caudal portions, to reach their target in the archistriatum). In some cases (including the injection shown in figure 6.2), HVC boundaries were determined by placing fluorogold into area X (five days prior to biocytin injection) and examining the field of backfilled cells in the dorsal N (not shown).

Shelf injections resulted in a great number of fibers running within the shelf under HVC. This effect was particularly visible with small biocytin injections, when brains were sectioned sagittally. Some examples shown in figure 6.1A to D represent a parasagittal series for an injection in the rostral shelf; a majority of fibers can be seen coursing anteriorly and posteriorly from the injection (figure 6.1B) and to a lesser extent medially and laterally (note how the fiber density decreases sharply in 6.1A and D; this was also confirmed in a brain cut coronally, not shown). Similar patterns were seen when injections were placed in rostral (figure 6.1B), medial (figure 6.1E) or caudal (figure 6.1F) portions of the shelf. The shelf fibers give off numerous small branches; in addition, varicosities and boutons suggest termination sites along the fiber course (figure 6.2B). In some cases fibers were seen running between HVC and the ventricular zone (figure 6.2A); these were particularly abundant after injections immediately caudal to HVC (not shown).

All birds with injections in the shelf showed stained fibers leading from the shelf into HVC (figure 6.3), where they traveled for various distances, usually within the same medio-lateral plane, before breaking up into thinner branches that eventually terminate in

FIGURE 6.1 - Injections of biocytin in the neostriatum immediately adjacent to HVC (shelf), viewed under dark-field illumination. Notice pattern of fibers running predominantly along the shelf. (A) to (D) represent a series of parasagital sections from medial to lateral to the injection; center of injection is antero-ventral to HVC and is shown in (B). (E) Injection placed ventrally to HVC. (F) Fibers extending rostrally along the HVC shelf from an injection caudal to HVC (center of injection not shown). Bar size: 200μm.

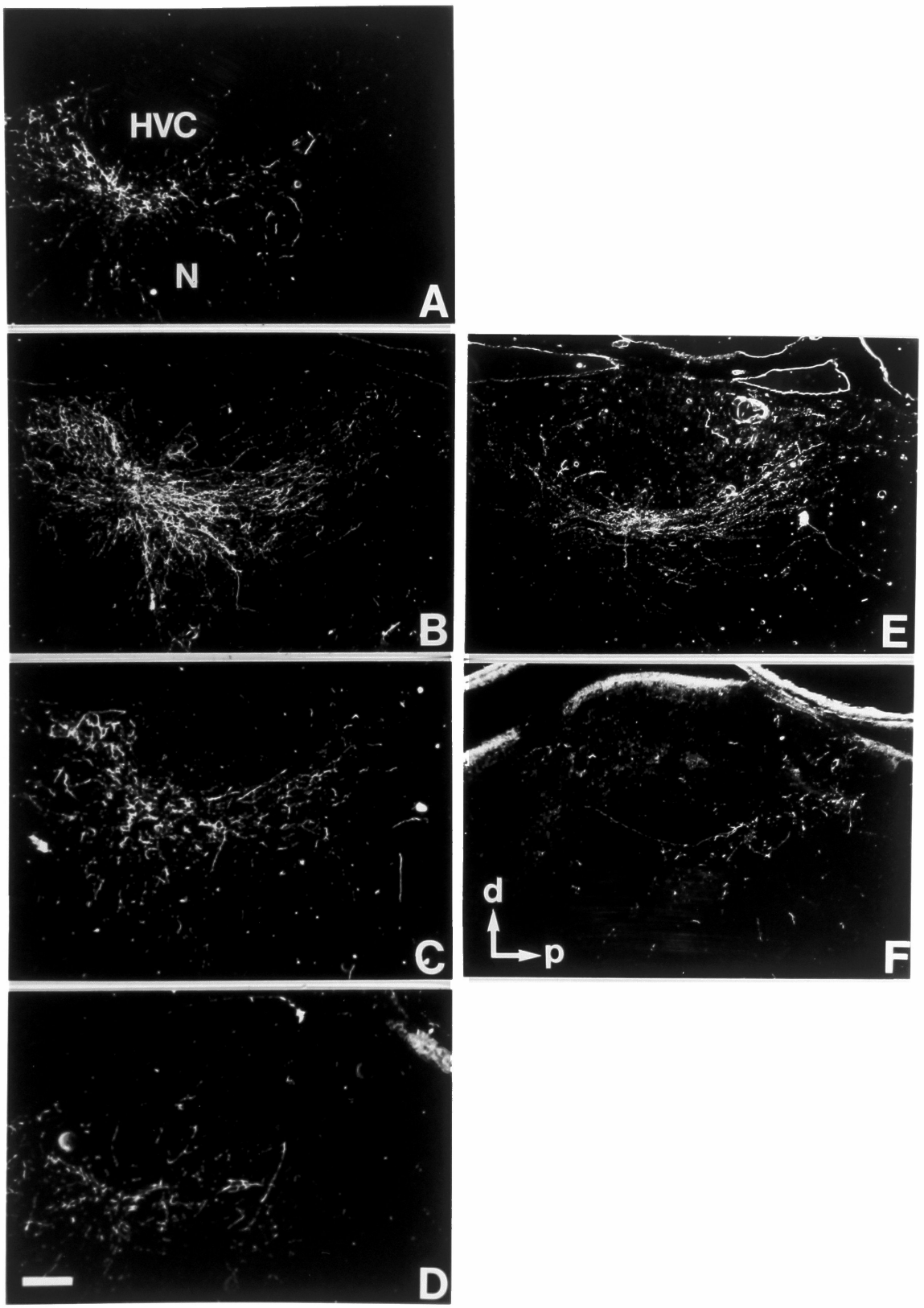
HVC
N
A
B
C
D
E
d
p
F

FIGURE 6.2 - Anterogradely-labeled fibers resulting from a biocytin injection rostro-ventral to HVC (same injection as in figure 6.3B). (A) Fibers running dorsal to HVC, under the ventricular zone; (B) fibers ventral to HVC (shelf). Bar size: 200μm.

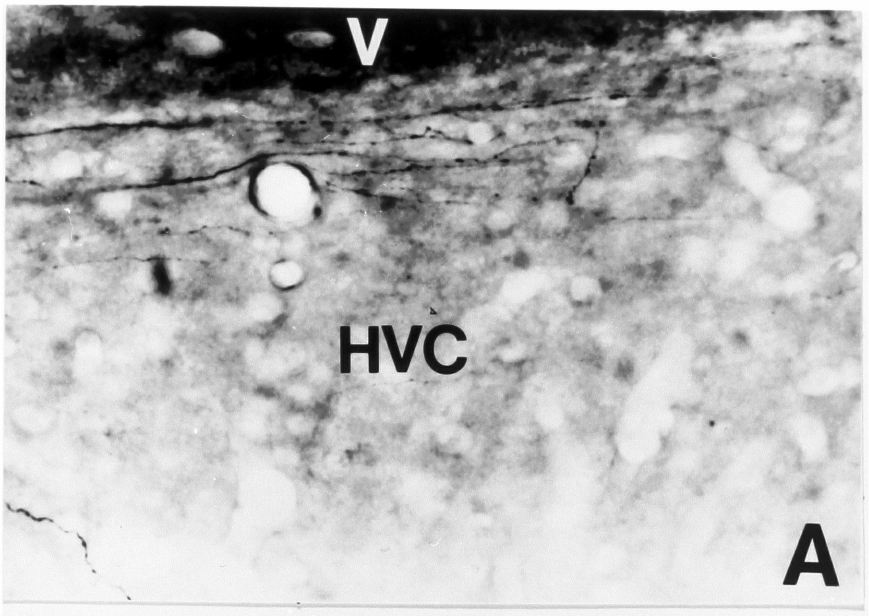
V
HVC
A

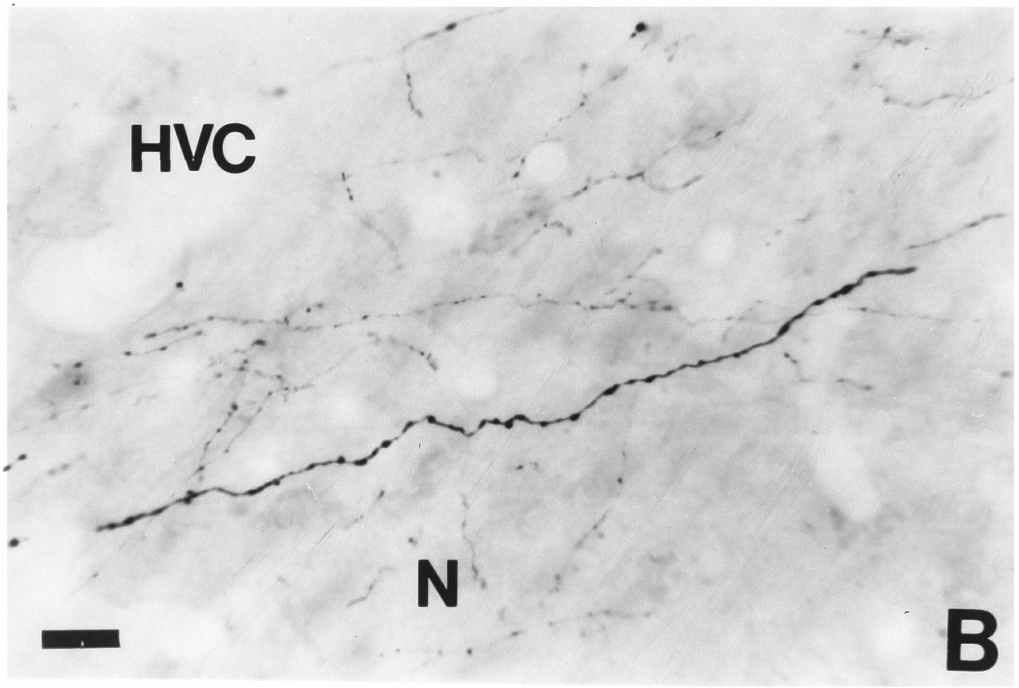
HVC
N
B

FIGURE 6.3 - Injection of biocytin in the neostriatum immediately adjacent to HVC (shelf). (B) Represents injection site; (A) enlargement of fibers seen within HVC in (B); (C) example of termination pattern in the dorsal portions of HVC. Notice presence of a blood vessel between injection site and HVC in (B). Orientation: dorsal is up and anterior is to the left. Bar sizes: (B), 50 μm; (A) and (C), 200μm.

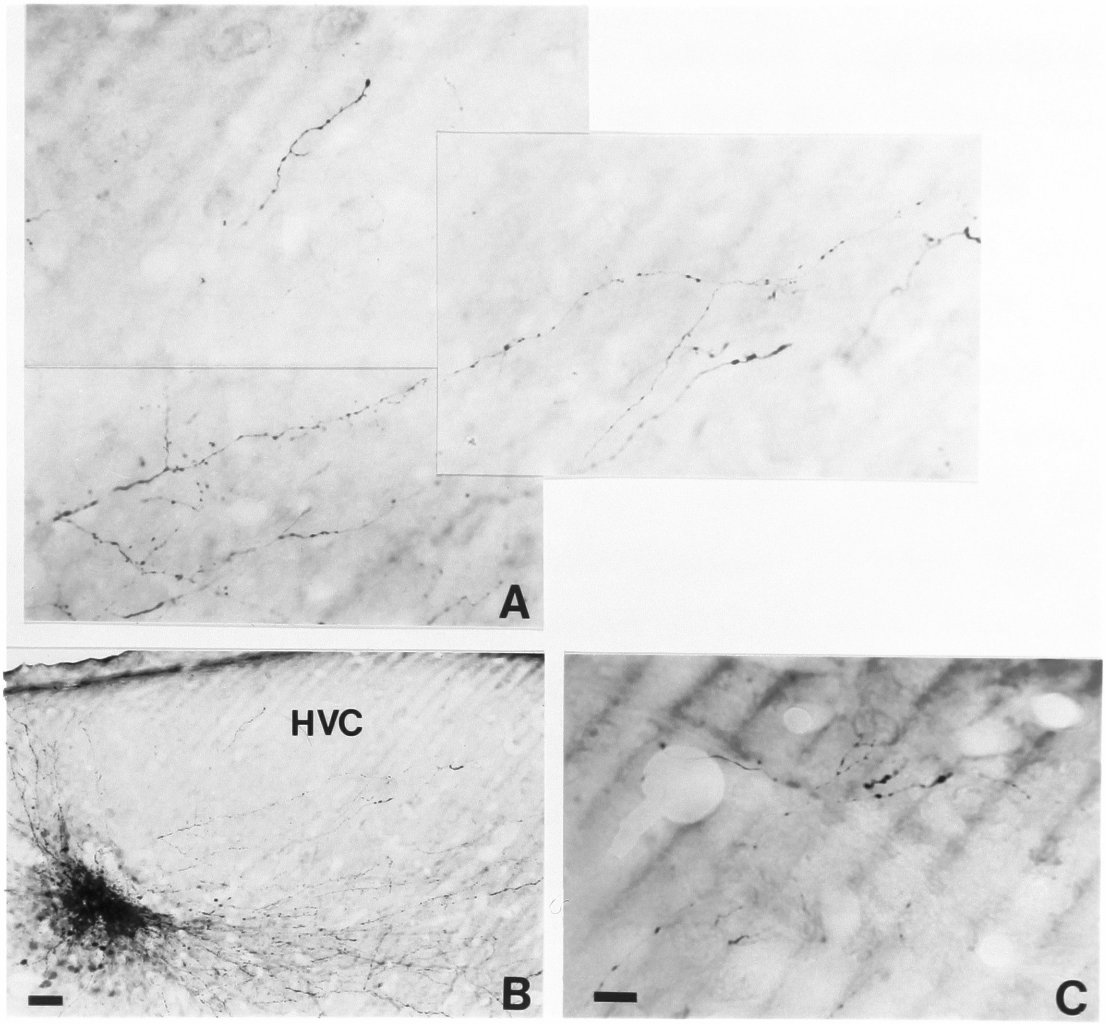
A
HVC
B
C

various small boutons, sometimes fairly close to cell bodies within HVC (6.3A and C). These fibers emerge either directly from the injection site or branch off from fibers running along the shelf, and enter HVC by crossing the HVC/shelf border. The number of such fibers is small compared with the number seen in the shelf and the impression one gets is that whereas individual shelf neurons can make contacts over broad regions of the shelf, their influence inside HVC may be restricted to a smaller domain. Fibers entering HVC seem to be most abundant in the same parasagittal plane as that of the injection, since the occurrence of stained fibers within HVC drops fast as one moves medial or lateral to the parasagittal plane that shows the injection; these projection domains may have, thus, a particularly narrow medio-lateral representation. Projections from the shelf into HVC may come preferentially from cell layers closest to HVC's ventral boundary, as the number of fibers within HVC seems to be greater in the shelf injections closer to HVC. The section shown in figure 6.3 comes from a brain that was injected with beads in area X five days prior to biocytin injection in the shelf. Visualization of backfilled cells in HVC under fluorescent light (not shown) helped define its boundary, which runs immediately caudal to the blood vessel seen in figure 6.3B.

Ten birds with shelf injections had stained fibers in the archistriatum, in close relationship with RA. A large PHA-L injection centered in the shelf resulted in an abundance of fibers in the A that surrounded RA; many of these fibers ended in a region rostro-ventral to RA known as the RA cup (figure 6.4). Since this injection did not respect the HVC boundary, many fibers are also seen

FIGURE 6.4 - Anterogradely labeled fibers after large injection of PHA-L in the HVC shelf. Notice abundant fibers around and ventro-rostral to RA; fewer fibers enter RA from its dorso-caudal aspect. Orientation: dorsal is up and anterior is to the left. Bar size: 250μm.

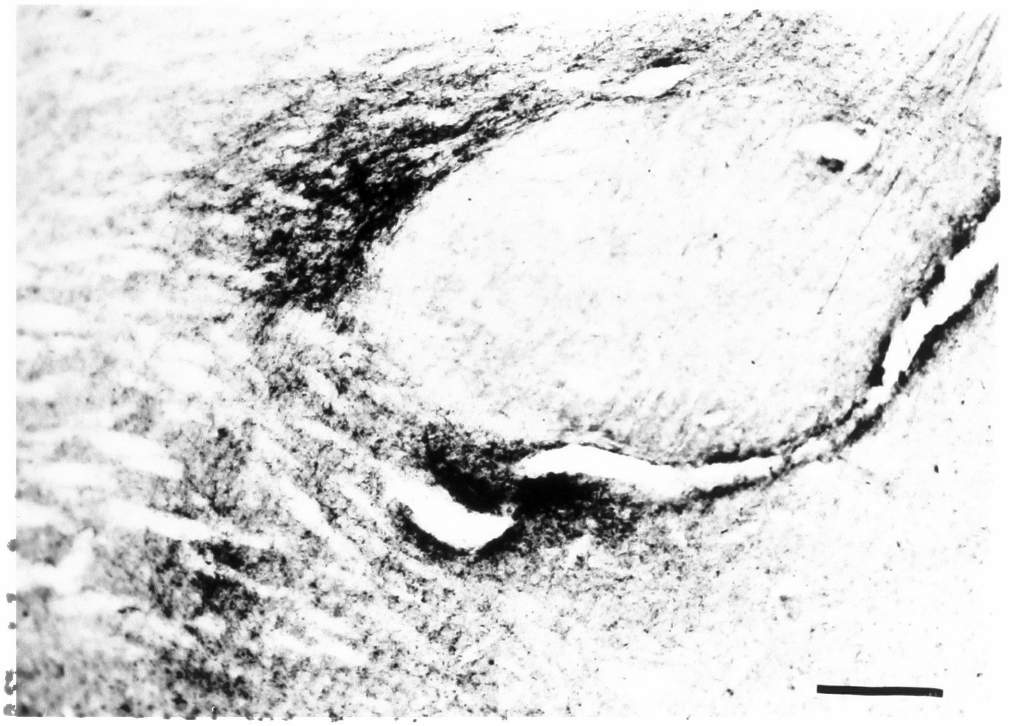

entering RA. The issue of which fibers originated in HVC and which in the shelf was clarified using smaller injections of biocytin (figures 6.5, 6.6 and 6.7). Injections centered in HVC resulted in fibers that entered RA and ramified into finer branches within RA (figure 6.5A and B); shelf injections that did not involve HVC, particularly those in the caudal shelf, resulted in fibers that came in close relationship with RA but did not enter it; instead, they ramified into finer branches that terminated in the surrounding A (figures 6.5C and D, 6.6 and 6.7). These observations strongly suggest that the projection to the cup is exclusively from the shelf, though the possibility that a small contingent of HVC fibers ends in the cup, especially in the domain dorso-caudal to RA, cannot be ruled out. Fibers from the shelf travelling towards the cup fasciculate together with a strong contingent of fibers travelling from HVC to RA and both kinds of fibers approach RA from above (figures 6.6 and 6.7). Notice that this approach is very different from that used by fibers that travel from Field L to the cup; the latter fibers approach RA from in front and below (Kelley and Nottebohm, 1979).

The number and position of stained fibers observed around RA following injections into the shelf varied between individuals, depending on the size of the injection. The medio-lateral position of the injection did not seem to matter; in some cases, a larger number of fibers was seen when the injection site was closer to the ventral border of HVC. A comparison between injections in the rostral and most caudal parts of the shelf suggests that there may be some organization along the rostro-caudal axis. Thus, the most rostral injections resulted in fibers that ran more rostrally towards A and,

FIGURE 6.5 - Comparison of projection patterns between biocytin injections placed in HVC or in the underlying neostriatum (shelf). (A) Anterogradely-labeled fibers after injection that included HVC and the shelf. (B) Detailed view of dorso-caudal portion of RA, enlargement from (A). (C) Anterogradely-labeled fibers after injection in the caudal shelf that completely excluded HVC. (D) Detailed view of dorso-caudal portion of RA and surrounding tissue, enlargement from (C). Orientation: dorsal is up and anterior is to the right. Bar size: 100μm

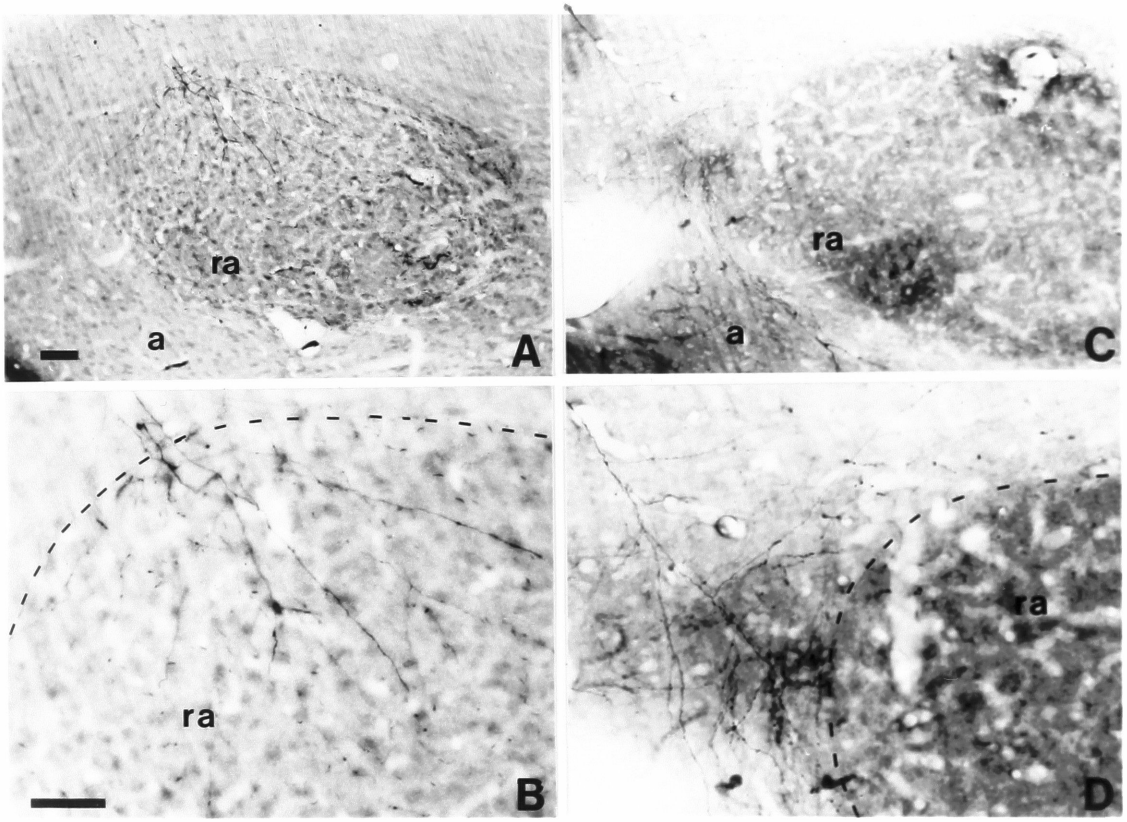
ra
a
A
ra
a
C
ra
B
ra
D

FIGURE 6.7 - Anterogradely-labeled fibers in the RA cup after small injection of biocytin in the HVC shelf. Diagram on the upper right shows injection site and levels of coronal sections shown in panels on the left. Panels (a), (b) and (c) are camera lucida drawings of the rectangular areas in the coronal sections at a level anterior to RA (a), at the transition between RA and A rostral to RA (b) and through RA. Bar size: 200μm.

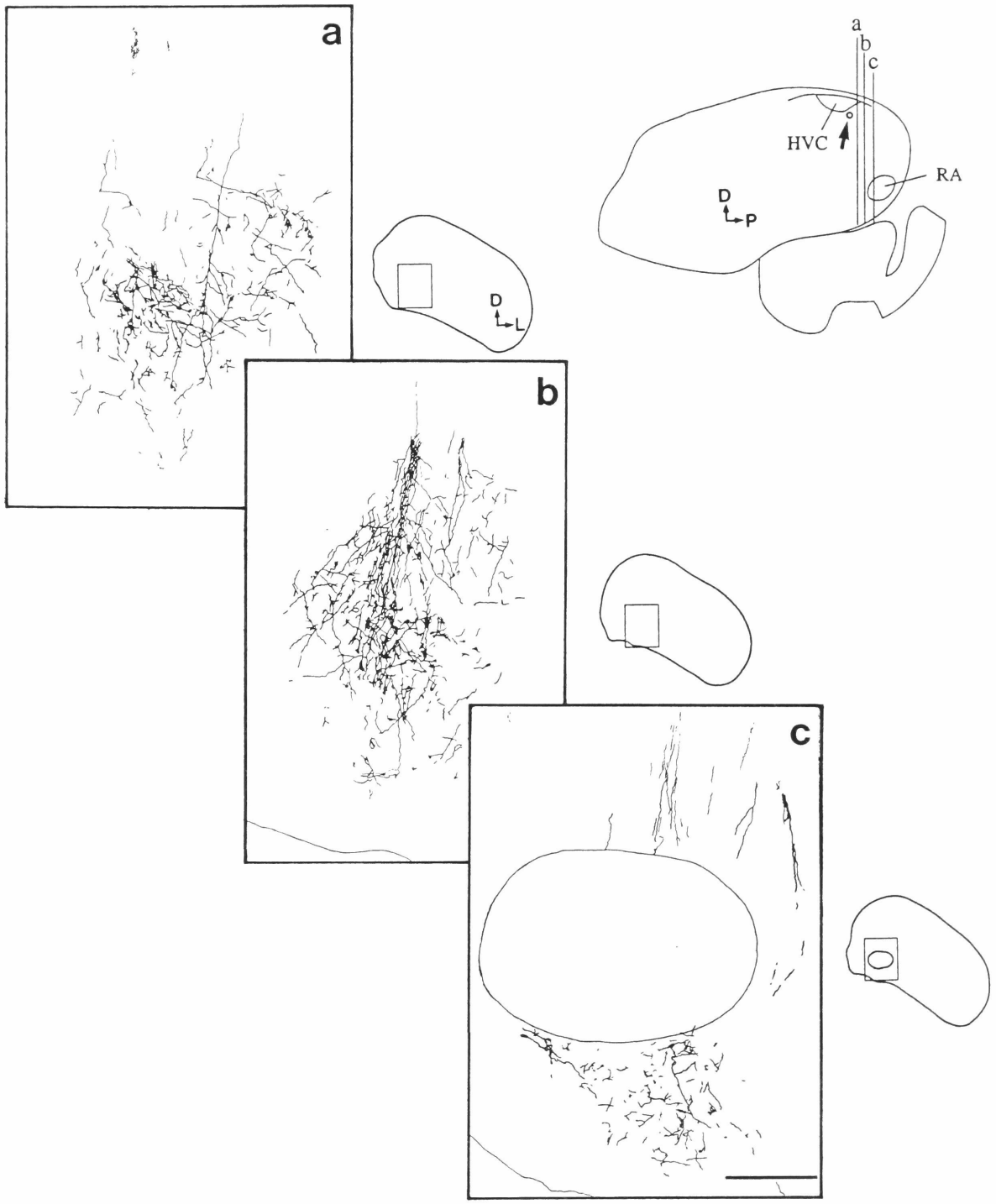
a
b
c
HVC
RA
D
P
D
L
a
b
c

upon reaching the dorsal surface of RA, bend rostrally and so avoided RA; they then terminate mostly in fields rostral and rostro-ventral to RA (RA cup), where stained fibers can be seen breaking up and forming a rich terminal field (figure 6.6, parasagittal series). A similar pattern was observed in a brain injected with biocytin in the middle portion of the shelf and which was sectioned in the coronal plane (figure 6.7). An injection of biocytin in the area caudal to HVC (where many of the shelf fibers seem to terminate) resulted in fibers that descended more caudally and reached the dorso-caudal surface of RA, where fibers branched and followed the contour of RA (6.5C and D); in this case, terminations were most abundant ventral to RA, although some fine terminal branches and boutons can be seen almost all around RA (not shown).

Injections of biocytin into the shelf resulted also in a few stained fibers going into the caudalmost tip of HV (not shown). This is probably a real, though sparse projection, and not all regions of the shelf may project to HV equally. Five birds with injections under HVC also had fibers going into dorsal NC. This is not a region with distinct anatomical boundaries, but this part of the NC lateral to NCM and ventral to HVC and its shelf could also process auditory signals.

Afferents to the cup

The RA "cup", as defined in Kelley and Nottebohm (1979) is relatively small and tightly apposed to RA, resulting in an odd shaped structure. Not surprisingly, it proved difficult to hit this cup while avoiding RA. As a result, many injections missed the goal, being either too medial, ventral, dorsal or anterior to the cup; in

many cases, RA was also partially labeled and the specificity of projection origins is inferred by comparing injections of tracers into the cup and into RA.

In general, the results of injections of retrograde tracers in the cup confirm the results obtained with injections of anterograde tracers in the shelf. Injections that included the cup resulted in a significant number of retrogradely-labeled cells in the dorsal neostriatum, including HVC (whenever RA was touched) and the areas underlying it. Most cells outside HVC are seen in the most caudal regions of the shelf, suggesting that this may be a preferential site of origin for fibers going to the cup. The density of labeled cells is not very large; there are two obvious possible explanations, which are not mutually exclusive: 1) it is very hard to completely target the cup, so we may be seeing just a portion of the projection; 2) it is possible that only a subpopulation of cells, distributed over a relatively large area in the shelf (when compared with HVC, for instance) is involved in the projection to the cup.

Labeled cells are also seen in a discrete portion of Field L ventro-caudal to L2 and caudal to the dorso-caudal tip of PA and which thus corresponds to L3 (not shown, but see figure 6.9). Besides clearly labeled cells, fibers can also be seen that leave the caudoventral portion of L3 and run towards the anterior cup when fluorogold is used as a tracer. Other labelled cells are occasionally seen in deep portions of P.

Efferents from the cup

One large PHA-L injection rostral to RA (and that did not cross into RA, as shown in figure 6.8) resulted in a few backfilled cells both in L3 and in the HVC shelf, confirming these as sources of projection to the cup (figure 6.9) In this same injection (figure 6.10) and in a couple of biocytin injections which completely avoided RA (not shown), a small number of very fine fibers is seen entering RA, with a correspondingly small number of boutons. Numerically this is a very minor input to RA; however, it is unclear whether these few fibers are stragglers or part of a significant circuit.

PHA-L injections in the cup resulted in anterogradely labeled fibers that enter the OM tract and descend towards lower brain structures. Thus, fibers can be followed that, upon reaching the thalamus, send short branches that terminate in a relatively rich plexus around Ov (figures 6.11 and 6.12), possibly in a pattern which is in part coextensive with the thalamic area that has been called the ovoidalis "shell"; Ov proper seems to be mostly spared, although some fine branches are seen in its more medial aspects (figure 6.11 A and E). A significant number of fibers can be seen reaching the tractus ovoidalis (figures 6.11D and G, 6.12 and 6.13), where a large density of varicosities and boutons is also detected, suggesting a rich termination field. The densest pattern of terminals is seen in a region immediately caudal to Ov, which may constitute a distinct nucleus (figure 6.11B, C and F).

A large number of fibers separate from the occipitomesencephalic tract (OM) and travel towards the caudo-lateral wall of the pons, where another termination-rich field is seen (figure 6.14). This may

FIGURE 6.8 - Schematic diagrams of parasagittal sections at the level of HVC and RA depicting site of PHA-L injection in A rostral to RA (shadowed area next to RA in the lower diagram). HVC, High Vocal Center; NC, caudal Neostriatum; A, Archistriatum; RA, nucleus Robustus Archistriatalis. Orientation: dorsal is up and anterior is to the right.

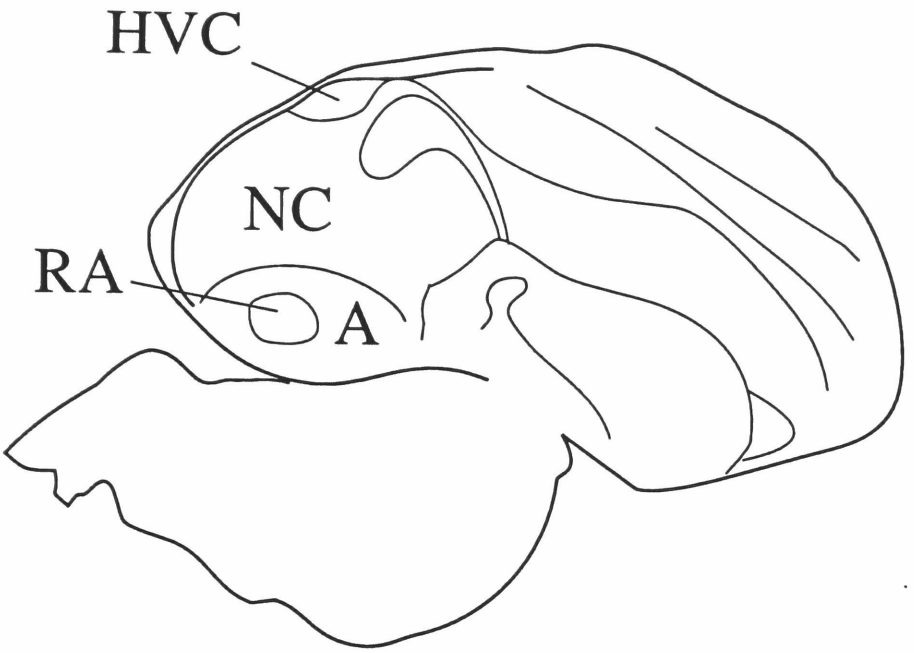
HVC
NC
RA
A

FIGURE 6.9 - Retrogradely-labeled cells after a PHA-L injection rostral to RA. (A) Labeled cells in L3; hatched lines are drawn over laminae that separate Field L subdivisions and the paleostriatum. (B) High power view of labeled cells in L3. (C) Labeled cell in the neostriatum adjacent to HVC (shelf). Bar sizes: (A), 200μm; (B) and (C), 40μm.

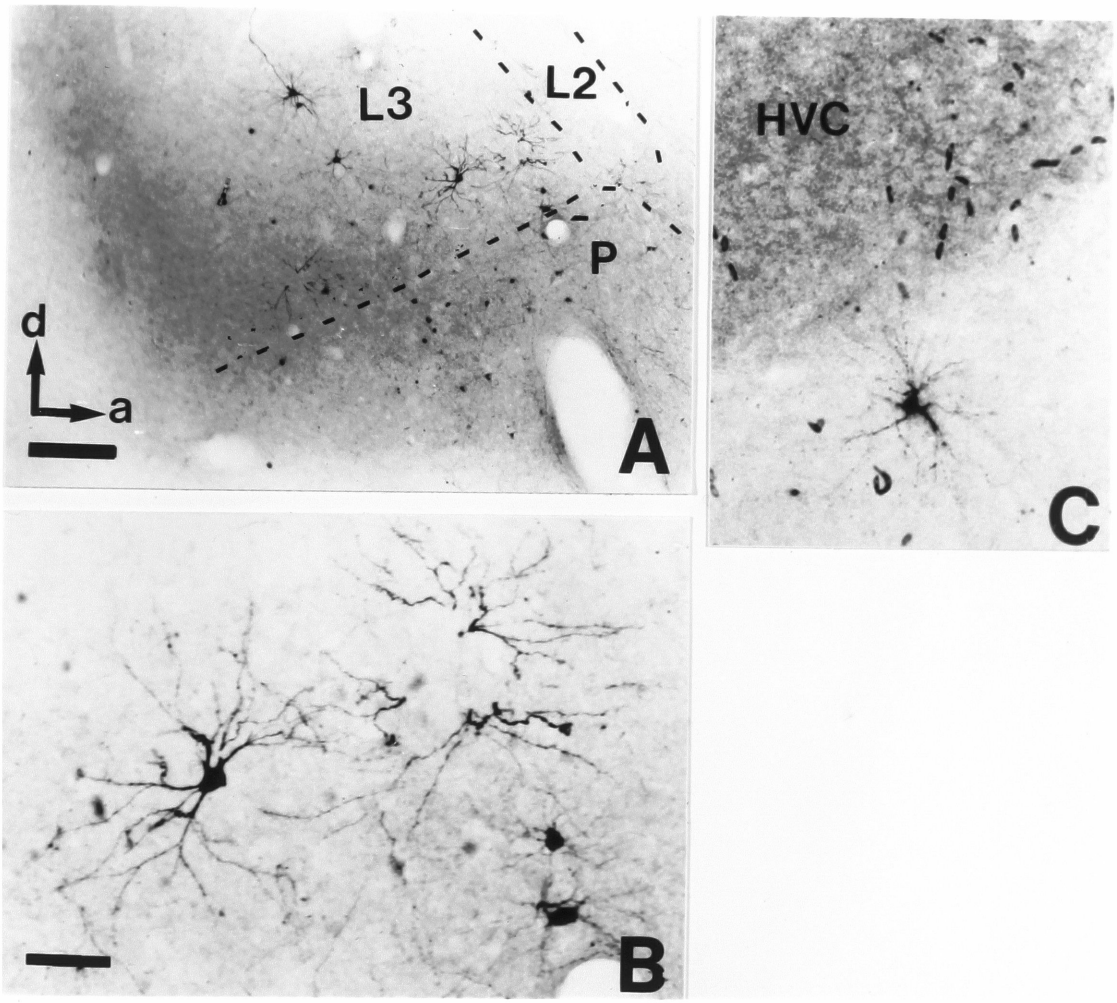
L3
L2
P
d
a
A
HVC
C
B

FIGURE 6.9 - Retrogradely-labeled cells after a PHA-L injection rostral to RA. (A) Labeled cells in L3; hatched lines are drawn over laminae that separate Field L subdivisions and the paleostriatum. (B) High power view of labeled cells in L3. (C) Labeled cell in the neostriatum adjacent to HVC (shelf). Bar sizes: (A), 200μm; (B) and (C), 40μm.

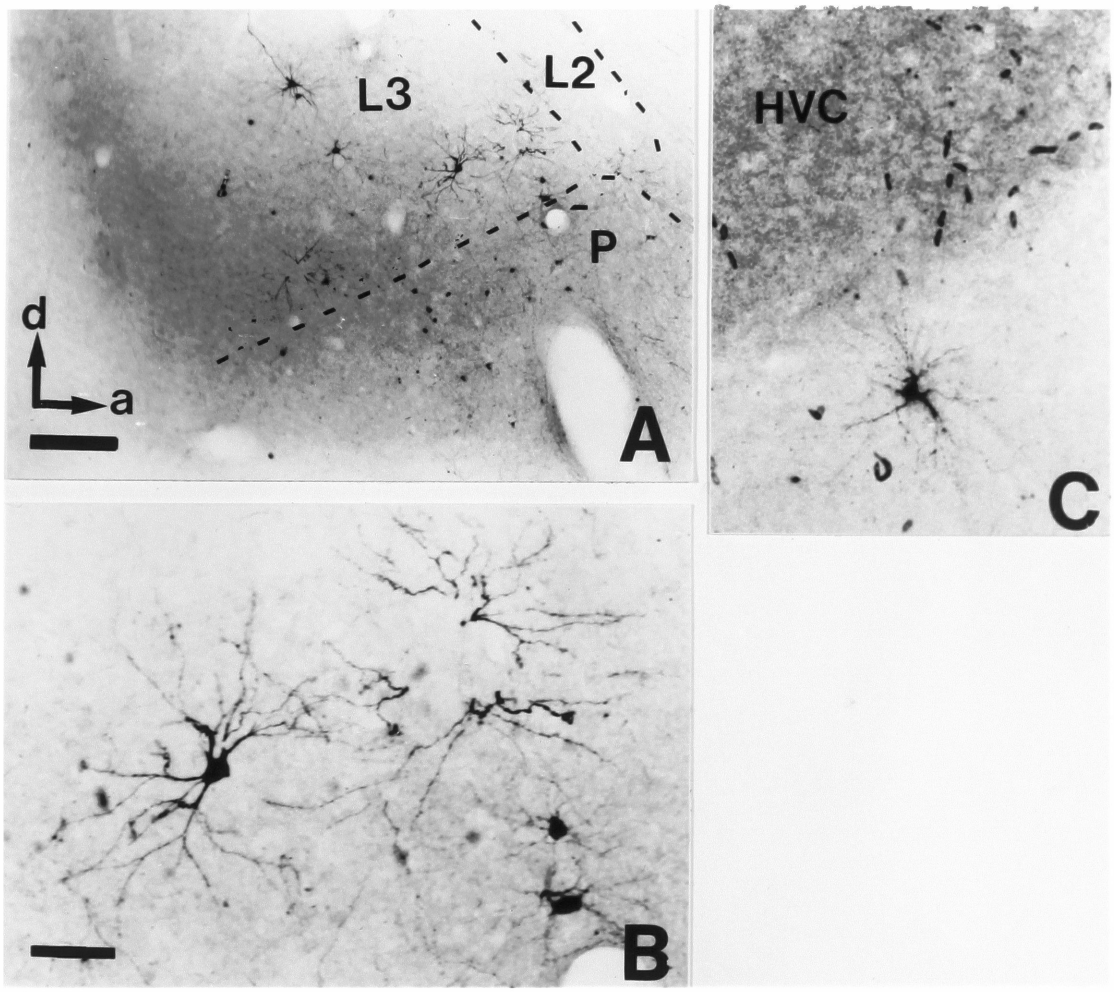
L3
L2
P
d
a
A
HVC
C
B

FIGURE 6.10 - Anterogradely-labeled fibers (arrowheads) entering RA from PHA-L injection rostral to RA, as shown in figure 6.8. (B) Enlargement of the rectangle in (A), showing a detailed view of fibers at a slightly different focal plane than in (A). Bar sizes: (A) and (B), 60μm.

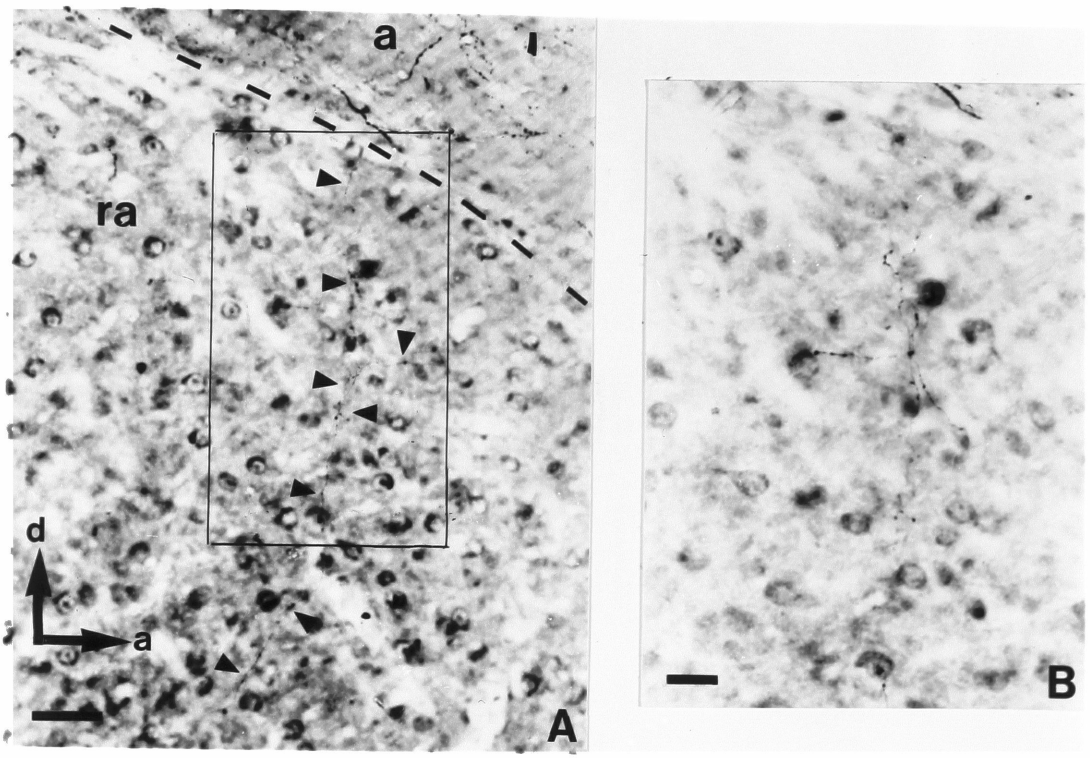
a
ra
d
a
A
B

FIGURE 6.11 - Anterogradely-labeled fibers in the auditory thalamus after PHA-L injection rostral to RA. (A) to (D) represent a detailed view of the vicinity of nucleus ovoidalis in serial parasagittal sections, as depicted in the diagram on the bottom right. (E) Enlargement of (A) showing fibers inside and around ovoidalis. (F) Enlargement of (B) showing dense termination zone caudal to ovoidalis. (G) Enlargement of (D) showing fine terminal arborization in the tractus ovoidalis. Ov., thalamic nucleus ovoidalis; OM, tractus occipitomesencephalicus; TO, tractus ovoidalis. Bar size: 200μm.

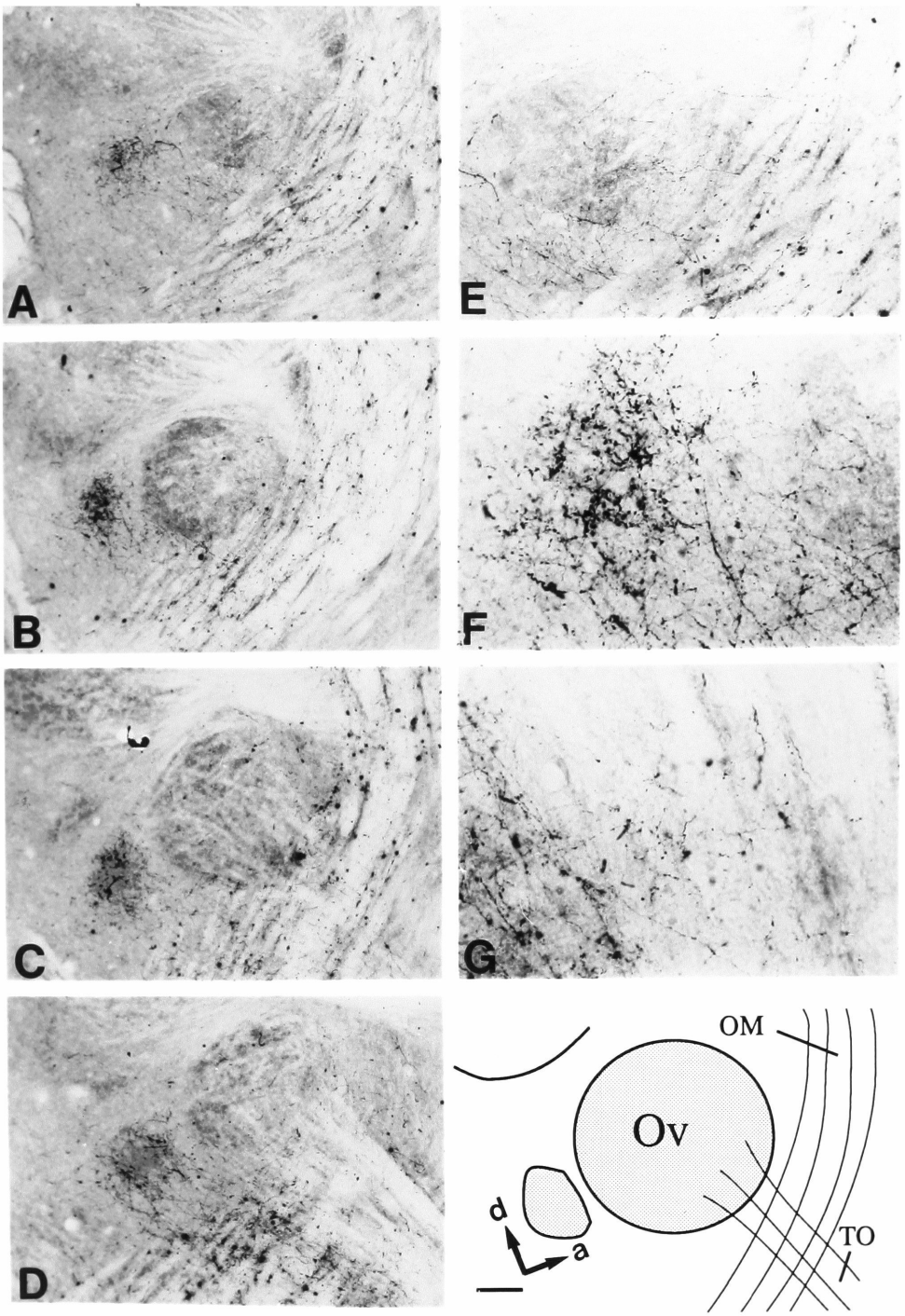
A
B
C
D
E
F
G
OM
Ov
d
a
TO

FIGURE 6.12 - Anterogradely-labeled fibers in the auditory thalamus after PHA-L injection rostral to RA. (A) Coronal section through ovoidalis showing dense staining in the periphery of ovoidalis. (B) Enlargement of the rectangle in (A) showing fibers and possible termination fields ventro-lateral to ovoidalis. Bar sizes: (A), 250μm; (B), 80μm.

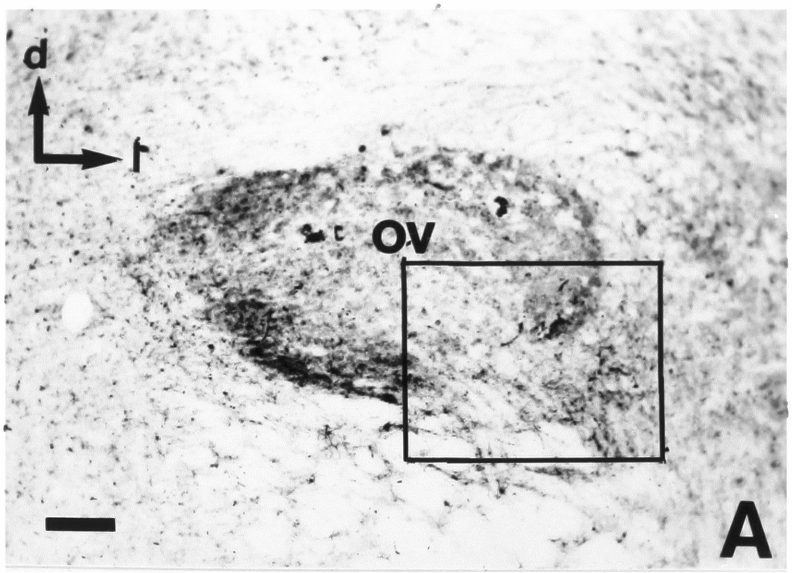
d
OV
A

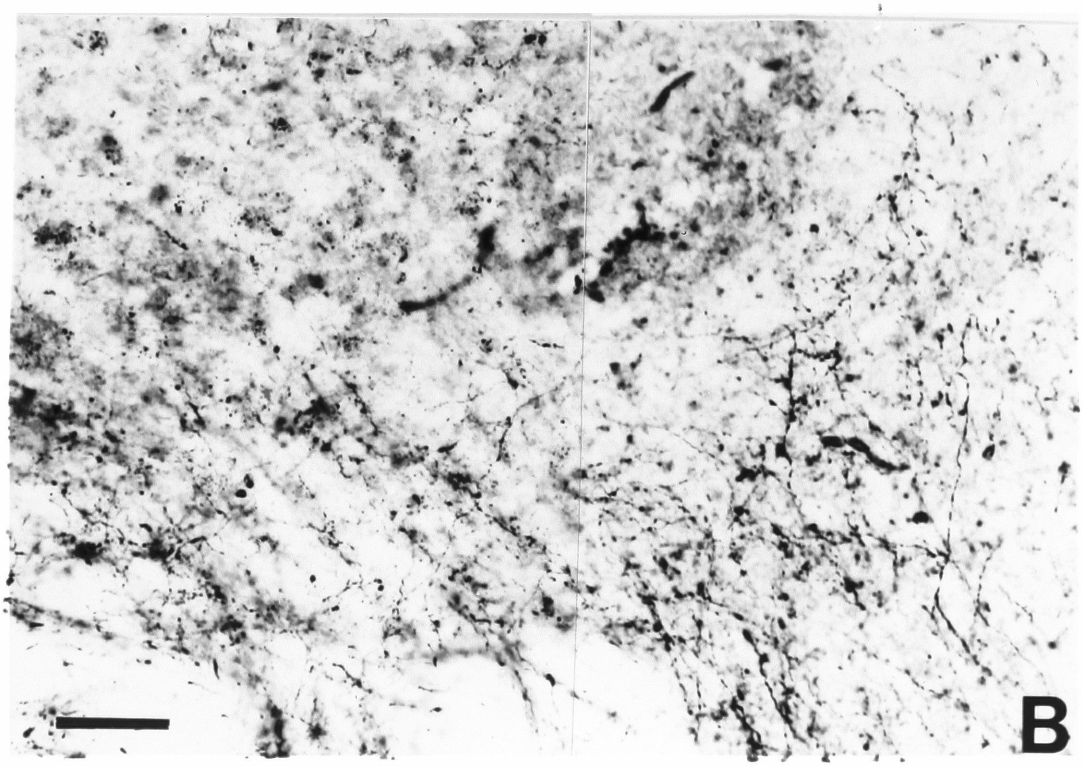
B

FIGURE 6.13 - Anterogradely-labeled fibers in the auditory thalamus after PHA-L injection rostral to RA. (A) Coronal section at a slightly more rostral plane than figure 6.10, showing fibers along the tractus ovoidalis. (B) Enlargement of the rectangle in (A) shows fibers and numerous boutons and fine terminal branches, suggesting termination zone. Rt, nucleus rotundus; TO, tractus ovoidalis. Bar sizes: (A), 250μm; (B), 75μm.

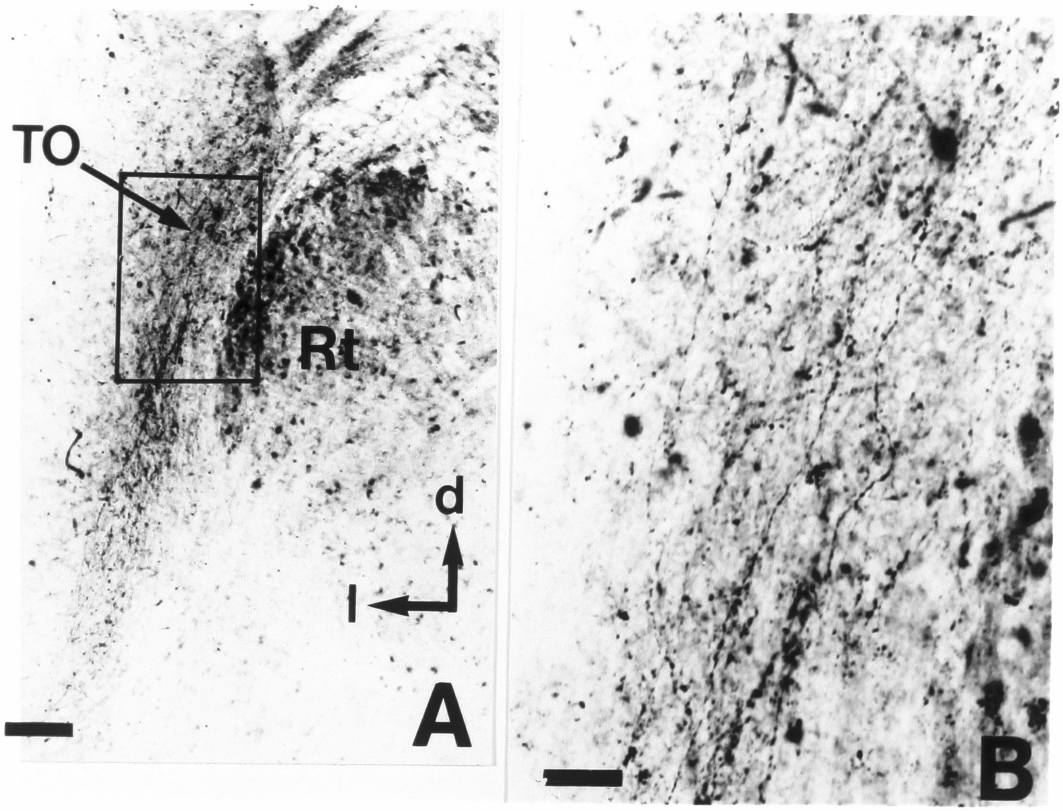
TO
Rt
d
l
A
B

FIGURE 6.14 - Anterogradely-labeled fibers in the lateral wall of the caudal pons after PHA-L injection rostral to RA. (A) Coronal section (B) High-power view of the rectangle in (A). Bar sizes: (A), 500μm; (B), 200μm.

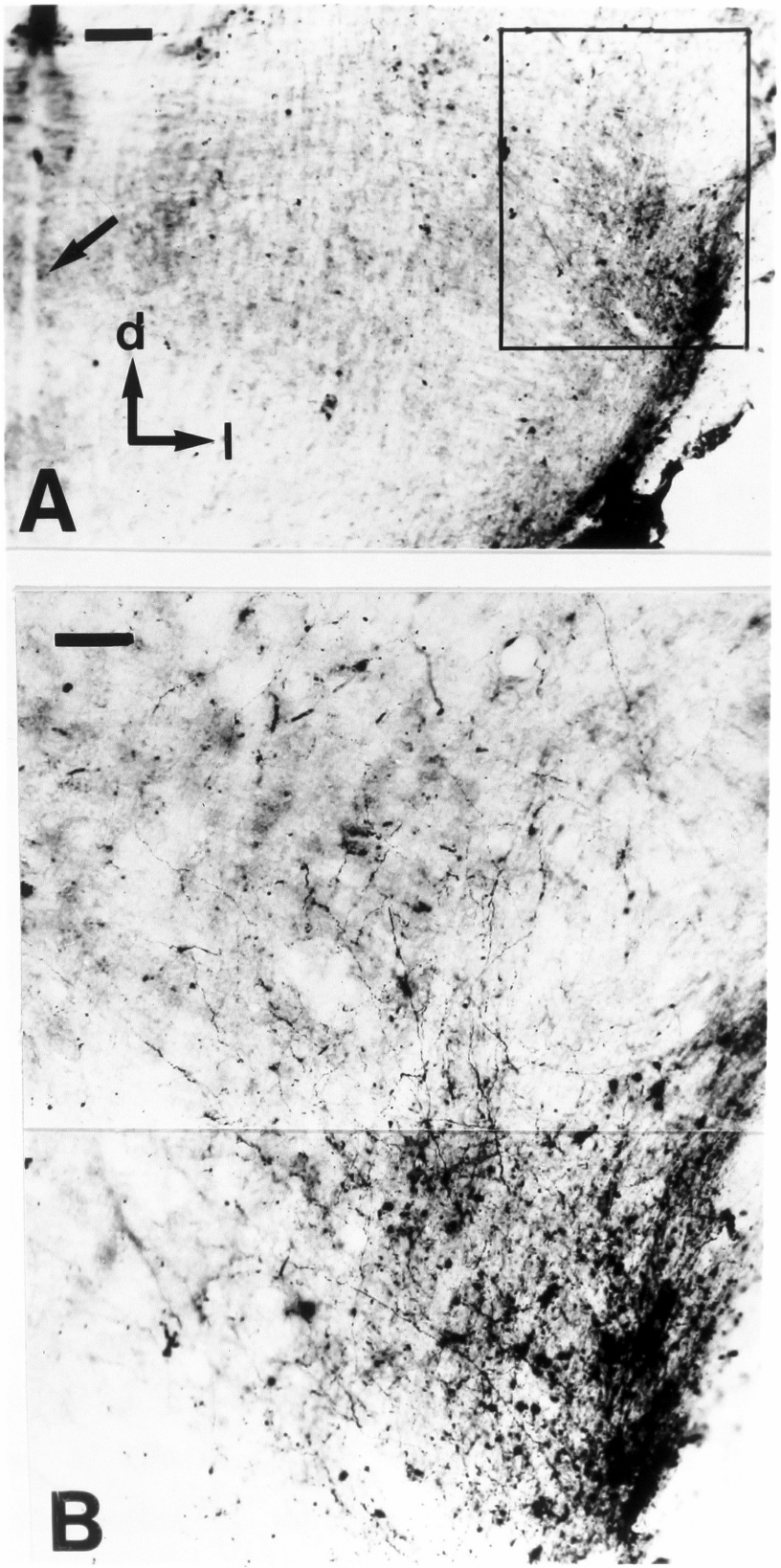
d
l
A
B

correspond to the general area where lateral lemniscal nuclei are localized, but this awaits further confirmation.

Many stained fibers arising from the PHA-L injections into the cup and adjacent A can be seen travelling all the way into the intercollicular (ICo) complex (possibly along TO), where a vast majority of them seem to terminate in the MLd/ICo border (figure 6.15 A to D), in a pattern that suggests colocalization with the source of input to the "shell" of Ov (Durand et al., 1992); a smaller but significant number of fibers penetrate MLd, where they seem to terminate (figure 6.15 E). DM was completely devoid of stained fibers in birds that received cup injections that respected RA. Some variability in the pattern of stained anterograde projections seen in these injections suggests that there may be some topographical organization of this descending system, especially along the AP axis, but this possibility was not explored in a systematic manner.

Injections of retrograde tracers completely restricted to discrete nuclei of the auditory thalamus were difficult due to the relatively small size of targets and proximity to the OM tract, where many fibers of archistriatal origin also travel. Ov was found by using coordinates obtained from neurophysiological recordings of auditory responses and the resulting injections were centered in Ov and its surrounding tissue, with varying degrees of leakage into the tractus ovoidalis or along the injection tract, which went through OM. The best example is shown in figure 6.16 (injection site not shown). A large number of backfilled cells is seen, that have a spatially well-delimited distribution in the intermediate medial portion of the archistriatum, grouped around nucleus RA, which is completely

FIGURE 6.15 - Anterogradely-labeled fibers in the auditory portions of the midbrain after PHA-L injection rostral to RA. (A) Coronal section through MLd. (B) High-power view of the left rectangle in (A). (C) High-power view of the right rectangle in (A). (D) Coronal section through MLd, rostral to (A). (E) High-power view of the rectangle in (D). Bar sizes: (A) and (D), 300μm; (B) and (C), 100μm; (E), 60μm.

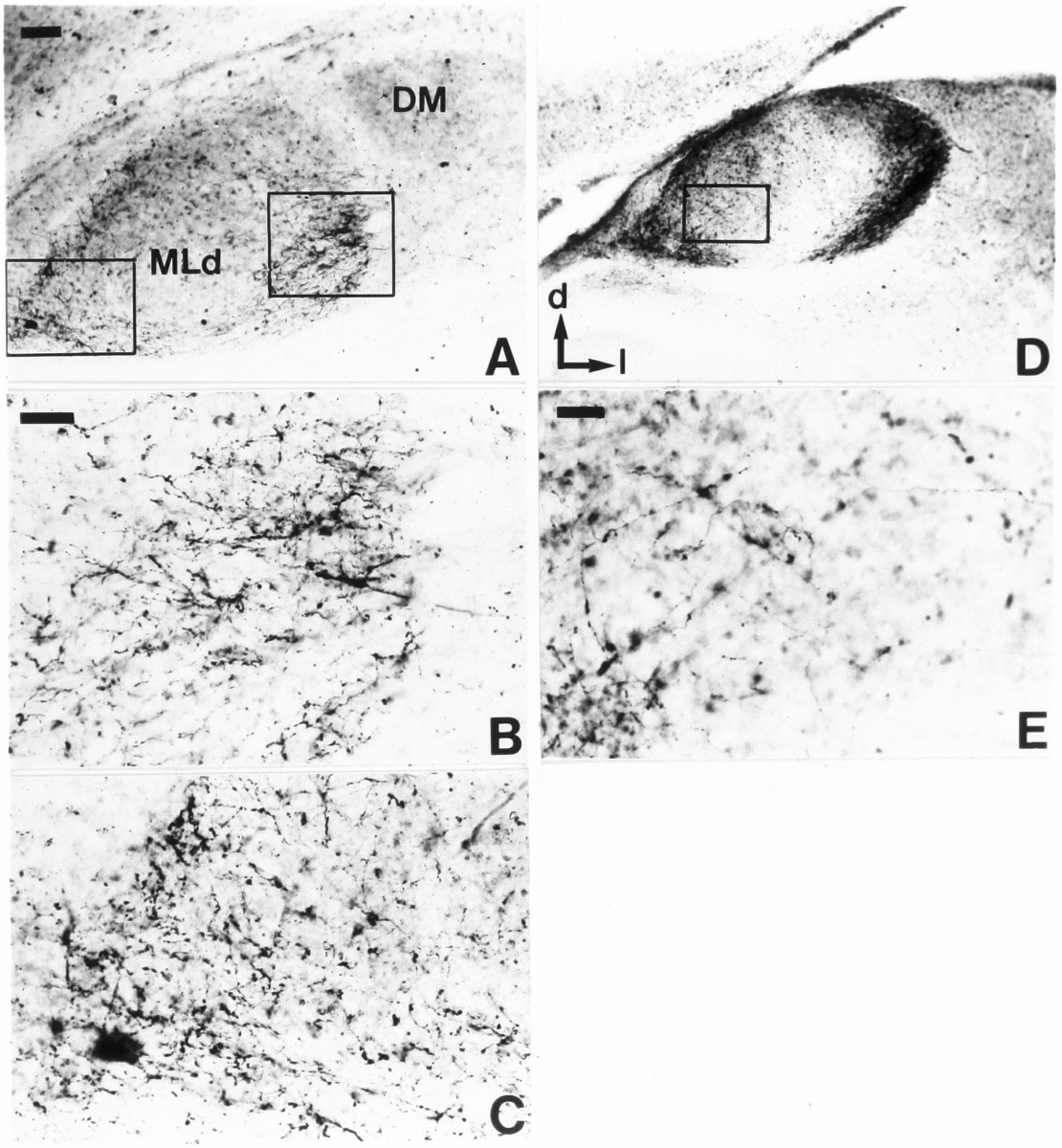
DM
MLd
A
d
l
D
B
E
C

FIGURE 6.16 - Retrogradely-labeled cells after injection of fluorescent beads centered in ovoidalis (injection site not shown). Diagrams represent serial parasagittal sections from L2.0 (upper left) to L3.3 (lower right); labeled cells are seen in the archistriatum next to RA and in MLd. Bar size: 2mm.

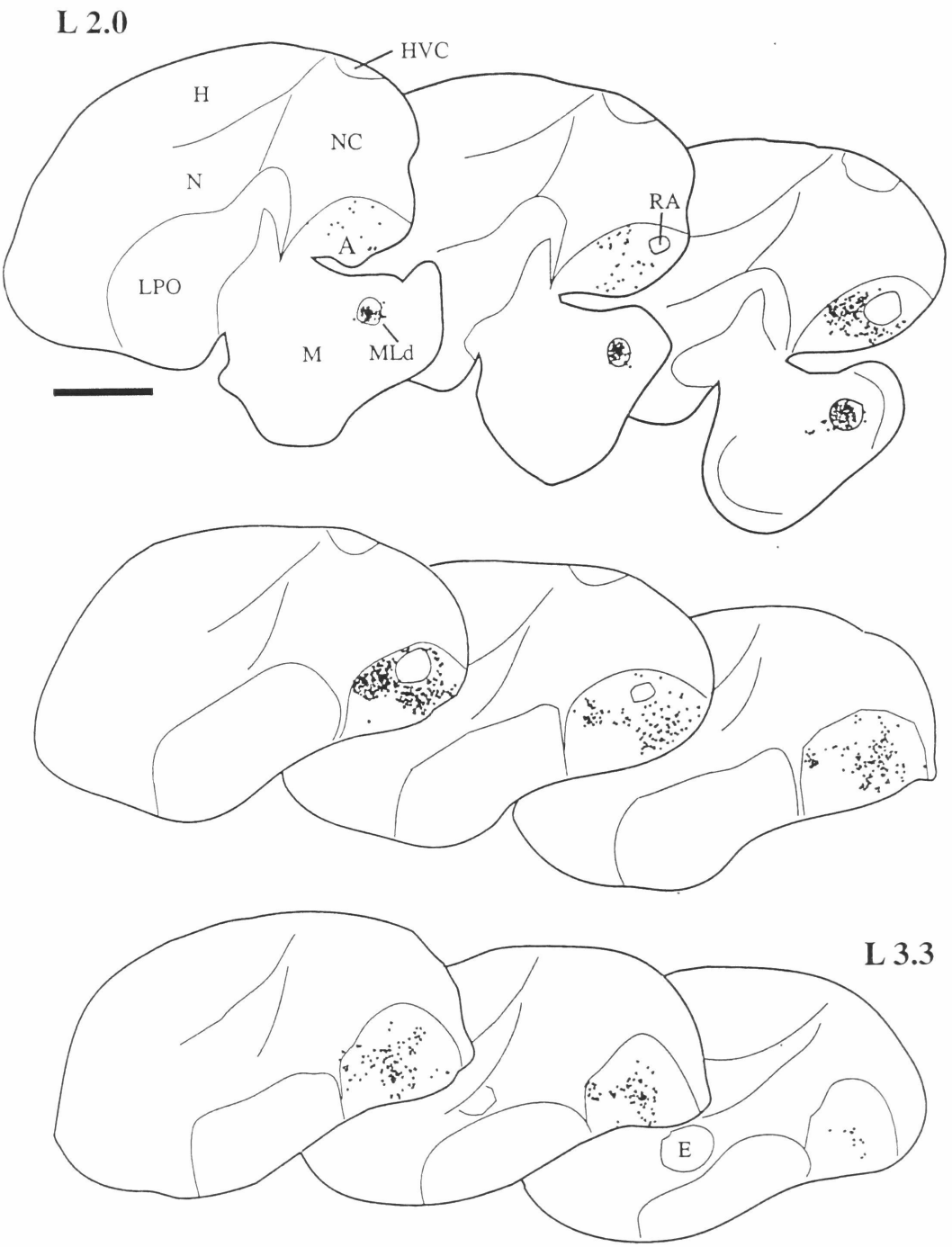
L 2.0
HVC
H
NC
N
RA
A
LPO
M
MLd
L 3.3
E

respected (this is strong evidence that the pattern of backfills is not just the result of damage to fibers in the OM tract). This array of backfilled cells may represent a good definition of the cup: notice that most cells are localized rostrally or ventrally to RA, although a few cells are also seen in its dorsal and caudal aspects. A large number of retrogradely labeled cells are also seen in MLd, confirming that the injection site did include termination sites of fibers from the auditory midbrain, as found in n. ovoidalis.

Auditory responses were also used to define coordinates for MLd, where beads were placed at various dorso-ventral and rostro-caudal levels. One example is shown in figure 6.17, where backfilled cells are seen in A in close relationship with RA, especially ventrally. In the particular injection shown in figure 6.17, very few cells are seen rostral to RA; more of these cells are seen when injections are placed in more rostral portions of MLd (not shown), suggesting a possible topographical organization. Whenever DM is respected, no backfilled cells are seen inside RA (figure 6.17; notice that this injection also included a portion of ICO that surrounds MLd).

FIGURE 6.17 - Retrogradely-labeled cells after injection of fluorescent beads in MLd. Diagrams represent coronal sections from A1.0 to P0.5; brain stem areas are only shown for the upper diagram. Shadowed area in the left tectal area (upper diagram) represents injection site; dots represent labeled cells in the archistriatum in close relation with RA. Bar size: 2mm.

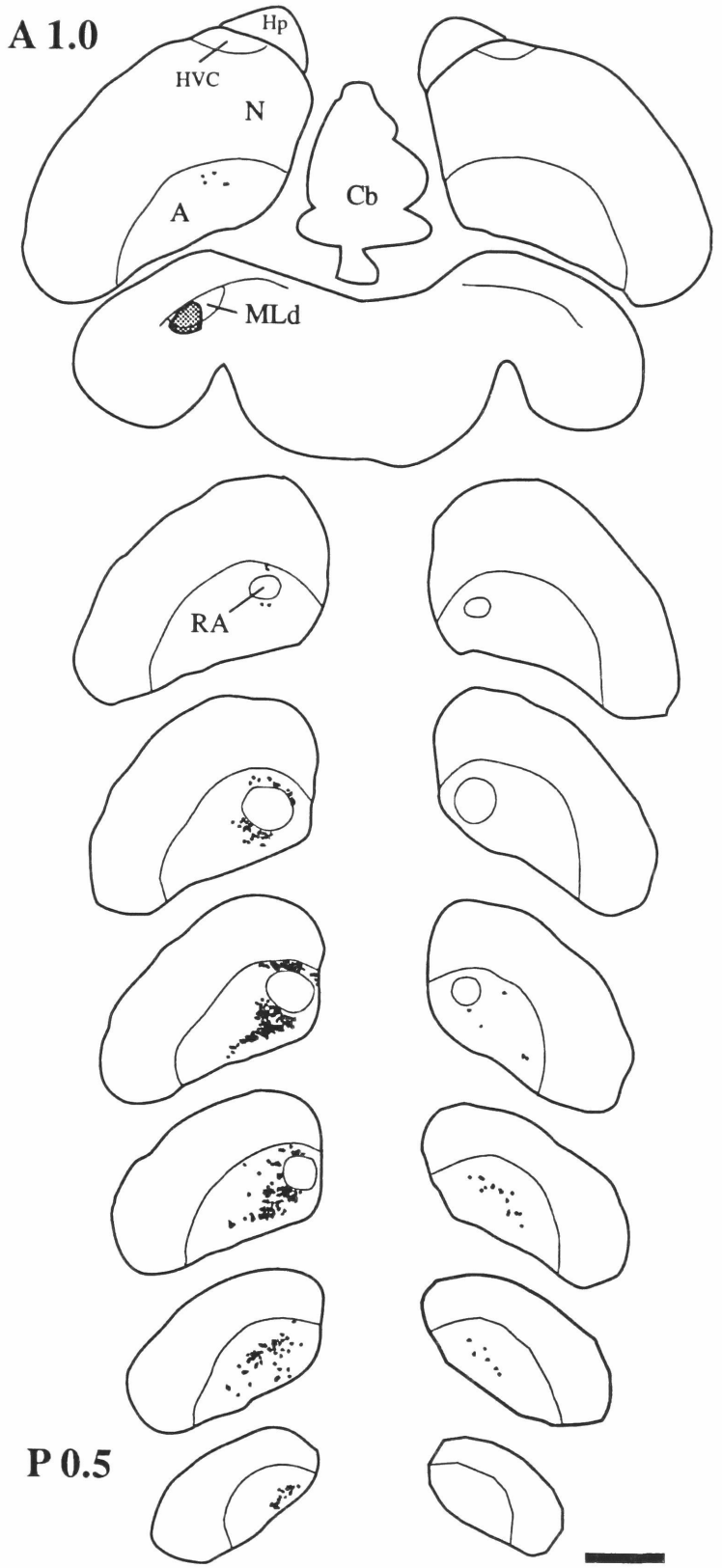
A 1.0
Hp
HVC
N
A
Cb
MLd
RA
P 0.5

DISCUSSION

The results presented in this chapter confirm that auditory structures project to the shelf under HVC and to the RA cup. They also show that the shelf projects to the cup, which in turn projects to thalamic and midbrain auditory relays. The projection from the shelf into HVC provides for a rich interface between the higher reaches of the ascending auditory pathway and the highest nucleus of the efferent pathway that controls learned song. More specific comments follow.

Shelf.

The shelf is one of the main terminal fields for fibers from Field L. The source of this input seems to be mainly subfields L1 and L3, although based only on the present injections and previously published work one cannot completely discard the possibility that the NIf/Uva pathway may also contribute to the shelf innervation as well as to HVC. In the previous chapter it is shown that the shelf may also receive input from more medial neostriatal areas (NCM), possibly also involved in auditory processing. Shelf cells form complex connections within the shelf what suggests that this area could be organized into various domains (especially along the medio-lateral axis). Thus, the shelf could work as an integrative center for auditory information from various sources, which it then sends either further down to the archistriatum or to a central component of the song control circuit, HVC. The richness of fiber patterns seen within the shelf suggests that a lot of song relevant auditory information may be integrated in this area before transmittal into

HVC or elsewhere. Densest termination sites are seen around the anterior and posterior poles of the shelf, which suggests that those could be particularly active integration areas.

Neurons in HVC are known to show patterned activity both during song perception and during song production (MacCasland and Konishi, 1981). The connection between the shelf and HVC seems to have a topographical relation and to be organized into discrete domains. This apparent orderliness offers the potential for an interfacing between a song relevant auditory map which is may be available in the shelf, and a song motor map represented in HVC.

Cup.

Our injections of retrograde tracers into the auditory thalamus and midbrain, have helped redefine the structure of the RA cup. Cells surrounding RA are the origin of forebrain fibers that project down to lower auditory structures. These cells have an asymetrical distribution around RA, being more numerous around its rostral and ventral aspects; these cells are distributed over an area that includes the region that receives input from Field L (presumably L3) as shown in Kelley and Nottebohm (figure 4 of their article). This pattern also corresponds to termination sites of fibers from the shelf, particularly parts of A ventral and rostral to RA, although terminals are also seen all around RA when injections are placed in the caudal pole of the shelf. RA is thus imbedded in a region which is intimately related with forebrain auditory pathways.

Auditory responses have been shown to travel down from HVC to RA (Williams, 1989, Doupe and Konishi, 1991 and Vicario and Yohay, in preparation). RA also receives inputs from the recursive pathway

that links HVC to RA (Williams, 1989) and in particular from lMAN. lMAN and the rest of the recursive loop are known to process auditory signals (Doupe and Konishi, 1991). In addition, a small number of fibers that travel from the RA cup into RA proper was also seen. Thus the archistriatal region of RA and the RA cup emerges as another site for integration of auditory information. It would be interesting to know whether the same cells that receive the auditory projections (from L3 or the shelf) are the origin of the descending fibers or of fibers that go into RA.

Auditory inputs into the song control circuit.

The exact source of auditory information to the song control circuit is undoubtedly a central question in the biology of birdsong that has not yet been completely resolved. The initial studies of Field L projections and the position of HVC in the hierarchy of nuclei within the song control circuit suggested HVC as a nodal point of entry for auditory information into the song control circuit. Recent observations suggest a more complex array of possibilities which are not mutually exclusive: 1) the shelf, for which further evidence is shown here; 2) a direct input from Field L into HVC: this was not observed initially (see Kelley and Nottebohm, 1979), but the more recent studies of Fortune and Margoliash (personal communication) suggest that cells in some L subfields (L1, L3) may project directly into HVC; these cells seem to be distributed over relatively large areas with a resulting lower density than, for instance, HVC projecting cells inside NIf, which makes their detection more difficult. In the injections described here, the possibility could not be eliminated that L cells backfilled from HVC injections are a result of

tracer uptake by fibers in the shelf. Another possibility which has been recently examined by Fortune and Margoliash is that dendrites of HVC cells may reach out to the shelf, where they could also receive a direct input from L cells; 3) auditory information could enter HVC from the Uva/NIf projection; Uva has indeed been shown to have auditory responses of short latency, whose origin is still unclear but which may be independent from the auditory thalamus (Okuhata and Nottebohm, in preparation); NIf is also closely apposed to Field L, from where it could receive some input.

Even though the contribution of each of these sources of auditory information to HVC is unclear, their existence suggests that multiple channels or pathways auditory information to HVC, which could be related to different aspects of sound processing such as temporal, or frequency analysis or some combination of these. This convergence could then play a major role in the generation of the highly specific patterns of auditory responses observed in units inside HVC and the song control circuit (Margoliash, 1983 and 1986; Williams, 1985). Another possible source of entry into the song circuit which probably deserves further investigation is the cup/RA interface. The cup could work as an integration center for auditory information which influences firing patterns inside RA, even though this may be a small contribution, since the pathway linking the cup to RA seems to have relatively few fibers. It would be very important to investigate patterns of electrophysiological response to auditory stimuli in areas like the shelf and cup; a particularly interesting question is whether cells in these areas show any kind of selectivity to complex stimuli

which could be then related to the acquisition of song models and to response patterns within nuclei of the song control circuit.

Organization of forebrain auditory pathways. Evolutionary considerations

Early research on the avian Field L tended to equate it with the mammalian auditory cortex, since it is the primary avian telencephalic structure which receives input from the auditory thalamus. Nevertheless, the absence of a descending projection which would correspond to the mammalian cortico-thalamic system was puzzling. It suggested that either this very distinctive feature of the mammalian cortex was not common to other vertebrates or that important information on the auditory pathway of birds was still missing. A projection to lower auditory centers is described in this chapter, that originates in a subregion of the archistriatum receiving at least a direct (from L3) and an indirect (through the shelf) projection from the primary auditory area. This seems to be very suggestive evidence that a descending auditory system originating from a telencephalic structure may be a conserved feature of vertebrates and not specific to mammals. It is, thus, probably wrong to equate Field L with the whole mammalian auditory cortex; it seems more reasonable to think of Field L as a complex that includes the primary forebrain target for the auditory thalamus (Fields L2a and 2b) and its surrounding areas and primary targets (L1 and L3); Field L2 may thus correspond just to the granular layer of mammalian auditory cortex while L1 and L3 represent targets for cells in this primary thalamo-recipient zone (in mammals, usually supra-granular layers).

It seems that in songbirds the auditory thalamo-recipient zone is physically separated from the area originating the descending auditory pathway, although they are connected. That this may be a general feature of the organization of avian sensory systems is suggested by the findings on the avian visual system (Karten and Shimizu, 1989). The ectostriatal visual component is also characterized by a separation of a primary visual target (ectostriatum) from the origin (in the archistriatum intermedium) of descending fibers to the visual thalamus and tectum. The ectostriatum is connected to the archistriatum by a forebrain circuit that involves periectostriatal, hyperstriatal and neostriatal areas, and which has been compared to the intracortical circuitry connecting thalamo-recipient layers to infragranular layers (similar relationships are also seen for nucleus basalis; see Dubbeldam and Visser, 1987). The results presented here and in the preceding chapter suggest that there is a complex telencephalic circuit that processes sound. This pathway involves various subdivisions of the avian forebrain, including portions of the caudal neostriatum (Field L, NCM and HVC shelf), the archistriatum intermedium (the area around RA) and possibly paleostriatum and hyperstriatum as well. It is suggested that these regions, which receive inputs from the auditory thalamus and in turn, directly or indirectly, project to thalamus and auditory midbrain may correspond to the mammalian auditory cortex. A general conclusion that emerges from the study of these sensory systems is that a large proportion of the connections between various avian telencephalic subdivisions may be comparable to mammalian intra- and intercortical connections.

It is surprising to find the origin of song motor fibers (RA) and of descending auditory fibers (RA cup) so closely apposed. The archistriatum is a complex structure, and the origin of the main descending forebrain tract, OM (Zeier and Karten, 1973). The archistriatum intermedium (Zeier and Karten, 1973), in particular, of which RA and its cup are both constituent parts, has been seen as a major source of descending motor fibers and of fibers related to at least one sensory system, the visual. The localization of the origin of descending auditory fibers in the archistriatum intermedium suggests that this subdivision of the forebrain could be generalized as the source of descending fibers originating in telencephalic structures, independent of whether they are related to motor or sensory systems. The homology that again comes to mind is that between archistriatum intermedium and infragranular layers of the cortex, the mammalian source of descending fibers from both sensory and motor systems.

It seems extremely interesting that two of the main nuclei in the descending motor pathway for control of song production - HVC and RA - are so intimately surrounded by and related to auditory areas. A similar relation can be seen at other levels of the song pathway - e.g. the proximity between DM (motor) and MLd (auditory), that between NIf and Field L and that between Uva and a shell of tissue around Uva which also shows auditory responses (Okuhata and Nottebohm, in prep.). A well developed telencephalic vocal control circuit occurs in birds as Passeriformes and Psittaciformes, that show vocal learning, but seems to be absent in suboscines, where vocal learning is not a distinctive feature (Kroodsma and Konishi, 1992).

All these observations suggest that the development of telencephalic circuits for the acquisition and production of learned vocalizations may have evolved from pre-existing and highly conserved auditory pathways.

If telencephalic auditory circuits had to decide on the nature of vocal responses given to conspecific vocal signals, then this could have led to the assumption of a motor role by some of the auditory neurons. Changes toward neoteny, favoring the late development of vocal motor pathways, may then have encouraged the emergence of vocal learning. Thus, a better understanding of the relation between pathways serving the perception and production of vocal signals should help us understand the evolution and machinery of vocal learning.

CHAPTER 7: SUMMARY AND CONCLUSIONS

The results presented in this thesis demonstrate that expression of an IEG, ZENK, is regulated in the brain of songbirds by a behaviorally relevant stimulus, song. This fact is used to map brain areas activated by song; a series of such areas is described, some of which had not been previously implicated in song production or perceptual processes. Based on comparisons with other studies where electrophysiological and metabolic methods were used, it is concluded that ZENK induction occurs in a subset of areas that respond to auditory stimuli. ZENK encodes a transcription factor and, in other systems, its induction correlates with activation of cell differentiation programs and synaptic plasticity; it is suggested that areas where ZENK induction is observed after song presentation could represent sites of active modification or plasticity in response to cellular activation.

Anatomical studies of areas highlighted by ZENK induction in response to song reveal that these areas are intimately associated with forebrain auditory pathways. Furthermore, a subset of these are closely apposed and contribute significant inputs to nuclei of the song control circuit; these areas could thus represent important sites for sensory-motor integration.

By focusing on NCM, the area with the most robust and consistent induction, it is demonstrated that ZENK induction has a preference for conspecific song and is habituated by repetitive presentations of the same song stimulus; however, cells do not enter an absolute refractory period after habituation to one particular song, since a full

genomic response can be elicited after habituation by introducing a new song stimulus. Thus, cells in NCM seem to be performing tasks related to auditory processing and song discrimination and may somehow play a role in the bird's ability to tell different songs apart.

ZENK response to a particular stimulus does not seem to influence the ability of cells to respond to other stimuli; this is important for deciphering whether a genomic response can recur at relatively brief intervals and code for successive memories. A gene regulatory mechanism that is sensitive to the properties of different songs could play an important role in the daily life of normally behaving songbirds.

Some directions for future research include:

- Electrophysiological experiments are needed to determine the response properties of cells in areas revealed by ZENK induction in response to song presentation and whether they contribute to the song-selectivity described within nuclei of the song control circuit;

- What are the mechanisms that regulate ZENK induction and permit discrimination between different songs? The answer to this question could lie: 1) regulation at the system or network level of activity in the ascending auditory pathways; 2) at the level of cells in NCM, for instance in the geometry of dendritic arborizations; 3) at a subcellular level; it would be interesting to determine what second-messenger systems are involved in the ZENK response and whether specificity can be achieved by differential activation of different transduction systems by different stimuli or by different contexts of stimulus presentation.

- What other genes are induced by song? Do they have similar or divergent patterns of expression as compared with ZENK (for instance, induction within nuclei of the song control circuit) that could help shed some light on IEG function?

- What are the consequences of ZENK induction? These can be further subdivided into three groups: 1) molecular: what genes are activated/repressed in consequence of ZENK activation?; 2) electrophysiological: does ZENK induction lead to any changes in the response properties of activated cells, such as potentiation/depression or changes in selectivity?; 3) does ZENK induction lead to morphological changes (e.g., in dendritic arborization, synaptic density, size and shape)?

REFERENCES

Alvarez-Buylla, A., Kirn, J. R. and Nottebohm, F. (1990). Birth of projection neurons in adult avian brain may be related to perceptual or motor learning. **Science, 249**:1444-1446.

Alvarez-Buylla, A. and Nottebohm, F. (1988). Migration of young neurons in adult avian brain. **Nature, 335**:353-354.

Alvarez-Buylla, A. and Vicario, D. S. (1988). Simple microcomputer system for mapping tissue sections with the light microscope. **J. Neurosci. Meth., 25**:165-173.

Anokhin, K. V. and Rose, S. P. R. (1991). Learning-induced increase of immediate early gene messenger RNA in the chick forebrain. **Eur. J. Neurosci., 3**:162-167.

Anokhin, K. V., Mileusnic, R., Shamakhina, I. and Rose, S. P. R. (1991). Effects of early experience on c-Fos gene expression in the chick forebrain. **Brain Res., 544:**101-107.

Arnold, A. P. (1975). The effects of castration on song development in zebra finches (Poephila guttata). **J. Exp. Zool., 191**:309-326.

Arnold, A. P., Nottebohm, F. and Pfaff, D. W. (1976). Hormone-concentrating cells in vocal control and other areas of the brain of the zebra finch (Poephila guttata). **J. Comp. Neurol., 165**:487-512.

Bailey, C. H. and Chen, M. (1983). Morphological basis of long-term habituation and sensitization in Aplysia. **Science, 220:**91-93.

Ball, G. F. and Casto, J. M. (1991). Autoradiographic localization of NMDA receptors in the avian song control system using [^{3}H]MK-801. **Soc. Neurosci. Abstr., Vol. 17:**p.1053.

Bartel, D. P., Sheng, M., Lau, L. F. and Greenberg, M. E. (1989). Growth factors and membrane depolarization activate distinct programs of early response gene expression: dissociation of fos and jun induction. **Genes Dev., 3**:304-313.

Berry, M. P., McConnell, P. and Sievers, J. (1980). Dendritic growth and the control of neuronal form. **Curr. Top. in Dev. Biol., 15**:67-101.

Bialy, M., Nikolaev, E., Beck, J. and Kaczmarev, L. (1992). Delayed c-Fos expression in sensory cortex following sexual learning in male rats. **Mol. Brain. Res., 14**:352-356.

Bliss, T. V. P. and Lomo, T. (1973). Long-lasting potentiation of synaptic transmission in the dentate area of the anaesthetized rabbit following stimulation of the perforant path. **J. Physiol., 232**:331-356.

Bliss, T. V. P. and Collingridge, G. L. (1993). A synaptic model of memory: long-term potentiation in the hippocampus. **Nature, 361:**31-39.

Bonke, B. A., Bonke, D. and Scheich, H. (1979a). Connectivity of the auditory forebrain nuclei in the guinea fowl (Numida meleagris). **Cell Tissue Res., 200**:101-121.

Bonke, D., Scheich, H. and Langer, G. (1979b). Responsiveness of units in the auditory neostriatum of the guinea fowl (Numida meleagris) to species-specific calls and synthetic stimuli. I.Tonotopy and functional zones of field L. **J. Comp. Physiol., 132**:243-255.

Bottjer, S. W., Miesner, E. A. and Arnold, A. P. (1984). Forebrain lesions disrupt development but not maintenance of song in passerine birds. **Science, 224**:901-903.

Braun, K., Scheich, H., Schachner, M. and Heizmann, C. W. (1985). Distribution of parvalbumin, cytochrome oxidase activity and 14C-2-deoxyglucose uptake in the brain of the zebra finch. I. Auditory and vocal motor systems. **Cell Tissue Res., 240**:101-115.

Brennan, P. A., Hancock, D. and Keverne, B. (1992). The expression of the immediate-early genes c-Fos, Egr-1 and c-Jun in the accessory olfactory bulb during the formation of an olfactory memory in mice. **Neuroscience, 49:**277-284.

Brenowitz, E. (1991). Altered perception of species-specific song by female birds after lesions of a forebrain nucleus. **Science, 251**:303-305.

Castellucci, V. F., Kennedy, T. E., Kandel, E. R. and Goelet, P. (1988). A quantitative analysis of 2-D gels identifies proteins in which labeling is increased following long-term sensitization in Aplysia. **Neuron,1**:321-328.

Chang, F. F. and Greenough, W. T. (1984). Transient and enduring morphological correlates of synaptic activity and efficacy change in the rat hippocampal slice. **Brain Res., 309**:35-46.

Changelian, P. S., Feng, P., King, T. C. and Milbrandt, J. (1989). Structure of the NGFI-A gene and detection of upstream sequences responsible for its transcriptional induction by nerve growth factor. **Proc. Natl. Acad. Sci. USA, 86**:377-381.

Christy, B., Lau, L. and Nathans, D. (1988). A gene activated in mouse 3T3 cells by serum factors encodes a protein with "zinc finger" sequences. **Proc. Natl. Acad. Sci. USA, 85**:7857-7861.

Christy, B. and Nathans, D. (1989). DNA binding site of the growth factor-inducible protein Zif268. **Proc. Natl. Acad. Sci. USA, 86**:8737-8741.

Clayton, D. F., Huecas, M. E., Sinclair-Thompson, E. Y., Nastiuk, K. L. and Nottebohm, F. (1988). Probes for rare mRNAs reveal distributed cell subsets in canary brain. **Neuron, 1**:249-261.

Cole, A. J., Saffen, D. W., Baraban, J. M. and Worley, P. F. (1989). Rapid increase of an immediate early gene messenger RNA in hippocampal neurons by synaptic NMDA receptor activation **Nature, 340**:474-476.

Cotman, C.W. and Nieto-Sampedro, M. (1984). Cell biology of synaptic plasticity. **Science 225:**1287-1294.

Cotman, C.W., Nieto-Sampedro, M. and Harris, E.W. (1981). Synapse replacement in the nervous system of adult vertebrates. **Physiol. Rev., 61:**684.

Davis, H. P. and Squire, L. R. (1984). Protein synthesis and memory: a review. **Psychol. Bull., 96:**518-559.

DeVoogd, T. J. and Nottebohm, F. (1981). Gonadal hormones induce dendritic growth in the adult avian brain. **Science, 214**:202-204.

Doupe, A. J. and Konishi, M. (1991). Song-selective auditory circuits in the vocal control system of the zebra finch. **Proc. Natl. Acad. Sci. USA, 88**:11339-11343.

Dragunow, M. and Robertson, H. A. (1987). Generalized seizures induce c-fos protein(s) in mammalian neurons. **Nature, 329**:441-442.

Dubbeldam, J. L. and Visser, A. M. (1987). The organization of the nucleus basalis-neostriatum complex of the mallard (Anas

platyrhyncos L.) and its connections with the archistriatum and the paleostriatal complex. **Neuroscience, 21**:487-517.

Durand, S.E., Tepper, J.M. and Cheng, M-F. (1192) The shell region of the nucleus ovoidalis: a subdivision of the avian auditory thalamus. **J. Comp. Neurology, 323**:495-518.

Falls, J. B. (1982) in Acoustic Communication in Birds, eds. Kroodsma, D. E. and Miller, D. H., New York: Academic Press, pp. 237-278.

Fortune, E. and Margoliash, D. (1992). Cytoarchitectonic organization and morphology of cells of the Field L complex in male zebra finches (Taenopygia guttata). **J. Comp. Neurology, 325:** 388-404.

Gahr, M. (1990). Delineation of a brain nucleus: comparisons of cytochemical, hodological, and cytoarchitectural views of the song control nucleus HVC of the adult canary. **J. Comp. Neurology, 294:**30-36.

Gall, C. M and Isakson, P. J., (1989). Limbic seizures increase neuronal production of messenger RNA for nerve growth factor. **Science, 245**:758-761.

George, J. and Clayton, D. F. (1992). Differential regulation in the avian song control circuit of an mRNA predicting a highly conserved protein related to protein kinase C and the bcr oncogene. **Mol. Brain Res., 12**:323-329.

Gerfen, C. R. and Sawchenko, P. E. (1984). An anterograde neuroanatomical tracing method that shows the detailed morphology of neurons, their axons and terminals: immunocytochemical

localization of an axonally transported plant lectin, Phaseolus vulgaris leucoagglutinin. **Brain Res. 290**:219-238.

Ginty, D. D., Bading, H. and Greenberg, M. E. (1992). Trans-synaptic regulation of gene expression. **Current Opinion Neurobiology, 2**:312-316.

Gius, D., Cao, X., Rauscher III, F. J., Cohen, D. R., Curran, T. and Sukhatme, V. P. (1990). Transcriptional activation and repression by Fos are independent functions: the C terminus represses immediate-early gene expression via CArG elements. **Mol. Cell Biol., 10**:4243-4255.

Godard, R. (1991). Long-term memory of individual neighbors in a migratory songbird. **Nature, 350**:228-229.

Goelet, P., Castelucci, V., Schacher, S. and Kandel, E. (1986). The long and the short of long-term memory - a molecular framework. **Nature, 332**:419-422.

Goldman, S. A. and Nottebomh, F. (1983) Neuronal production, migration and differentiation in a vocal control nucleus of the adult female canary brain. **Proc. Natl. Acad. Sci. USA, 80**:2390-2394.

Greenough, W., and Bailey, C.H. (1988). The anatomy of a memory: converge of results across a diversity of tests. **TINS, 11:**142-147.

Grisham, W. and Arnold, A. P. (1992). GABA-like immunoreactivity in the song system of the zebra finch. **Soc. Neurosci. Abstr., 18 (Part 1)**: p. 528.

Gupta, M. P., Gupta, M., Zak, R. and Sukhatme, V. P. (1991). Egr-1, a serum-inducible zinc finger protein, regulates transcription of the rat cardiac α-myosin heavy chain gene. **J. Biol. Chem.**, 266:12813-12816.

Gurney, M. E. (1981). Hormonal control of cell form and number in the zebra finch song system. **J. Neurosci., 1**:658-673.

Herrmann, K. and Arnold, A. P. (1991). Lesions of HVC block the developmental effects of estradiol in the female zebra finch song system. **J. Neurobiol., 22**:29-39.

Hunt, S. P., Pini A. and Evan, G. (1987). Induction of c-fos like protein in spinal cord neurons following sensory stimulation. **Nature, 328**:632-634.

Isakson, P. J., Huntsman, M. M., Murray, K. D. and Gall, C. M. (1991). BDNF mRNA expression is increased in adult rat forebrain after limbic seizures: temporal patterns of induction distinct from NGF. **Neuron, 6**:937-948.

Immelman, K. (1969). Song development in the zebra finch and other estrildid finches. In: Bird Vocalizations (Ed. by Hinde, R. A.) Cambridge: Cambridge University Press, pp. 61-74

Izzo, P. N. (1991). A note on the use of biocytin in anterograde tracing studies in the central nervous system: application at both light and electron microscopic level. **J. Neurosc. Meth., 36:**155-166.

Karns, L. R., Ng, S. -C., Freeman, J. A. and Fishman, M. C. (1987). Cloning of complementary DNA for GAP-43, a neuronal growth-related protein. **Science, 236**:597-600.

Karten, H. J. (1967). The organization of the ascending auditory pathway in the pigeon (Columba livia). I. Diencephalic projections of the inferior colliculus (nucleus mesencephalis lateralis, pars dorsalis). **Brain Res., 6**:409-427.

Karten, H. J. (1968). The ascending auditory pathway in the pigeon (Columba livia) II. Telencephalic projections of the nucleus ovoidalis thalami. **Brain Res., 11**:134-153.

Karten, H. J. (1991). Homology and evolutionary origins of the "neocortex". **Brain Behav. Evol., 38**:264-272.

Karten, H. J. and Dubbeldam, J. L. (1973). The organization and projections of the paleostriatal complex in the pigeon (Columba livia). **J. Comp. Neurol., 140**:35-52.

Karten, H. J. and Shimizu, T. (1989). The origins of neocortex: connections and lamination as distinct events in evolution. **J. Cogn. Neurosci., 1**:291-301.

Katz, L. C., Burkhalter, A. and Dreyer, W. J. (1984). Fluorescent latex microshperes as a retrograde neuronal marker for *in vivo* and *in vitro* studies of visual cortex. **Nature, 310**:498-500.

Katz, L. C. and Gurney, M. E. (1981). Auditory responses in the zebra finch's motor system for song. **Brain Res., 221**:192-197.

Kelley, D. B. and Nottebohm, F. J. (1979). Projections of a telencephalic auditory nucleus - field L - in the canary. **J. Comp. Neurol., 183**:455-469.

King, M. A., Louis, P. M., Hunter, B. E. and Walker, O. W. (1989). Biocytin: a versatile anterograde neuroanatomical tract-tracing alternative. **Brain Res., 497**:361-367.

Kirn, J. and Nottebohm, F. (1990). Neuronal clusters: incorporation sites for neurons born in adult canary forebrain. **Soc. Neurosci. Abstr., Vol. 16.**

Konishi, M. (1989). Birdsong for neurobiologists. **Neuron, 3**:541-549.

Konishi, M. & Akutagawa, E. (1985). Neuronal growth, atrophy and death in a sexually dimorphic songnucleus in the zebra finch brain. **Nature, 315**:145-147.

Kornhauser, J. M., Nelson, D. E., Mayo, K. E. and Takahashi, J. S. (1990). Photic and circadian regulation of c-fos expression in the hamster suprachiasmatic nucleus. **Neuron, 5**:127-134.

Kroodsma, D.E. (1976). Reproductive development in a female songbird: differential stimulation by quality of male song. **Science, 192**:574-575.

Kroodsma, D. E. (1982). Learning and the ontogeny of sound signals in birds. In Acoustic Communication in Birds, eds., Kroodsma, D. E., Miller E. H. and Oullet H., New York: Academic Press. Vol. 2, pp. 1-23.

Kroodsma, D. E. and Konishi, M. (1992). A suboscine bird (eastern phoebe, Sayornis phoebe) develops normal song without auditory feedback. **Anim. Behav., 42**:477-487.

Lee, K., Schottler, F., Oliver, M. and Lynch, G. S. (1980). Brief bursts of high-frequency stimulation produce two types of morphological changes in rat hippocampus. **J Neurophysiol., 44**:247-258.

Lemaire, P., Revelant, O., Bravo, R., and Charnay, P. (1988). Two mouse genes encoding potential transcription factors with identical DNA-binding domains are activated by growth factors in cultured cells. **Proc. Natl. Acad. Sci. USA, 85**:4691-4695.

Leppelsack, H. and Vogt, M. (1976). Responses of auditory neurons in the forebrain of a songbird to stimulation with species-specific sounds. **J. Comp. Physiol., 107**:263-274.

Margoliash, D. (1983). Acoustic parameters underlying the responses of song-specific neurons in the white-crowned sparrow. **J. Neurosci., 3**:1039-1057.

Margoliash, D. (1986). Preference for autogenous song by auditory neurons in a song system nucleus of the white-crowned sparrow. **J. Neurosci., 6**:1643-1661.

Marler, P. (1970). A comparative approach to vocal learning: song development in white-crowned sparrows. **J. Comp. Phys. Psych., 71**:1-25.

Marler, P. and Peters, S. (1977). Selective vocal learning in a sparrow. **Science, 198**:519-527.

Marler, P. and Peters, S. (1987). A sensitive period for song acquisition in the song sparrow, Melospiza melodia: a case of age-limited learning. **Ethology, 76**:89-100.

Marler, P. and Tamura, M. (1964). Culturally trasmitted patterns of vocal behavior in sparrows. **Science, 146**:1483-1486.

McLean, I. W. and Nakane, P. K. (1974). Peryodate-lysine-paraformaldehyde fixative, a new fixative for immunoelectron microscopy. **J. Histochem. Cytochem., 22**:1077-1083.

McMahon, S.B. and Monroe, J.G. (1992). Role of primary response genes in generating cellular responses to growth factors. **FASEB J., 6**:2707-2715.

Mello, C. V., Vicario, D. S. and Clayton, D. F. (1992). Song presentation induces gene expression in the songbird forebrain. **Proc. Natl. Acad. Sci. USA, 89**:6818-6822.

Milbrandt, J. (1987). A nerve growth factor-induced gene encodes a possible transcriptional regulatory factor. **Science, 238**:797-799.

Milbrandt, J. (1988). Nerve growth factor induces a gene homologous to the glucocorticoid receptor gene. **Neuron, 1:** 183-188.

Montarolo, P. G., Goelet, P., Castellucci, V. F., Morgan, J., Kandel, E. R. and Schacher, S. (1986). A critical period for macromolecular sysnthesis in long-term heterosynaptic facilitation in Aplysia. **Science, 234**:1249-1254.

Morgan, J. I., Cohen, D. R., Hempstead, J. L. and Curran, T. (1987). Mapping patterns of C-fos expression in the central nervous system after seizure. **Science, 237:**192-197.

Morgan, J. I. and Curran, T. (1989). Stimulus-transcription coupling in neurons: role of cellular immediate-early genes. **TINS, 12**:459-462.

Morrison, R. (1992). Doctoral dissertation, Rockefeller University.

Müller, C. M. (1988). Distribution of GABAergic perikarya and terminals in the centers of the higher auditory pathway of the chicken. **Cell Tissue Res., 252**:99-106.

Müller, C. M. and Leppelsack, H. (1985). Feature extraction and tonotopic organization in the avian auditory forebrain. **Exp. Brain Res., 59**:587-599.

Müller, S. C. and Scheich, H. P. (1985). Functional organization of the avian auditory field L - a comparative 2-deoxyglucose study. **J. Comp. Physiol., 156**:1-12.

Nastiuk, K. (1992). Doctoral dissertation, Rockefeller University.

Nikolaev, E., Kaminska, B., Tischmeyer, W., Matthies, H. and Kaczmarek, L. (1992). Induction of expression of genes encoding transcription factors in the rat brain elicited by behavioral training. **Brain Res. Bul., 28**:479-484.

Nikolaev, E., Werka, T. and Kaczmarek, L. (1992). C-Fos protooncogene expression in rat brain after long-term training of two-way active avoidance reaction. **Beh. Brain Res., 48:** 91-94.

Nordeen, K. W. and Nordeen, E. J. (1988). Projection neurons within a vocal motor pathway are born during song learning in zebra finches. **Nature, 344**:149-151.

Northcutt, R. G. (1981). Evolution of the telencephalon in nonmammals. **Ann. Rev. Neurosci., 4**:301-350.

Nottebohm, F. (1981). A brain for all seasons: cyclical anatomical changes in song control nuclei of the canary brain. **Science, 214**:1368-1370.

Nottebohm, F. (1989). From birdsong to neurogenesis. **Scientific American, 260**:74-79.

Nottebohm, F. and Arnold, A. P. (1976). Sexual dimorphism in sexual control areas of the songbird brain. **Science, 194**:211-213.

Nottebohm, F., Kelley, D. B. and Paton, J. A. (1982). Connections of vocal control nuclei in the canary telencephalon. **J. Comp. Neurol., 207**:344-357.

Nottebohm, F. and Nottebohm, M. E. (1988). Relationship between song repertoire and age in the canary, Serinus canarius. **Z. Tierpsychol., 46**:298-305.

Nottebohm, F., Nottebohm, M. E. and Crane, L. (1986). Developmental and seasonal changes in canary song and their relation to changes in the anatomy of song-control nuclei. **Behav. Neural Biol., 46**:445-471.

Nottebohm, F., Stokes, T. and Leonard, C. M. (1976). Central control of song in the canary, Serinus canarius. **J. Comp. Neurol., 165**:457-486.

Pavletich, N. P. and Pabp, C. O. (1991). Zinc finger-DNA recognition: crystal structure of a Zif268-DNA complex at 2.1Å. **Science, 252**:809-817.

Price, P. H. (1979). Developmental determinants of structure in zebra finch song. **J. Comp. Physiol. Psychol., 93**:260-277.

Purves, D., Hadley, R. D., and Voyvodic, J. T. (1986). Dynamic changes in the dendritic geometry of individual neurons visualized over periods of up to three months in the superior cervical ganglion of living mice. **J. Neurosci. 6:**1051-1060.

Purves, D., Voyvodic, J. T., Magrassi, L. and Yawo, H. (1987). Nerve terminal remodelling vizualized in living mice by repeated visualization of the same neuron. **Science, 238**:1122-1126.

Reiner, A., Davis, B. M., Brecha, N. C. and Karten, H. J. (1984). The distribution of enkephalinlike immunoreactivity in the telencephalon of the adult and developing domestic chicken. **J. Comp. Neurol., 228**:245-262.

Reiner, A., Karten, H. J., and Solina, A. R. (1983). Substance P: Localization within Paleostrial-tegmental pathways in the pigeon. **Neurosci., 9:**61-85.

Rose, S. P. R. (1991). How chicks make memories: the cellular cascade from C-fos to dendritic remodelling. **TINS, 14:** 390-397.

Rusak, B., Robertson, H. A., Wisden, W. & Hunt, S. P. (1990). Light pulses that shift rhythms induce gene expression in the suprachiasmatic nucleus. **Science, 248**:1237-1240.

Saffen, D. W., Cole, A.J., Worley, P.F., Christy, B. A., Ryder, K. and Baraban, J.M. (1988). Convulsant-induced increase in transcription factor messenger RNAs in rat brain. **Proc. Nat. Acad. Sci. USA, 85**:7795-7799.

Sagar, S. M., and Sharp, F. R. (1990). Light induces a Fos-like nuclear antigen in retinal neurons. **Mol. Brain Res., 7**:17-21.

Sagar, S. M., Sharp, F. R. and Curran, T. (1988). Expression of c-fos protein in brain: metabolic mapping at the cellular level. **Science, 240**:1328-1331.

Saini, K. D. and Leppelsack (1981). Cell types of the auditory caudomedial neostriatum of the starling (Sturnus vulgaris). **J. Comp. Neurol., 198**:209-229.

Sakaguchi, H., Asano, M., Yamamoto, K. and Saito, N. (1987). Release of endogenous g-aminobutyric acid from vocalization nucleus, the robust nucleus of the archistriatum of zebra finch in vitro. **Brain Res., 410**:380-384.

Sanger, F., Nicklen, S. and Coulson, A. R. (1977). DNA sequencing with chain-termination inhibitors. **Proc. Natl. Acad. Sci. USA, 74**:5463-5467.

Sassone-Corsi, P., Sisson, J. C. and Verma I. M. (1988). Transcriptional autoregulation of the proto-oncogene FOS. **Nature, 334:**314-319.

Scharff, C. and Nottebohm, F. (1991). A comparative study of the behavioral deficits following lesions of various parts of the zebra finch song system: **implications for vocal learning. J. Neurosci., 11**:2896-2913.

Scheich, H., Bonke, B. A., Bonke, D. and Langner, D. (1979). Functional organization of some auditory nuclei in the guinea fowl demonstrated by the 2-deoxyglucose technique. **Cell Tiss. Res., 204**:17-27.

Schmued, L. C. and Fallon, J. H. (1986). Fluoro-Gold: a new fluorescent retrograde axonal tracer with numerous unique properties. **Brain Res., 377**:147-154.

Searcy, W. A. and Marler, P. (1987). Response of sparrows to songs of deaf and isolation-reared males: further evidence for innate auditory templates. **Develop. Psychobiol., 20**:509-519.

Shatz, C. (1990). Impulse activity and the patterning of connections during CNS development. **Neuron, 5**:745-756.

Sheng, M. and Greenberg, M. (1990). The regulation and function of c-fos and other immediate early genes in the nervous system. **Neuron, 4**:477-485.

Sheng, M., McFadden, G. and Greenberg, M. (1990). Membrane depolarization and calcium induce c-fos transcription via phosphorylation of transcription factor CREB. **Neuron, 4**:571-582.

Siegel S. (1956). Nonparametric Statistics for the Behavioral Sciences, New York: McGraw-Hill, pp. 116-127.

Simpson and Vicario, 1991. Early estrogen treatment of female zebra finches masculinizes the brain pathway for learned vocalizations. **J. Neurobiol., 22**:777-793.

Sohrabji, F., Nordeen, E. J. and Nordeen, K. W. (1990). Selective impairment of song learning following lesions of a forebrain nucleus in the juvenile zebra finch. **Behav. Neural Biol., 53**:51-63.

Sonnenberg, J. L., MacGregor-Leon, P. F., Curran, T. and Morgan, J. I. (1989a). Dynamic alterations occur in the levels and composition of transcription factor AP-1 complexes after seizure. **Neuron, 3**:359-365.

Sonnenberg, J. L., Rauscher, F. J., III, Morgan, J. I. and Curran, T. (1989b). Regulation of proenkephalin by Fos and Jun. **Science, 246**:1622-1625.

Stokes, T. M., Leonard, C. M. and Nottebohm, F. (1974). The telencephalon, diencephalon, and mesencephalon of the canary, Serinus canaria, in stereotaxic coordinates. **J. Comp. Neurol., 156**:337-374.

Sukhatme, V. P., Cao, X., Chang, L. C., Tsai-Morris, C. H., Stamenkovitch, D., Ferreira, P. C. P., Cohen, D. R., Edwards, S. A., Shows, T. B., Curran, T., LeBeau, M. M. and Adamson, E. D. (1988). A zinc finger-encoding gene coregulated with c-fos during growth and differentiation, and after celular depolarization. **Cell, 53**:37-43.

Thorpe, W. H. (1958). The learning of song patterns by birds, with especial reference to the song of the chaffinch, Fringilla coelebs. **Ibis, 100**:535-570.

Watson, M.A., and Milbrandt, J. (1989). The NGFI-B gene, a transcriptionally inducible member of the steroid receptor gene superfamily: genomic structure and expression in rat brain after seizure induction. **Mol. Cell. Biol., 9:** 4213-4219.

Welty, J. C. and Baptista, L., (1988). The Life of Birds. New York: W. B. Saunders, pp.214-215.

Wild, J. M. (1987). Nuclei of the lateral lemniscus project directly to the thalamic auditory nuclei in the pigeon. **Brain Res., 408**:303-307.

Williams, H. and Nottebohm, F. (1985). Auditory responses in avian vocal motor neurons: a motor theory for song perception in birds. **Science, 229**:279-282.

Williams, H. (1989). Multiple representations and auditory-motor interactions in the avian song system. In: Modulation of Defined Vertebrate Neural Circuits. **Ann. N. Y. Acad. Sci., 563**:148-164.

Wingfield, J. C. and Wada, M. (1989). Changes in plasma levels of testosterone during male-male interactions in the song sparrow, Melospiza melodia: time course and specificity of response. **J. Comp. Physiol., 166**:189-194.

Winer, J. A. and Larue, D. T. (1987). Patterns of reciprocity in auditory thalamocortical and corticothalamic connections: study with horseradish peroxidase and autoradiographic methods in the rat medial geniculate body. **J. Comp. Neurol. 257**:282-315.

Wisden, W., Errington, M. L., Williams, S., Dunnett, S. B., Waters, C., Hitchcock, D., Evan, G., Bliss, T. V. P. and Hunt, S. P. (1990). Differential expression of immediate early genes in the hippocampus and spinal cord. **Neuron, 4**:603-614.

Worley, P. F., Christy, B.A., Nakabeppu, Y., Bhat, R. V., Cole, A.J. and Baraban, J.M. (1991). Constitutive expression of Zif268 in neocortex is regulated by synaptic activity. **Proc. Nat. Acad. Sci. USA, 88**:5106-5110.

End